Natural Hazards
Risk Assessment and Vulnerability Reduction

Edited by José Simão Antunes do Carmo

NATURAL HAZARDS - RISK ASSESSMENT AND VULNERABILITY REDUCTION

Edited by **José Simão Antunes do Carmo**

Contributors

Shakeel Mahmood, Razia Rani, Luca Franzi, Gennaro Bianco, Alessandro Pezzoli, Angelo Besana, Bruno Barroca, Hasanuddin Zainal Abidin, Heri Andreas, Teguh P Sidiq, Irwan Gumilar, Dina Anggreni Sarsito, Dhota Pradipta, Liliasari S, Eko Hariyono, Selma Lendelvo, Margaret Angula, Immaculate Mogotsi, Karl Aribeb, Michihiro Ohori, Yuri Masukawa, Keisuke Kojima, Marco Conedera, Claudio Bozzini, Patrik Krebs, Ueli Ryter, Thalia Bertschinger, Nafise Moghaddasi, Iman Karimirad, Vahedberdi Sheikh

Notice

Statements and opinions expressed in the chapters are these of the individual contributors and not necessarily those of the editors or publisher. No responsibility is accepted for the accuracy of information contained in the published chapters. The publisher assumes no responsibility for any damage or injury to persons or property arising out of the use of any materials, instructions, methods or ideas contained in the book.

We are IntechOpen,
the world's leading publisher of Open Access books
Built by scientists, for scientists

3,900+
Open access books available

116,000+
International authors and editors

120M+
Downloads

151
Countries delivered to

Our authors are among the
Top 1%
most cited scientists

12.2%
Contributors from top 500 universities

Interested in publishing with us?
Contact book.department@intechopen.com

Numbers displayed above are based on latest data collected.
For more information visit www.intechopen.com

Meet the editor

José Simão Antunes do Carmo completed his master's degree in Hydraulics and Water Resources in 1990 from the University of Lisbon and his PhD in Engineering Sciences in 1995 from the University of Coimbra, Portugal. He was director of several undergraduate and master courses in Civil Engineering and Environmental Engineering in the period 1995–2010. He was a scientific advisor of 23 master's dissertations and two PhD theses in Hydraulics and Water Resources. He has been a member of the Ocean & Coastal Management Editorial Board since 2012. He has published more than 60 papers in scientific journals, 12 book-chapters, and more than 100 papers in international conferences. He has authored two books and edited eight others. His main areas of scientific research are: hydrodynamics, morphodynamics, river and coastal processes, coastal management, climate change, natural hazards, risks, and vulnerabilities.

Contents

Preface

At a time when human and material losses caused by natural disasters, such as earthquakes, tsunamis, volcanic eruptions, landslides, floods, and wildfires, are intensifying throughout the world, it is imperative to evaluate these events to mitigate the social, economic and environmental damage that they cause.

It is also of paramount importance to raise awareness of hazards, develop possible actions, procedures, and measures to curb the growing number of increasingly devastating events, and reduce vulnerability; and for that there are no borders.

It is something to bear in mind that natural hazards occur in all parts of the world across different time and area scales, although some regions are more vulnerable to certain hazards than others. Earthquakes, tsunamis, flash floods, landslides, and avalanches are short-lived, violent events, affecting in general relatively small regions. Others, such as prolonged rainfall, lead to floods lasting for weeks or months. Still others, such as droughts, develop slowly, but can affect entire countries for months or even years. In addition, a single-type disaster may develop into a compound disaster, as may be the case under extreme continuous rainfall conditions, for example.

According to the European Environment Agency (EEA) Technical Report No. 13/2010, between 1998 and 2009 a total of 928 natural hazards and technological accidents recorded in Europe caused nearly 100,000 fatalities and, overall, a loss of about EUR 150 billion in the 32 EEA member countries.

Based on data from the Swisse Re Institute (http://www.sigma-explorer.com/) on global disasters from 1970 to 2017, collected in May 2018, the following graphs show the increase in the number of events and growth in economic loss. It seems clear from these trends that the world should prepare for greater losses in the future.

In addition to the increase in the number of disasters and economic loss, the growing trend in greenhouse gas emissions (to say nothing of its current value) and the consequent increase in the global temperature of our planet make it difficult to reverse the trends shown in those graphs, as many studies have shown. We must also keep in mind that human livelihoods will be affected by the chain effects of climate change, which will inevitably lead to irreversible conditions of unsustainability, especially in the second half of this century.

Therefore, on the one hand, it is urgent and essential to predict, plan, and reduce disaster risks to more effectively protect people, communities, and countries, as well as people's livelihoods, health, cultural heritage, socioeconomic assets, and ecosystems, and thus strengthen their resilience.
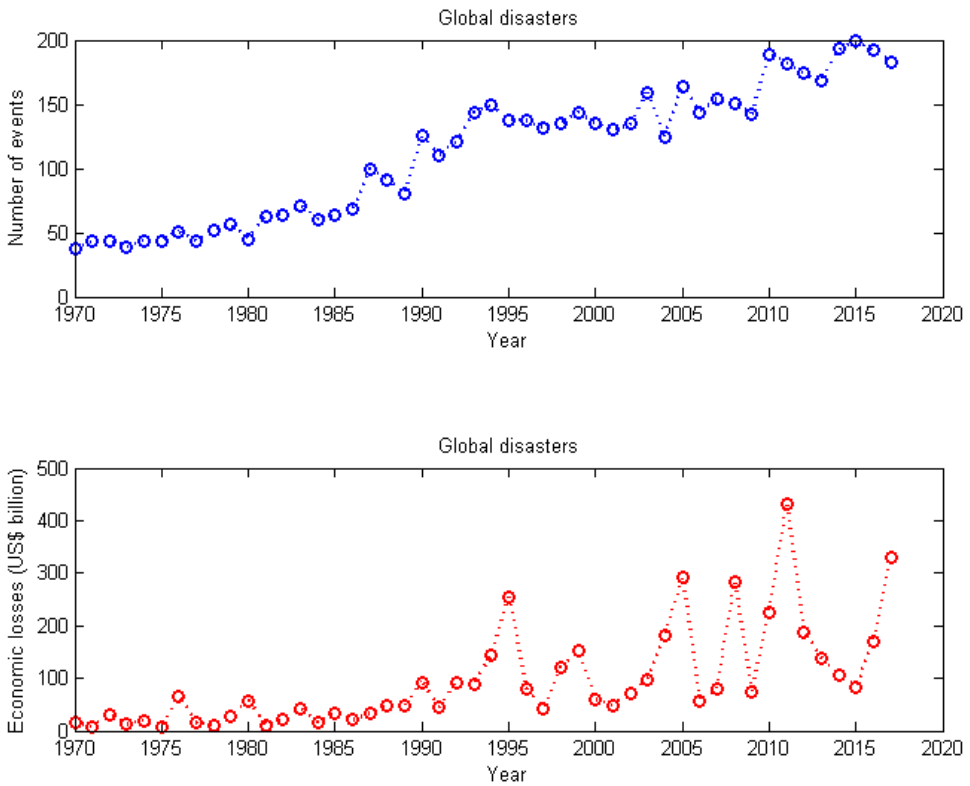
Global Disasters: Number of events and economic losses recorded between 1970 and 2017 (data from the Swisse Re Institute, May 2018).

On the other hand, it is important to promote the incorporation of knowledge about disaster risk, including prevention, mitigation, preparedness, response, recovery, and rehabilitation, into formal and non-formal education, civic education at all levels, and vocational training.

It is recognized that effective disaster risk management contributes to sustainable development. However, it should be noted that disasters can disproportionately affect the least developed countries, in particular Small Island Developing States because of their specific vulnerabilities. The effects of disasters, some of which have increased in intensity and been exacerbated by ongoing climate change, hinder progress towards sustainable development.

To be effective, particularly in less-prepared countries, policies and practices for disaster risk management must take local specificities into account and be based on a clear understanding of risks with respect to vulnerability, capacity, exposure of people and assets, risk characterization, and environmental sustainability.

It is worth recalling that the outcome of the United Nations Conference on Sustainable Development 2012, "The Future We Want," was a call for disaster risk reduction issues and increased disaster resilience to be addressed with a renewed sense of urgency in the context of sustainable development.

However, while some progress has been made towards increasing resilience and reducing loss and damage, a substantial reduction in disaster risk requires perseverance and persistence, with a more explicit focus on people and their livelihoods, and regular monitoring.

Preventing new disaster risks and reducing existing disaster risks through the implementation of integrated economic, structural, legal, social, cultural, educational, environmental, technological, political, and institutional measures will contribute to:

- the prevention and reduction of exposure to hazards and vulnerability to disasters;
- an increase in readiness for response and recovery, and thus an increase in resilience.

This book presents case studies and discusses concepts, methods, and techniques to assess risks and vulnerabilities relating to a wide range of natural events: floods, droughts, avalanches, rockslides, landslides, tsunamis, earthquakes, and volcanoes. Selected chapters, which were identified as offering meaningful information and scientific knowledge, underwent a rigorous review process.

The book consists of nine chapters: five on flood events addressing vulnerabilities, risk assessments, impacts, sensitivity analyses, and mitigation measures, two on climate change and reconstruction of natural hazard events such as avalanches and rockslides, and two devoted to tsunamis and volcanoes. All chapters contribute relevant information and useful content for scientists and other readers interested in possible measures to protect people, property, and economic activities. The lack of action and ineffectiveness of measures implemented to contain the vulnerabilities and risks of natural hazards worldwide are also addressed.

I believe this book comprises material of sufficient quality and quantity to make it a reference document in the field of natural hazards

Acknowledgments

I would like to thank all collaborators who directly or indirectly helped to set up this project, in particular the invited referees and my Publishing Process Managers, Ms. Renata Sliva and Ms. Kristina Jurdana, and my Author Service Manager, Ms. Marijana Francetic, for the opportunity to work with them.

José Simão Antunes do Carmo
University of Coimbra
Coimbra, Portugal

Flood Events: Vulnerabilities and Risk Assessments

Vulnerability, Urban Design and Resilience Management

Bruno Barroca

Additional information is available at the end of the chapter

Abstract

After 30 years without any serious flooding, and over half a century without any major floods (the river Seine's last "important" flooding in Paris took place in January 1955), the 2016 event questions our capacity to evaluate the flood hazard and its impacts. For the Ile-de-France region, the hazard occurred outside defined periods of vigilance, as a result of heavy rains downstream of the main protection structures formed by reservoirs. For this reason, these large protection works only had a very moderate influence on the event. Management of the 2016 event has been analysed on the basis of local measures whose effectiveness varied depending on the context. Among the positive lessons to be drawn, the 2016 floods revealed the high level of resilience of the Matra district in Romorantin. This resilient district, which has high urban qualities, has shown that, in the French regulatory context, flood risks can be treated effectively by appropriate development projects.

Keywords: urban resilience, urban design, flood, vulnerability, Romorantin, Matra district, critical infrastructure

1. Introduction

In both civil society and scientific fields, the frequency with which the term "resilience" is used has increased dramatically since 2005 [1, 2] in discourses on climate change, natural risk management and urban and territorial development. Etymologically, the word "resilience" comes from the Latin "resilio, resilire," which means taking a step backward and having the ability to restart. Coming from fields as varied as psychology, ecology and materials sciences, it has also been adopted by disciplines such as economics, information technology, and so on

with varied meanings revealing not only polysemous wealth but also many contradictions [3]. Currently, the field of resilience covers a great deal more than just post-disaster questions; resilience applies to all aspects of temporality and the actions related to risk management.

For this reason, if the term of resilience has invaded the risk management landscape, as far as urban floods are concerned, this gives rise to two complementary dynamics: on the one hand, "adaptation" by local strategies that integrate flood risks for sites in urban development projects, and, on the other hand, "resistance" by means of protection strategies based on so-called structural measures (anti-flood walls, dikes, dams) aimed at reducing flood risks in urban areas.

This chapter reviews the floods that affected France in June 2016. It analyses national and regional strategies. The chapter also presents a resilient local experience that has shown all its effectiveness during the flood period. The singularity of the hydrological situation and flood prevention in the Ile-de-France region implemented by development work are covered in Sections 2.1 and 2.2. Section 2.3 focuses on the limits of this flood-prevention strategy and reveals its impacts and effects. In Section 2.4, positive elements are highlighted, including innovative experiences for adapting urban forms and local strategies for resilient development.

2. Urban vulnerability and local resilience design

2.1. France in the face of flooding

In France at present, flood risks cost an average of 250 million euros per year or 80% of the total cost of damage attributable to natural hazards. One "commune" in three is concerned, including some 300 major towns and cities. A total of 17.1 million people reside in "approximate potential flood areas" and are exposed to the various consequences of overflow floods, including 16.8 million in mainland France [4]. Regarding coastlines, which are undergoing considerable urban growth, 1.4 million inhabitants are exposed to risks of marine submersion (without taking account of seasonal populations), and more than 20% of them live in single-floor buildings.

It is surprising to see such sizable and ever-increasing stakes at issue in flood zones because, after decades of strategy for protecting land against flooding that was applied until the 1980s, flood risk in new developments has only been taken into account since the mid-1990s mainly through Flood Risk Management Plans (FRMPs). FRMP planning regulations are compulsory for all urban planning documents. On the one hand, FRMP comprise a study of the hazard that uses the largest historical flood known as a reference if it is at least a 100-year flood, or a model of a 100-year hazard, which is the most common place solution. On the other hand, FRMPs categorise issues affected by the hazard, an operation defined by national guidelines. In fact, when compared, FRMP offer different solutions for grouping issues depending on the territories concerned, either by their economic damage potential or by the danger levels for large numbers of populations, or by vital networks concerned, and so on [5]. The FRMP regulatory map is the result of a correlation of maps covering hazards and major issues. It indicates risk areas ranging from low, medium and high to very high levels (very high being associated with 100-year events). Regulations are also created per zone. They specify any

constraints liable to prohibit new constructions (homes, services, shops, equipment …) or make recommendations and exclude certain functions (bans on homes or establishments open to the public for example).

Generally, recommendations indicate the super-elevation of occupied levels and hydraulic transparency (the ability not to block the water flow). Despite the many criticisms concerning the elaboration of FRMP [6], the opacity of technical selection stages and expert negotiation processes [7], FRMP regulations impose significant constraints on local planning. Faced with these constraints, which are difficult to accept locally, especially when the effectiveness of FRMPs is regularly challenged, other approaches have come into being, born by the will to live with water and to integrate risk not in terms of controlling the use of land, but in terms of regional planning and organisation aspects [8]. The increasing use of the term "resilience" is part of this shift, and government authorities are now looking for ways for taking better account of resilience in specific regions. In 2015 [9] and 2016, the Ministries of Housing and Ecology even launched a Grand Prix for urban development on building land liable to be flooded. In terms of the regulations for this prize, the ministries want to promote "urban development or […] buildings designed for undergoing frequent or rare floods and which are respectful of urban, environmental and heritage constraints in areas with low to medium hazard levels where building operations have not been prohibited "[10].

2.2. How does the Ile de France area protect itself?

With nearly 500 km^2 of its area flooded in the event of a 100-year flood, large areas of the Île-de-France region are likely to undergo flooding for exceptionally long periods (12 days of rising water levels and 5 weeks of receding water levels in 1910). Ninety-four per cent of the flood zones in Paris and neighbouring departments are already built-up areas [11].

The increase in the number of homes in these flood-prone urban areas more particularly stems from demographic pressure that is reflected just as much in plots exposed to flood risks as elsewhere [12]. In the last few decades, departments of the Ile-de-France region have built largely in flood-prone areas. The Val-de-Marne department, more particularly prone to flooding by the river Seine and its tributary, the Marne, is one of the three departments that stand out on national levels for the largest number of constructions they have in flood-prone zones. In this respect, over 8000 homes were built between 1999 and 2006. Before 1999, the Val-de-Marne department already had a large number of homes built in flood zones. The result of these phenomena is an increase in exposure not only to extreme events, but also to events that were considered in the past as being common place.

Until the beginning of the twentieth century, there were no major protection works in the Paris region and only local measures and suitably designed constructions made any form of risk management possible. At the beginning of the twentieth century, works were carried out on improving the flow of the river Seine by digging out the river bed and limiting obstacles where it crossed Paris.

Four reservoirs, created in the Yonne valley for diverting the Seine, Marne and Aube rivers (tributaries of the Seine upstream of Paris) were also built between 1950 and 1990 to limit their high flows.

These reservoirs serve a dual purpose, first to reduce the effects of flooding by the river Seine and its main tributaries, and second to replenish low-water levels so that they remain sufficiently high for maintaining regular water supplies to downstream regions, including the Paris area. These four reservoirs can store and release up to 830 million cubic meters of water. In this way, each one of them can influence the flow of the river Seine in the Ile-de-France region and further downstream. Locally, structures in the form of dikes or small walls along water courses complete the reservoirs' action by protecting land against so-called "frequent" flooding in the departments around Paris and "medium" flooding" in Paris [13]. Unfortunately, these walls sometimes suffer from lack of maintenance and are in poor condition or even have gaps in them.

Climate change in the Ile-de-France area is likely to lead to more extreme and more frequent flood and low-water situations in the coming years, both of which are liable to cause malfunctions in all urban networks [14], especially for critical infrastructures (**Figure 1**). Critical infrastructures form the backbone of modern societies [15], and the vulnerability of critical infrastructures will become a major issue in urban risk management [16] as and when it generates collective vulnerability due to relationships with and between these infrastructures. Interdependencies can cause cascade-effect failures because the failure of one infrastructure can directly or indirectly affect other infrastructures and thus impact large geographic areas [17]. The study of natural hazards applied to critical infrastructures is currently focused on notions of vulnerability, i.e., "the propensity of exposed elements such as physical or capital assets, as well as human beings and their livelihoods, to experience harm and suffer damage and loss when impacted by single or compound hazard events" [18].

For the Ile de France region, the economic stakes in Flood Risk Territory (100-year flooding) concern 107,200 companies (13.2% of all companies) and 745,900 jobs (18.4% of all jobs in the region). However, we must also add 119,350 companies and 636,100 jobs located in areas where the electricity grid is fragile, i.e., areas liable to be deprived of electricity in case of a 100-year flood (**Figure 1**).

Under these circumstances, a total of 226,550 establishments (28%) and 1.38 million jobs (34.1%) are liable to be affected by the direct consequences of flooding. It must be noted that more than half of the companies deprived of electricity are located outside the flood zone [19]. Power cuts will affect 1.5 million people. A total of 140 km of public transport networks (Metro, RER, Train) will be impacted as well as three major railway stations. Many bridges and five motorways will be cut and 5 million Ile-de-France inhabitants will be affected by drinking water problems, as well as 295 schools [20].

Relatively recent awareness of the numerous interactions fostered between each other by networks, infrastructures and urban services recognised as being critical, essential or vital has totally modified methods of risk management for urban environments. Current research in urban engineering leads to a more systemic approach that takes shape via the concept of resilience and gives rise to studies of critical infrastructures on more local levels [21].

2.3. The 2016 floods, a hazard that reveals the limits of the protection system

Flooding caused by tributaries in the central Seine and Loire basins, which, for the most part, took place between May 25 and June 6, 2016, has brought the question of summer floods
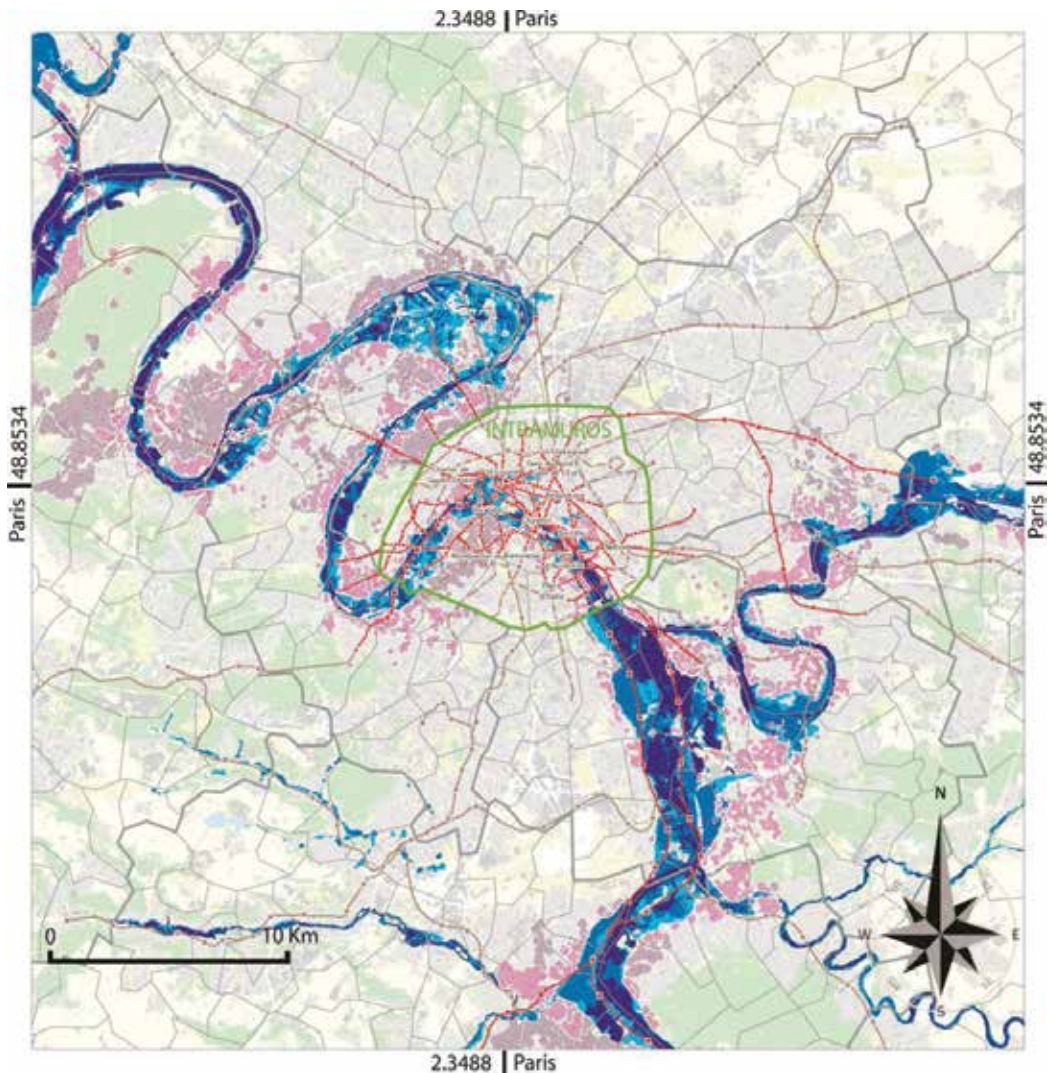
Figure 1. The impact of major flooding on the electricity network. Blue areas represent flooding, and pink areas represent electricity grid fragility (areas without any power connections during a 100-year flood). Source IAU and Ludovic Faytre.

back to the forefront. Temporal and spatial aspects were abnormal. In the case in question, flooding occurred exceptionally in late spring, while management of flood crises in the Seine basin—and more particularly in the Ile-de-France area—is centred on the probability of major flooding occurring during the winter, a period during which reservoirs' efficiency is the maximum, as regulations require them to be almost empty at this time of the year (December–January), unlike the spring when they are filled up for anticipating low-water levels during the summer. As stated before, reservoirs have a dual function inasmuch as they protect against flooding but they also replenish low-water levels during dry spells. This dual function considerably limited the role played by reservoirs[1] during the 2016 floods. A year

---

[1]Reservoirs only enabled water-levels in Paris to be lowered by a few centimetres at the most.
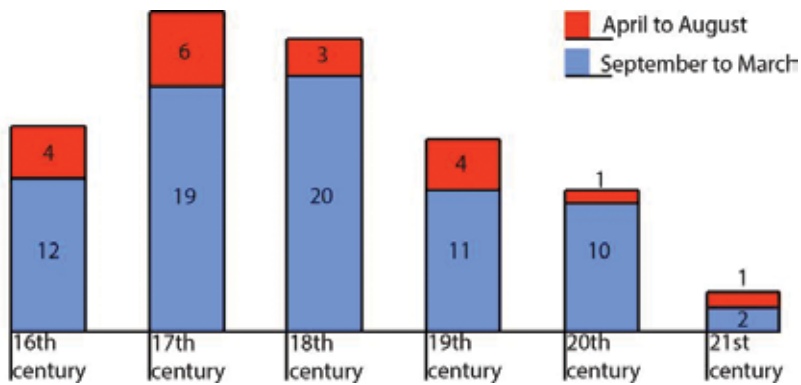
Figure 2. The number of floods in Paris between April and August (1500–2016). According to National Archives, H2 1778–1880. Register of deliberations drawn up by the Bureau of the City of Paris. Source [22].

later, in early June 2017, the reservoirs even needed to release water to maintain the flow of the river Seine, which was very low at the time. Contrary to June 2016, the release of water from the reservoirs for replenishing low flow-levels in June 2017 constituted a record of precociousness. As far as flooding is concerned, an analysis of the events that have occurred over the last four centuries shows that, with just a few exceptions, very large floods (above 7 m in Paris-Austerlitz) most often occur between December and January. This forms an initial limit for reducing spring flood levels because reservoirs are full at the time so that they can carry out their low-water replenishment mission between June and November. Three years earlier, during the period of May 7–10, 2013, flood levels had completely saturated the reservoirs[2]. Although they are less frequent than winter floods, summer floods are not uncommon, as shown in **Figure 2**. However, they do not seem to attain either the frequency or the heights of the great winter floods. Even so, the Seine basin hydrological manual, written in 1884, enables us to relativize this assertion as the book indicates that at least two summer floods over 7 m high have occurred in Paris since 1650 (June 1693: 7.55 m and June 1697: 7.35 m) together with two others that were close to 6 meters, in May 1836 and September 1866 [22].

The second singularity was due to the location of flood-generating rainfalls, which mainly occurred downstream of the reservoirs and upstream of Paris. The 2016 event was exceptional in local terms with accumulated rainfalls of 100–150 mm over the week of 28/05/2016 to 3/06/2016, which led to significant increases in water levels in the river Seine's tributaries (especially the river Loing) as well as those of the river Loire. This exceptional meteorological situation, which caused the Seine to flood due to heavy rain downstream of the reservoirs, made it impossible for them to reduce flood water levels. This phenomenon forms the second limit to a risk management system that is based on the use of reservoirs.

Assessment forecasts on the impacts made by this type of flooding carried out a few years earlier in 2014 also illustrated significant limits because reality was very different from

_____

[2]An exceptional section comprised of reservoirs (excepted for the Pannecière reservoir which was undergoing renovation works at the time.

economic forecasts. In fact, following the flood, damage to insured property amounted to approximately 1.2–1.3 billion euros, but, according to the insurers, these figures needed to be doubled to take uninsured damage (such as assets belonging to the French state) into account. The real amount of damage was certainly between 3.6 and 3.9 billion euros for the Seine and Loire basins, while the heart of the Greater Paris area was relatively spared by surface water overflows [22]. Studies made over recent years did not provide for such high amounts of damage for this type of flooding [11]. Although they caused a great deal of damage, the May–June 2016 floods cannot be considered as constituting major floods caused by the river Seine, (a 20-year flood-level at Paris-Austerlitz), while this was the case for some of its tributaries, such as the river Loing (higher than the 100-year level), the Yvette (the 50-year level) or the rivers Almont and Yerres further upstream [22].

All things said and done, flood levels caused by the river Seine were relatively modest in Paris *intramuros* (the physical space outlined by the green line in **Figure 1**) and in the most built-up areas of the Ile-de-France metropolis. The maximum water level on the Paris-Austerlitz scale was 6.10 m, while the 1910 level (the so-called 100-year flood) was at 8.62 m. However, the actual volumes for the 6 m 10 water level, which did not over-run local protections, are comparable to those envisaged during studies published in 2014 for flood-levels 7 m 30 high[3]- or a flood level 1 m20 higher than the event of June 2016!

2.4. Resilience assessed by experience: The example of Romorantin

Less than a month after the floods, on June 27, 2016, the Minister of Environment, Energy and the Sea, and the Minister of the Interior asked the General Council for the Environment and Sustainable Development (CGEDD in France) and the General Inspectorate of Public Administration (IGA) to conduct a feedback mission. The report [23] that followed this mission came back on the points presented above, and it proposed a series of recommendations on crisis management, evacuation of inhabitants, a return to normal, and so on. Two recommendations strongly influence urban planning aspects. In this respect, it was stated that "to take account of the fact that a policy of prescriptive zoning does not cover all the realities of exposure to risk, and that, on the other hand, manufacturers need relatively simple and reproducible rules to be able to industrialize construction processes, the mission proposes that rules for building be drawn up in the form of 'Unified Technical Documents (UTD),' which would more especially make buildings more resilient and lead to a faster return to normal."

Without naming it, this recommendation introduces the concept of resilience, as it concerns "living in the city with risk, understanding, and knowledge." Prescriptive zoning follows a completely reversed logical process, which consists of separating building land from flood areas. A second recommendation specifies the importance of local circumstances: "[In plans and strategy it is necessary] to introduce the need to explain protection objectives, quantified in terms of frequency and adapted to local circumstances. To differentiate these objectives and the measures that respond to them for the protection of persons, goods, and economic activities." The shift from a hazard control approach to an integrated approach to urban planning

---

[3]7.30 m is the maximum level of the January 1924 flood recorded at the Paris-Austerlitz station.

and construction is emphasised by this report and its ensuing recommendations. This is consistent with what is gradually being initiated in Europe with the construction of resilient districts. For France, current regulations strongly limit "urban innovations" of this type, but the stakes in Île-de-France, a particularly vulnerable region, encourage changes to be made to the current framework. It is not a question of reducing risks by physical protections in the form of dikes whose effectiveness is highly questionable, but of reducing risks by integrating watercourses into the urban system. This will create a risk management system that works on the aspects of vulnerability and resilience within urban forms and urban programming and which is more especially applicable on the scale of urban planning operations [24, 25]. The influence of urban design on risk is therefore fundamental, and urban design is sometimes studied on the basis of moderate to extreme risks [26]. Over recent years, resilience through urban design has been highlighted in New York by the "rebuild by design" operation. In Europe, redevelopment of the old German ports of Hafencity in Hamburg, Zollhafen in Mainz or Westhafen in Frankfurt is also evident of the potential for implementing development projects in floodplains [27]. Even though France is not deeply involved in these approaches, the 2016 floods have revealed a little-known district located in Romorantin which has undergone extreme local flooding without damage (**Figure 3**).

The district is located on the banks of a tributary of the river Cher (in the Loire basin) and is the result of recent development of an old industrial area closed in 2006. In June 2016, the district was flooded to levels well beyond what had been projected by models and what regulations required. The industrial zone, mainly comprised of the old Matra factory, was located close to the town centre on a large floodplain shared with various old abandoned industrial

Figure 3. Romorantin, in the foreground marked by a red dotted line, the "Matra" district flooded in June 2016.

buildings. The global project was designed by the architect, teacher and researcher Eric Daniel Lacombe from the EDL architectural firm, which was awarded the Grand Prix for architecture in constructible zone floodplains in 2015 [9]. The project defined risk adaptation objectives by proposing building foundations that served to channel floodwater, creating a situation where road vehicles were not washed away and causing serious damage as is unfortunately common, and with accesses to buildings for pedestrians, even disabled, which remain accessible during flood periods. Design work maintained architectural objectives at flood levels 50 cm higher than those imposed by regulations. As a result, the newly built district complies with FRMP recommendations on the height of flooring and hydraulic transparency and has established other, even more demanding restrictions (**Figures 4** and **5**). If water levels exceed FRMP models by more than 50 cm, the area has been architecturally designed for enabling rescue boats to access buildings without difficulty. In this way, urban design has developed resilience by implementing sustainable urban development measures integrating risk at the heart of development projects over and above existing scenarios. Therefore, contrary to an elaborate form of protection applicable to just one water-level threshold, the district's design consisted of studying to what level of urban, technical, morphological, programmatic and social configurations its resilience could be imagined for covering frequent to very rare hazard events.

Figure 4. Romorantin, "Matra" district in non-flood conditions, pedestrian paths in black and old factories in light grey. Source EDL - Eric Daniel Lacombe.

Figure 5. Romorantin, a study of hydraulic transparency during a 100-year flood in "Matra" district (the flow of water through the district marked in red). Source EDL - Eric Daniel Lacombe.

The new district also stands out for the wide range of architectural solutions it proposes for foundation supports. Old buildings that have been kept have deep hard stone foundations that have already withstood a number of flood episodes, and new collective buildings are raised off the ground and protected from rises in water levels by long "floodable" parking lots that form a water retaining channel. Detached houses are also raised off the ground on piles which enable water to pass through without restriction. In this way, we can imagine the future movement of any water liable to invade the district by observing the meeting points between facades and ground: the protective dike on the boundaries to the north and west, the water retaining channel in the centre and the vertical piles to the south. It is certainly simpler to understand this by walking through the district during flood periods, but which is undoubtedly easier to do outside flood periods. Inhabitants of the town can cross the area by two parallel ways, one alongside the public square to the north, and the other skirting the detached homes to the south. Pedestrians and residents in the district have pathways between homes and the garden. Each of these ways offers a different perspective of the whole project, and they all entwine with the watercourse in different ways depending on the frequency of rainfalls [28]. To the south, the route crosses buildings on piles and runs along islands with large trees heralding the proximity of the river. The results of any rise in water levels are easy to imagine. The situation is

Figure 6. View from the public garden of Matra district (in Romorantin) without flood.

different on the road to the north and in the public square, where only one residential building has a special construction system giving the impression that it "floats" above the ground. We can most certainly visit these routes and not pay any attention to this element of mystery, but, once it has been discovered, it invites us to imagine the route taken by water under flood conditions, to reflect on the height of the lowest balconies in private homes, to look at the marks kept by the town on the level of the last major flood and the future of the plants in the public garden during any forthcoming flood. The architectural project aims at making the answers provided by inhabitants to these questions become supports for the identity of the district and foster the creation of a new culture of relationships between the town and its river.

Just as the district opens at the west onto the river, here too the concern for removing any limits is combined with the refusal to impose any separation of the urban district from nature. Different water-inspired metaphors are integrated into architectural design with "ripples" on the facades and sinusoids formed by the eaves of roofs, and where raised ground floors are reached via sloping wooden footbridges (that look like pontoons). These floating paths lead to pontoon terraces offering just as many opportunities for looking over the flood gardens (**Figure 6**), which are transformed by successive passages of water [28]. In this way, the architectural, urban and landscape make-up creates a dialogue with water's regular or exceptional presence on the site.

3. Conclusion

Although the Ile de France region has managed to create structures for limiting the most frequent floods and droughts over the last 60 years, it is clear that large structures show

their limitations in the face of less frequent events. As such, the 2016 flood was a remarkable indicator of dysfunctions, whereas the climatic event was not very intense in itself. Various options exist for coping with more significant events, and creating an additional storage facility in the area of La Bassée is part of this objective. If the project is realised, storage capacity will be increased, but by themselves, these works will not be capable of protecting downstream areas from flood risks. The French version of the 2007 Flood Directive [13] gives more prominence to local flood risk management strategies and resilience dynamics are intensifying. The Ile de France region has developed a strategy [20] on a scale corresponding to the size of the high-risk area. The strategy has eight targets, one of which (Target 6) deals specifically with "Resilient Neighbourhood Design." Moreover, since December 2014, Paris has been part of the global network of resilient cities[4], an initiative launched by the Rockefeller Foundation and it has also set up a multi-hazard resilience strategy [29].

The case study presented in this chapter deals with a sector subject to slow floods and proves the existence of a capacity to manage exceptional events at local levels. From a historical point of view, this is all the more interesting because the possibility exists, very credible in view of the great floods of 1846, 1856 and 1866 [23], 1910, and so on that most of the major French rivers may be in spate simultaneously and that many large urban centres can be flooded in a matter of weeks. It shows that it is possible to manage floods effectively by means of urban design, even floods that are very significant at local levels, without losing qualities of architecture and urban planning. By means of its local response, Romorantin has illustrated that the examples usually published on resilient neighbourhoods can also be conceived in economically less privileged areas and within the framework of French regulations. Will architects, town planners, and decision-makers know how to take advantage of current evolutions and will this experience to innovate towards urban forms of resilience be capable of meeting all the very significant challenges seen during the 2016 floods?

Author details

Bruno Barroca[1,2]*

*Address all correspondence to: bruno.barroca@univ-mlv.fr

1 National Center for Scientific Research - Research Centre on Technologies, Territories and Societies (LATTS), Marne-la-Vallée, France

2 Paris-Est University –Urban engineering, Environment and Housing (Lab'Urba), Marne-la-Vallée, France

---

[4] In this network, urban resilience is defined by "the capacity of persons, communities, institutions, companies and systems to survive, adapt themselves and grow, irrespective of the types of chronic tensions and acute crises they may undergo."

References

[1] Serre D, Barroca B. Preface "natural hazard resilient cities". Natural Hazards and Earth System Sciences. 2013;**13**(10):2675-2678

[2] Barroca B, Di Nardo M, Mboumoua I. De la vulnérabilité à la résilience: Mutation ou bouleversement? EchoGéo. 2013;(24) [En ligne]

[3] Reghezza-Zitt M, Rufat S. Resilience imperative. In: R.a.D. Uncertainty. 1st ed. Elsevier & ISTE Press; 2015

[4] Ministère de l'écologie du développement durable et de l'énergie, Première évaluation nationale des risques d'inondation; 2012. p. 15

[5] Gralepois M, Rode S. Flood resilient city and urban distortion. Urban Risks. 14 December 2017;**1**(2). Available at : DOI: 10.21494/ISTE.OP.2018.0205 [Accessed 12/06/2018]

[6] Hubert G, de Vanssay B. Le risque d'inondation et la cartographie réglementaire. Analyse de l'efficacité, des impacts et de l'appropriation locale de la politique de prévention. In: Programme "Evaluation et Prise en compte des Risques naturels et technologiques". Paris: Ministère de l'Ecologie et du Développement Durable; 2005. p. 188

[7] Hubert G, Reliant C. Cartographie réglementaire du risque d'inondation: Décision autoritaire ou négociée? Annales des ponts et chaussées. La gestion des risques naturels; 2003. pp. 24-31

[8] Daluzeau J, Gralepois M, Oger C. La résilience face à la normativité et la solidarité es territoires. EchoGéo [En ligne]. 2013;**24**:22

[9] Ministère de l'environnement de l'énergie et de la mer and Ministère du logement et de l'habitat durable, Comment mieux bâtir en terrains inondables constructibles ? In: Grand prix d'aménagement/Projets 2015. France: La défense; 2016. p. 102

[10] Ministère de l'environnement de l'énergie et de la mer and Ministère du logement et de l'habitat durable. Comment mieux bâtir en terrains inondables constructibles - Réglement. 2015; Available from: https://www.ecologique-solidaire.gouv.fr/sites/default/files/20160930_GPATIC_Reglement.pdf

[11] OCDE. Étude de l'OCDE sur la gestion des risques d'inondation : la Seine en Île-de-France 2014. Paris: OECD Publishing; 2014

[12] Commissariat général au développement durable, S.d.l.o.e.d.s., Croissance du nombre de logements en zones inondables, O.e. statisitiques, Editor. Paris; 2009. p. 4

[13] European Commission. Directive 2007/60/EC of the European Parliament and of the council on the assessment and management of flood risks. Official Journal of the European Union. 2007:8

[14] Serre D, Heinzlef C. Assessing and mapping urban resilience to floods with respect to cascading effects through critical infrastructure networks. International Journal of Disaster Risk Reduction. 2018

[15] Serre D. La ville résiliente aux inondations Méthodes et outils d'évaluation. Vol. 173. Marne-la-Vallée: Université Paris-Est; 2011

[16] Robert B, Morabito L. Réduire la vulnérabilité des infrastructures essentielles. Innovations - Sciences du risque et du danger, ed. TEC&Doc. Lavoisier; 2009

[17] Robert B, Morabito L. Interdependent Critical Infrastructures: From protection towards resilience. West Point, NY, USA: Critical Infrastructure Symposium (TISP); 2013

[18] Birkmann J et al. Framing vulnerability, risk and societal responses: The MOVE framework. Natural Hazards. 2013;**67**(2):193-211

[19] Faytre L. Evaluation des enjeux économiques exposés aux inondations dans le TRI de la Métropole Francilienne. Paris: Institut d'Aménagement et d'Urbanisme - Ile-de-France; 2017. p. 23

[20] Robert S, Montoya B. Stratégie locale de gestion des risques d'inondation TRI. Paris: Métropole francilienne; 2016. p. 79

[21] Serre D et al. Contributing to urban resilience to floods with neighbourhood design: The case of Am Sandtorkai/Dalmannkai in Hamburg. Journal of Flood Risk Management. 2018;**11**(S1):S69-S83

[22] Gache F. Comment la crue modérée de la Seine en mai-juin 2016 réinterroge les politiques franciliennes de gestion des inondations ? In: Barroca B, editor. Quelles stratégies pour quels risques ? La ville en question. Presses des ponts; 2018 (in press). p. 20

[23] Perrin F et al. Inondations de mai et juin 2016 dans les bassins moyens de la Seine et de la Loire - Retour d'expérience. Paris: Ministère de l'Environnement de l'Energie et de la Mer & Ministère de l'Intérieur; 2017. p. 210

[24] Barroca B et al. Considering hazard estimation uncertain in urban resilience strategies. In: Etingoff EBK, editor. Ecological Resilience, Response to Climate Change and Natural Disasters. Apple Academic Press; 2016. pp. 197-220

[25] Barroca B et al. Indicators for identification of urban flooding vulnerability. Natural Hazards and Earth System Sciences. 2006;**6**:553-561

[26] Raven J et al., Urban planning and urban design, in Climate Change and Cities, C. Rosenzweig, et al., Editors. 2018, Cambridge University Press. p. 806 p

[27] Balsells Mondéjar M et al. Analysing urban resilience through alternative stormwater management options: Application of the conceptual spatial decision support system model at the neighbourhood scale. Water Science and Technology. 2013;**68**(11):2448-2457

[28] Lacombe E-D. L'architecture aux risques de l'eau, in Quelles stratégies pour quels risques ? In: Barroca B, editor. La ville en question. (sous presse), Presses des ponts; 2018. p. 22

[29] Ville de Paris, Stratégie de Résilience de Paris. Ville de Paris et 100 resilient cities; 2017. p. 126. Available at: https://api-site-cdn.paris.fr/images/95335. [Accessed 11/06/2018]

Index of Proportional Risk (IRP) Flood-Risk Assessment Model and Comparison to Collected Data

Luca Franzi, Gennaro Bianco,
Alessandro Pezzoli and Angelo Besana

Additional information is available at the end of the chapter

Abstract

After the publication of the flood directive hazard and risk maps, risk assessment and risk evaluation became useful tools to set priorities for flood management and for countermeasure financing. Regione Piemonte, in collaboration with Politecnico di Torino and University of Turin, proposed a procedure for risk assessment (named IRP model, Index of Proportional Risk), already applied in different case studies. The comparison among the obtained results and the collected data on damages recorded during the recent 2016 flood in Piemonte region showed the effectiveness of the IRP procedure for the quantitative assessment of direct damages. The IRP model can also be usefully applied to the revision and the updating of flood directive risk maps and to assess the cost/benefit ratio of the designed countermeasures (National Repository for Soil defense (Re.N.Di.S.) procedure).

Keywords: European flood directive, flood risk, vulnerability, flood mapping, flood-risk maps, flood damage

1. Introduction

In 2007, with the European Flood Directive (EFD) [1], legislation came into force, with the aim "*to reduce the risk of adverse consequences from flooding, especially for human health and life; the environment; cultural heritage; economic activity; and infrastructure.*"

The EFD has been implemented in the Italian Legislation with the Legislative Decree 49/2010, taking into account the applicable national legislation.

The concept of flood risk in the EFD, that is,

"'flood risk' means the combination of the probability of a flood event and of the potential adverse consequences for human health, the environment, cultural heritage and economic activity associated with a flood event".

is similar to that already adopted in the PAI (Hydrogeological Asset Plan), a plan adopted by the Po Basin District Authority (PBDA [2]) in 2001, which aims at assessing and managing natural hazards and risks in the Po watershed basin (Italy). Risk was defined as ([2], p. 190).

"expected value of the damage that the receptors can undergo on average in a predetermined period of time".

therefore implying the concept of damage and of probability of occurrence.

According to PAI, risk can be considered the superposition of the three elements, corresponding to a conceptual formula of this kind:

$$R = E x V x H \tag{1}$$

where E is the exposure, V is the Vulnerability, and H is the hazard.

The aim of PAI was to express *relative* comparison of risks on the Po watershed basin, highlighting, in relative terms, the distribution of natural risks on the territory. The flood risk was not quantified in economic terms, but only qualitatively assessed with the use of indicators. The risk was determined through the use and superposition of indicators and aggregated into four classes with increasing value (1 = moderate, 4 = very high); a risk level was associated to each municipality.

Therefore, the risk maps in PAI showed the different classification of municipalities in terms of relative risks.

The presence of PAI on the Italian territory has provided an adequate base, suitably updated, homogenized, and valued, to fulfill the obligations referred to the Article 6 of EFD. Therefore, the hazard and flood-risk maps have been obtained starting from those contained in PAI and in accordance with the "Operational guidelines" issued by the Ministry for the Environment, Land and Sea (MATTM) [3], with the contribution of ISPRA (*Superior Institute for Protection and Environmental Research)*, of the National Basin Authorities and State Regions technical board.

The EFD requirements about risk mapping forced public administration to find different methodologies to assess and map risk on the territory. Actually, the EFD, Article 5, forces Member state to *"identify those areas for which … potential significant flood risks exist or might be considered likely to occur,"* and risk maps have to be referred to the scale of areas at risk. Therefore, the municipality scale of PAI had to be changed according to the EFD requirements.

Italian Ministry fulfilled the requirements of the flood directive, as far as the following steps are concerned: (i) preliminary assessment, (ii) hazard and flood-risk maps, and (ii) management plans of flood risk (PGRA).

In Po river basin, flood maps and risk management plan came into force with the acts of the General Secretary decree (n.122/2014) and of the decree of the President of the Ministry Council (DPCM 26.10.2016), respectively.

As far as flood hazard assessment is concerned, the item has been widely described in other papers and is here summarized.

2. Risk assessment in land-use planning (Po basin)

The "Operational guidelines" issued by MATTM explain the contents of EFD and highlight the difficulties in risk mapping, that is ([3], p. 20),

"By considering the difficulties in quantifying parameters and the unavailability of reliable data of sufficient detail (…) it is reasonable to adopt, at least in this first phase, simplified methodological criteria for an assessment and representation of risk".

and, as far as vulnerability is concerned ([3], p. 20),

"Therefore, in this first phase of drawing up the risk maps, we refer to an estimate of the vulnerability … assuming an equal value (vulnerability equal to 1) in the flood prone areas; consequently exposure and potential damage (…) have been considered to be equivalent."

Consequently, damage has been deduced in a simplified way, that is, by associating the categories of exposed receptors to the *potential damage*. In practice, three potential damage classes have been identified: (i) D4—very high potential damage, (ii) D3—high potential damage, (iii) D2—medium potential damage, and (iv) D1—moderate (or null) damage, which are described in **Table 1**.

As a consequence of the damage ranking in four classes, the risk has been assessed by means of a matrix method. Risk categories have been deduced by those proposed by the former decree of the Prime Minister (D.P.C.M. 29.09.98, which contains the guidelines for the adoption of urgent countermeasures against natural hydro-geological risks, regarding hazard assessments).

Damage class	Description of the damage class
D1	(Moderate or null potential damage). It includes areas with no urban or productive settlements; free flow of floods on floodplain is possible.
D2	(Medium potential damage). It includes (i) areas where floods have limited effects on people, on productive activities (agriculture), (ii) secondary infrastructures, and (iii) public green areas.
D3	(Very high potential damage). It includes (i) areas with relevant damages for people and economic system, (ii) areas with relevant communication lines, and (iii) important productive activities.
D4	(Very high potential damage). It includes areas which can be affected by floods with serious risks for human life, relevant damages to economic activities, and/or environmental disasters.

Table 1. List of the classes of damage, according to the act of MATTM ([3], p. 24).
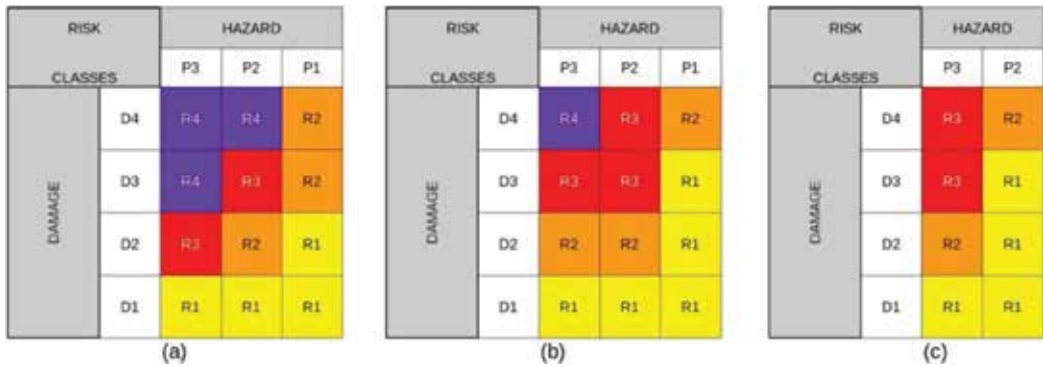
Figure 1. The matrices adopted in PGRA, by Po basin District Authority. Hazard classes P1, P2, and P3 refer to the return period indicated in EFD (P1 for T = 20–50; P2 for T = 100–200; P3 for T = 500).

As far as the Po basin District Authority ([4], p. 17) is concerned, the risk is assessed by the combination of the damage and hazard classes, through a matrix approach. The rows show the damage classes and the columns the hazard levels, that is, the probability of flood occurrence. The implementation of this matrix allowed associating a risk class to each exposed element (receptor).

To distinguish the different impacts in terms of human life and anthropic activities risk, three different matrices were used, each for a different flooding process: (i) first matrix (a) in **Figure 1** refers to flooding in main rivers, (ii) second matrix (b) to lake flooding and Apennines rivers, and (iii) third matrix (c) refers to plane secondary rivers.

On the basis of hazard and flood-risk maps, the District Authorities prearrange the flood-risk management plans (PGRA), coordinated at the level of river basin district.

3. Limitations in the approach to risk and vulnerability assessment

Risk matrices approaches are widely used by public administration as a basis for risk management decisions, with applications [5] from terrorism risk analysis, to highway construction project management, to dam and levee safety and climate change risk management. Risk matrices are widely used for risk reporting, risk prioritization, and risk monitoring [6].

On one hand, they are easy to use and intuitive, and they are often defended as a practical way to flood-risk management, especially when quantitative information is scarce or nonexistent [7]. On the other hand, their theoretical basis is superficial and their employ in decision making is hard, especially when different technical solutions for flood-risk management have to be compared to each other.

At present state, it is sustained that "*the flood directive asks for vulnerability parameters only. The risk as such is not explicitly requested, but implicitly the notion of risk is an integrated part*" (*Handbook on good practices for flood mapping in Europe* [8]). In other terms, the EFD does not

require a quantitative estimation of risk. The cited handbook addresses the map of assets at risk (i.e., the distribution of population, vulnerable groups, and buildings at risk) more than to "*risk maps.*"

The same *Floods Directive Reporting Schemas* [9], which should be followed by countries in reporting to European Commission, allow different methods for reporting, and quantitative estimation is optional. Actually, according to the reporting schema, damage can be indicated (i) as a range, (ii) as a percentage of the total GDP for the flood event, (iii) by classes (Insignificant, Low, Medium, High, Very high), or (iv) by means of other numerical measure indicative of the degree of (potentially) adverse consequences, leaving a wide choice for implementation.

Therefore, the report of quantitative damage is not compulsory, qualitative estimations are widespread, even if the risk formula, which implies the quantification of risk, is often reported in official documents (see [9], p.23).

There are several practical problems with matrix approach, either with respect to the guidelines of the EFD or theoretical.

First, the scales shown in the matrix are ordinal (i.e., rank-ordered); consequently, mathematical operations with ordinal scales are meaningless.

Second, the risk matrix generally shows only probability and consequence, and rank risks by that pair of measures; vulnerability is implicitly considered in the matrix or set equal to a constant value.

Third, communication to people may reveal to be captious; for example, the damage in D4 class in **Table 1** is not necessarily twice the damage of D2 class, in spite of the damage class indication.

Fourth, it is questionable if risk matrices actually improve decision making. Cox has been particularly critical of risk matrix and hazard ranking systems, concluding that "*Applying portfolio optimization methods instead of risk prioritization ranking, rating, or scoring methods can achieve greater risk-reduction value for resources spent*" [10].

The present limitations of risk mapping approach adopted in the implementation of EFD can be reviewed and in the next step of "*…reconsideration and updating…*" in the flood directive.

Actually, the *management plans for flood risk (PGRA)* should be periodically reviewed, and if necessary updated, taking into account "*…the likely impacts of climate change on the occurrence of floods*" (EFD, art.14). Italian legislation provides the time limits to review the preliminary flood-risk assessment (before 09/22/2018 and at a later stage, every 6 years), the hazard maps and flood risk (before 22.9.2019 and thereafter every 6 years) as well as the Management Plans (before 22.09.2021 and thereafter every 6 years).

To this aim, ISPRA edited "*Methodological proposal for updating hazard and risk maps for risk mapping*" [11]. The document aims at proposing some approaches, taken from scientific literature, to be implemented in the revision and updating of the flood-risk maps.

On the basis of the proposal of the ISPRA document, a model (named IRP model) has been proposed by public administration in Piemonte region to quantify and evaluate risks, in view of the revision of the flood-risk maps. The model can also be a usable instrument to fulfill the requirements of the Re.N.Di.S. (National Repository for Soil defense) platform, described in the following paragraph.

4. The Re.N.Di.S. platform for planning

Flood damage quantification and assessment is not only a (optional) requirement for the implementation of EFD, but it has recently become a requirement for the evaluation of the projects of countermeasures and for the eligibility of public financing.

Actually, with the recent 2015 decree of the President of the Ministry Council (2015DPCM in the following), a new discipline to evaluate the priority of public financing for flood protection projects came into force in Italy. To set priorities is fundamental when financial resources are scarcer than necessities. Actually, at the moment, the total needs for protection (by considering all the kinds of natural hazards, which are floods, landslides, flash floods, debris flows) amount to about 30G€, by far higher than the resources available at the moment (**Table 2**).

The model for prioritization proposed by the 2015DPCM is based on a score approach.

According to the 2015DPCM, flood defense projects have to be collected into the so-called Re.N.Di.S. procedure, which is a national repository of projects for soil defense. For a given project, either the assessments by public administration, or the level reached by design, or the effectiveness of the designed countermeasures are scored. The Re.N.Di.S. procedure allows to associate a total score to each proposed project, included in the Re.N.Di.S. procedure. The criteria are listed in **Table 3**.

For the sake of simplicity, it can be said that, for a given project of flood protection measures included in the Re.N.Di.S procedure, the priority to financing is based on its total score: the higher is its score, the higher is its ranking and therefore the probability for public financing. As shown in **Table 3**, flood damage evaluation score is relevant with respect to other criteria: if the damage evaluation is given, there is a 10-point score.

	Total number of interventions eligible for financing	Total financing requirements	Public financing requirements
Floods in Italy	3284	15,046.00 M€	13,809.40 M€
Floods in Piemonte	417	1179.20 M€	(not available)
Total*	9397	29,110.00 M€	26,407.90 M€

*The total includes avalanches, soil-slips, coastal erosion, and other natural hazards.

Table 2. Total amount of proposed interventions for risk reduction and financing necessities (taken from [12]).

Criteria contained in the DPCM	Description of the criteria	Min-max score
Priority by public administration	The priority level is expressed by public administration and expressed in three levels. The cost/effectiveness rate should be considered	0–20
Design level (low/medium/high)	Italian laws consider three levels of design. The higher the level, the higher the score	3.3–10
Completion	Higher score for projects that are complementary to other projects	0–10
Directly endangered people	Higher score for a higher number of protected population	0–60
Goods at risk (properties, communication lines, etc.)	Higher score for projects that allow the protection of goods at risk	0–30
Frequency	Higher score if the project allows the protection to more frequent floods	4.2–30
Effectiveness of the project in terms of damage reduction	*The criteria allow a higher score for projects which quantify the effectiveness in terms of damage reduction*	*0—no quantification* *10—damage quantification*
Effectiveness of the project in terms of the reduction of the total number of involved people	*The criteria allow a higher score for projects which allow the reduction of the total number of people involved*	0–30
Compensation and mitigation measures	Presence of compensation and mitigation measures, which can mitigate the effects on environment	0–5

The higher is the total score, the higher is the ranking of the project for public financing.

Table 3. List of the evaluation criteria of the projects, with the respective scores (table taken from the 2015DPCM).

Without a uniform methodology for damage assessment and quantification, the damage assessment and the cost/benefit analysis (upon which also the prioritization of the public administration is based) is meaningless, either for the aims of EFD or for the Re.N.Di.S. procedure. Heterogeneity would undermine the usability of the analysis.

Therefore, a uniform methodology for risk evaluation is required. It should be homogeneous at the national scale and based on databases available and preferably free to public and updated.

5. The IRP model

In order to overcome the constraints of the present methodologies for risk mapping, Regione Piemonte public administration in collaboration with the Politecnico of Turin and the University developed a methodology for risk assessment and quantification, which is based on the quantification of the *Index of Proportional Risk* (IRP).

The model has been developed by referring to specific types of risk, according to **Table 4**.

The IRP is quantified by applying the following expression:

$$IRP = \frac{1}{T} \sum_{i=1}^{N} e_i A_i v(h) \tag{2}$$

where N: total number of receptors in the flooding area; T: return period (years); h: flow depth (m); A: area of the receptor (m²); e: OMI value (€/m²); $v(h)$: vulnerability (adim.); *IRP* dimension is €/year. The multiplication of the IRP and the return period is called *index of proportional damage* (IDP).

The model implicitly assumes the definition of risk contained in the EFD, as it refers either to the probability (the return period) or to the consequences of flood in terms of the flood damage.

According to Eq. (2), the model assumes that the total risk is proportional to the area of the receptor. A short description of the terms in Eq. (2) is given in **Table 5**.

The vulnerability V(h) is estimated by means of the JRC "European" curve in [13].

Flood depths maps can be easily obtained by following the procedure contained in [14, 15] and widely applied in the project of "Orco river flooding assessment," developed in collaboration with the former Po basin Authority [16].

The choice of the JRC curve has been guided by the necessity to adopt a "robust" formulation, which is based on a "…*globally consistent database…*" of depth-damage curve.

The proposal of a vulnerability curve usable for Po river floodplain is not simple, in particular due to the lack of detailed damage data, so that a vulnerability curve cannot be easily obtained for the receptors in Piemonte region and Padana plain.

As it is well known, many flood damage models using depth-damage curves have been proposed in scientific literature in different countries. They are generally based on analysis of past flood events and on regression of available data. However, such damage curves are not available for all regions, and their use can be questionable in some areas. Moreover, "*due to*

	Applicability	Possible extension
Type of risk	Direct and tangible risks; the model has been developed by referring to structural (and content) damage	The model allows to obtain a quantitative estimation of damages (and risks), to which other damages (and risks) can be correlated (e.g., indirect damages)
Type of processes	Major river flood processes in plains. By taking into account sediment transport, the model can also be applicable to stream floods	The model can be extended to processes like debris flows/soil-slips, as far as E is concerned. The approach to H and V should be revised
Main field of application/objective	Spatial and land planning	Possible extension to real-time risk (civil protection)

Table 4. Natural hazards and types of processes to which the IRP model refers to.

different methodologies employed for various damage models in different countries…damage assessments cannot be directly compared with each other, obstructing also supra-national flood damage assessments" [13].

The discussion about the depth-damage curve to be adopted for risk mapping is in course among regions in Po watershed basin, the Po District authority, the Turin University, the Politecnico of Turin, and of Milan.

In the proposed model [14, 15], exposure is evaluated by referring to the OMI (*estate market observatory*, free available online, [17]) database. The exposure E of each receptor has been computed by the product of the area A of the receptor for its economic value "e"; this parameter is reported in the *OMI* dataset and, as applied in [14, 15], varies depending on the prevalent use of receptors (commercial, residential) and their location in the urbanized areas (*OMI* zones), which are considered homogeneous from the economic market point of view.

Item	Description
h	Water depth, computed at the centroid of the receptor. For receptors outside the flooding area, it is h = 0. The depth h is calculated at the barycenter of the i-th receptor, that is, by using a GIS terminology, at its *centroid*
e	The value of the receptor expressed in €/m², as indicated in the OMI database; OMI database is periodically updated and available to public
A	Receptors are contained in the Regione Piemonte BDTRE database, available to public (in *shape* format). The area of the receptors can be easily and automatically quantified by means of GIS software (e.g., QGIS©)
V(h)	The equation for vulnerability is contained in the JRC publication for "Europe" [13]

Table 5. Constitutive elements in the proposed model (H, E, V) and discussion (see [14, 15] for details).
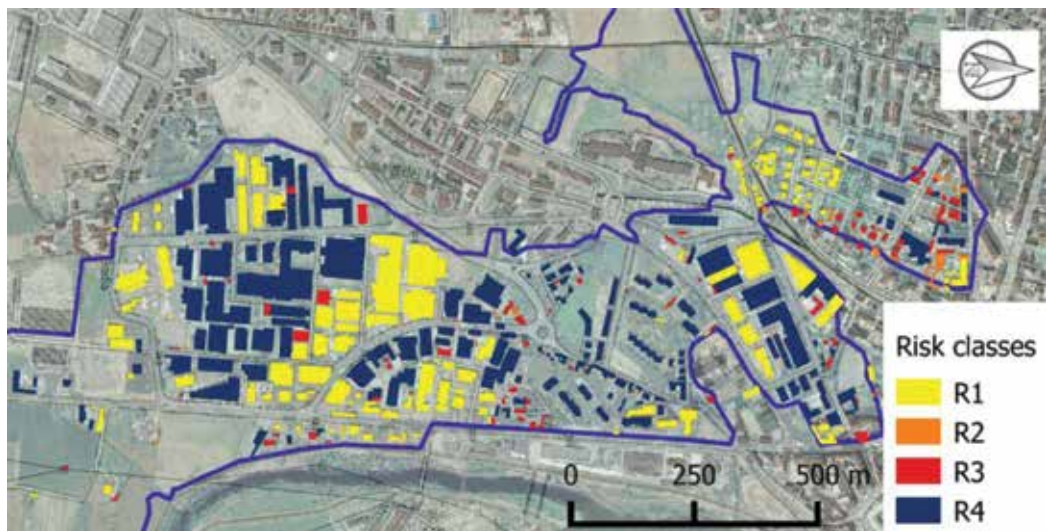

Figure 2. An example of the application of the procedure to the Chisola river. The map has been obtained by referring to the 2016 flood. Risk classes are on a log-scale (R1 class: 0–1000.00€; R2 class: 1000.00–10,000.00€; R3 class: 10000.00–100,000.00€; R4 class: >100,000.00€; the blue line indicates the borders of the flooding areas).

The IRP model can be easily used to rank flood risk, according to quantitative criteria. At present, it can be used to calculate the risk (and the damage) on receptors (buildings), as well as for risk mapping (**Figure 2**).

6. Model validation

The model has been extensively applied to different case studies, in Piemonte region, for the risk assessment and the cost/benefit analyses [14, 15].

In this work, a sort of validation of the model has been tried by comparing the IDP computed by the model and the damages recorded in the recent 2016 flood.

The term "validation" is not appropriate, as the comparison is not simple. Actually, it should be highlighted (see Section 8) that the real damages suffered by residential or commercial receptors may not be equal to the indemnifications by public administration [18]. This point will be discussed in the next paragraphs.

However, a comparison between the computed index damages and the requested indemnification for residential or commercial activities has been tried, in order to estimate the gap between the computer IDP and the available data.

In the following paragraphs, three applications will be shown and discussed, referring to 2016 flooding in Chisola river, Bormida river, and Tanaro river. A comparison between the computed IDP and the requested indemnifications is also shown.

7. Application

In the last 10 days of November 2016, Piemonte region was affected by a flood event with meteorological characteristics similar to other events of the past. According to ARPA Piemonte (*Regional Environment protection Agency of Piemonte*), the flood severity was similar to the most severe historic event occurred in the past in the Tanaro river watershed.

The flood event on November 24–25, 2016, has also significantly affected the basins of the Bormida di Millesimo and Bormida di Spigno rivers. In particular, the Bormida di Millesimo flood involved important production companies in the Bormida valley, as well as residential buildings and farms, causing considerable damage to the agricultural cultivation [19, 20].

According to the flood report ([20], p. 2), the event caused extensive damages to flood control structures, sediment deposits, bank erosions, and meander changes and extensive flooding with serious involvement of inhabited settlements and productive activities.

According to the report ([20], p. 3), important economic activities, generally insured against flood damage, risked not to benefit from reimbursements by insurance companies; these in fact generally cover the damage only in the presence of a *declaration* of an emergency *status*,

by the Council of Ministry. Consequently, some companies, which were affected by the flood and suffered extensive property damages, asked for the *declaration* of the emergency *status* and also claimed the restoration of damages and the reinstallation of adequate defenses in order to continue to stipulate insurance with adequate contractual conditions. The Council of Minister declared the emergency *status* on December 16, 2016, only for Turin and Cuneo Provinces. Afterwards, Regione Piemonte public administration asked to extend the *declaration* to Asti and Alessandria. On February 23, the Council of Ministers approved the resolution, extending the emergency *status* to the provinces of Asti and Alessandria, providing the allocation of financial resources.

After the flood event, the Regional Departments started some activities, aiming to map and assess the flood effects, upon which the hazard evaluations of the IRP model have been based. These activities are the following:

- systematic mapping of requested interventions by means of the EMETER (*Emergency and Territory Management Information System*) application; the EMETER is a web-GIS system useful for regional officials of the Public works Directorate, which operates both in ordinary situations and in case of extraordinary events;

- field surveys along the main rivers, including Bormida river and Tanaro river; the technicians carried out systematic surveys in order to integrate and evaluate the information deriving from remote sensing; analysis of satellite data from the Cosmo platforms and from the platforms belonging to the European Copernicus system was performed;

- acquisition and processing of aerial photographs; a flight was made in the week following the event; aerial photo interpretation allowed to integrate the satellite and ground surveys.

Flood maps were the basis upon which the hazard estimation procedure of IRP started from. The procedure to obtain the flood depth maps has been described elsewhere [14, 15].

In this application, the exposure of receptors in the flooded area refers to the 2018 OMI database. The variability in time of the asset value (i.e., from the date when the flood occurred to present days) is negligible. The total number of flooded receptors and municipalities is summarized in **Table 6**.

After the 2016 flood, data of damages have been collected by public administration according to the civil protection procedures [18]*"Procedure for the recognition of the needs for the restoration of damaged public and private structures and infrastructures, as well as for the damages to economic and productive activities, to cultural heritage, and to the housing assets."* The procedures are followed by Regione Piemonte administration [19, 20] and are available to public. According to them, the requests for residential and productive damage indemnification have to be collected in the so-called *B-sheet* (*Recognition of the needs for the restoration of private buildings* sheet, which contains all the requests regarding residential damages*) and *C-sheet* (*Recognition of damages suffered by economic and productive activities* sheet, which contains all the requests regarding damages to economic/productive activities), respectively. These have to be filled by privates and confirmed by technical assessments.

Case study	Total number of involved receptors	Municipalities included in the analysis
Tanaro reach	104 (85 residential)	Govone, San Martino Alfieri, Costigliole d'Asti, Antignano, Isola d'Asti, Revigliasco d'Asti, Asti, Azzano d'Asti
Bormida di Millesimo reach	170 (159 residential)	Vesime, Cessole, Loazzolo, Bubbio, Monastero Bormida, Sessame e Bistagno
Chisola reach	1858 (1243 residential)	Candiolo, Cumiana, La_Loggia, Moncalieri, None, Piobesi_Torinese, Piossasco, Vinovo, Volvera

The total number of receptors is referred to the flooding mapped area as described before. The analyses were focused only on the river reaches where damage data were available.

Table 6. Applications of the model to the case studies.
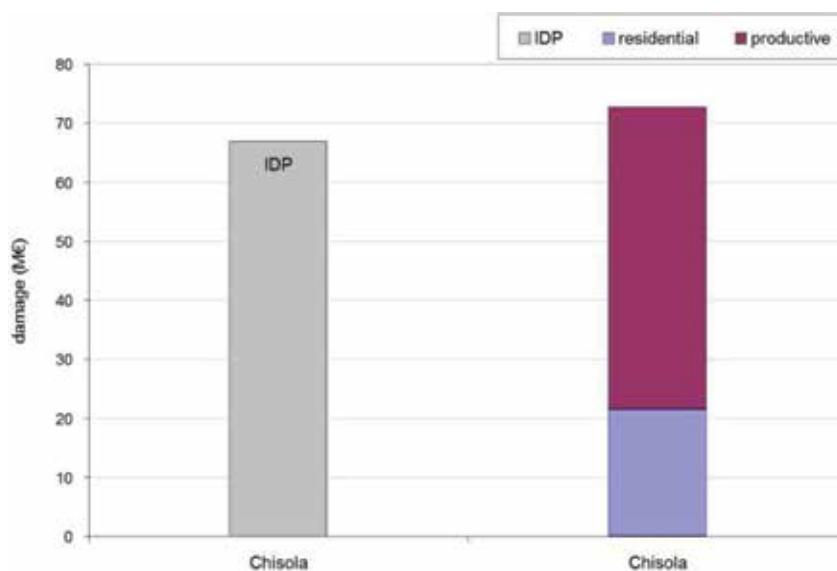
Figure 3. Comparison among the IDP and collected data in Chisola case study.

Comparison of IDP index has been made by referring to the total requests in B-sheet and C-sheet. The results of the comparison are shown in **Figures 3** and **4**.

It should be highlighted that the categories of damages refundable by Public administration are specified by the Council of Ministry. Actually, the recent deliberation of the Minister council (July 28, 2016; *Directional criteria for the determination and granting of contributions to private individuals for damage to buildings and housing assets*.) contains the list of the damages that can be eligible for indemnification. They may not match with the real damages.

Moreover, as it can be seen from the figures, the rate of residential and productive damages to the total damage varies in a wide range.
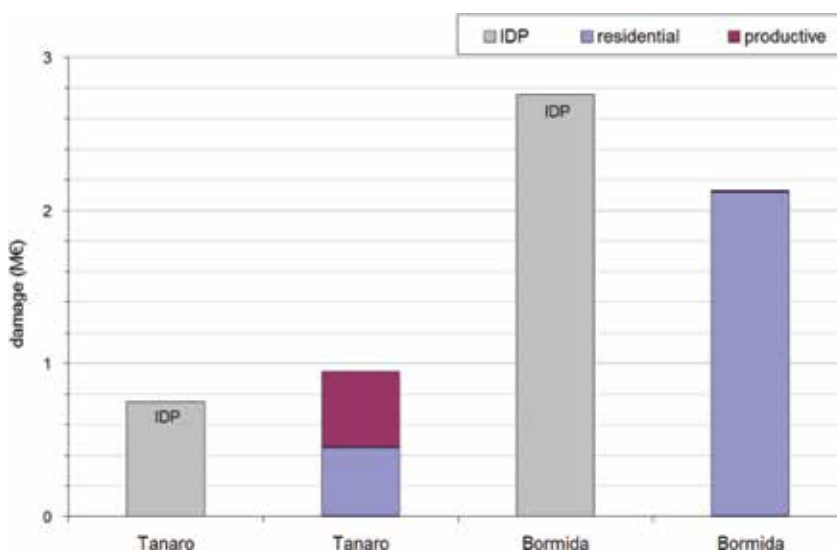
Figure 4. Comparison among the IDP and collected data in Bormida and Tanaro case studies.

River	IDP (total)	Damage to private properties	Damage to productive activities
Chisola	€ 6,933,305.00	€ 21,520,781.16	€ 51,191,427.49
Tanaro	€ 751,473.12	€ 451,153.28	€ 496,860.00
Bormida	€ 2,757,522.90	€ 2,116,426.00	€ 13,885.00

Table 7. Comparison among the IDP and the collected data.

The interpretation of the comparison, shown in **Figures 3** and **4** and summarized in **Table 7**, is not immediate, and a discussion is provided in the following paragraph.

8. Discussion

The IRP model, extensively applied to different case studies in Piemonte region, demonstrated to be a suitable tool to risk and damage estimation, either for the aims of the implementation of flood directive or for the design of the countermeasures. The model aims at expressing an "index," where estimation is based on a scientific approach (i.e., on the definition of damage and of risk) and on the basis of databases available at regional and national scale. The usability of the model has been proven elsewhere, and it is confirmed by the application to the 2016 case study, to Tanaro, Bormida and Chisola rivers (**Figures 3** and **4**).

The comparison shows that IDP can lead to an under/overestimation of the collected data. The use of the term "collected" is preferable to others, as it substantially refers to the kinds

of damages reported by privates for indemnification. These categories of damages may, or may not, match with the categories of "refundable" damages by Ministry. Moreover, the quantification of damage made by "not expert" privates after the flood can overestimate/ underestimate real damages assessed by professionals.

The gap between the collected damages (contained in the B-sheet and C-sheet) and the refundable damages can lead to an over (or under)estimation of the former with respect to the latter. **Table 8** shows a list of the main factors for this gap.

Consequently, the quantification of real damages, and the calibration of the model, is a very difficult task. The computed IDP cannot be easily compared to collected damage "data," as the latter refer to conditions which are highly influenced by regulations, personal attitudes, and so on.

For this reason, the proposed model aims at the computation of an *index* (the Index of Proportional Risk, or the index of proportional damage) more than to the precise computation of physical damages.

Moreover, it should be considered that the total flood damages can be by far higher than the residential and/or productive ones. Actually, in the recent *flood report* of Regione Piemonte administration ([19], p.84), "flood costs" have been divided into different groups:

Factors	Description	Effects
Bureaucracy	The procedures are felt to be "complex." Regulations [19, 20] indicate that different modules to be filled, with different obligations for the owners	The total number of collected B-sheet and C-sheet can be by far lower than the affected receptors
Necessity to produce a technical assessment	The technical assessment has to be made by professionals, to quantify the damages of residential houses. Professionals are paid by privates	The quantification by professionals can be different from assessment by privates (B-sheet, C-sheet)
Maximum amount of public contribution (e.g., max 1500.00€ for chattels)	Damages to chattels can be of the same order of the total maximum contribution or less. Bureaucracy costs can be too high with respect to the possible indemnification	Citizens avoid to produce B-sheet and C-sheet if the technical costs for bureaucracy are of the same order of refunds
Kinds of refundable damages	According to regulations, only some damage categories can be refunded. For example, • damaged or destroyed chattels in secondary houses are not refunded; • damages to secondary buildings are not refundable; • damages to cars and to mobile registered goods are not refundable	The requests in B-sheet and C-sheet can overestimate the total refundable damage
Insurance to natural disasters	Damages covered by private insurances are not contained in the available data	The available data can underestimate the real damage

Table 8. Main factors that cause a gap between the total amounts of real damages suffered by residential/commercial receptors and damages that can be eligible for public indemnification.
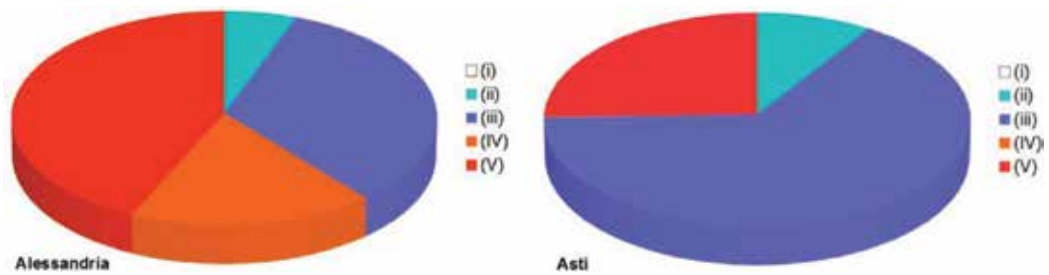
Figure 5. Total flood costs referred to 2016 flood event, recorded by public administration [19, 20] in Alessandria and Asti provinces.

(i) costs for people rescue; (ii) costs for highly urgent interventions: restoration of public services and infrastructures of strategic networks; (iii) interventions to reduce the residual risk (strictly connected to the event); (iv) costs contained in the *Recognition of the needs for the restoration of private buildings (B-sheet)*; and (v) costs contained in *Recognition of damages suffered by economic and productive activities (C-sheet)*.

As shown in **Figure 5**, the total flood costs are by far higher than the "collected" damages from private (residential and productive). The IDP can allow an estimation of the (iv) and (v) components.

In spite of the fact that model calibration is a very difficult task, the computation of IDP can prove to be a useful means for the estimation of the total damages after a flood.

Actually, the estimation of the (iv) and (v) components by means of the IDP can indirectly allow the estimation of total costs. For example, by referring to the damages to Alessandria and Asti provinces in 2016 flood, the total cost is 1.6 or 3.9 times (respectively) the private damage (i.e., given by the addition of the (iv) and (v) components).

The variability of the total damage with respect to the private one depends on variables that are highly dependent on the kind of processes and the affected area of flooding.

At present, it is preferable, for public administration, to focus on simple and robust models that can predict the order of magnitude of damages (preferably based on free- and open-source software [21]), more than to complex models hard to be applied in practical conditions.

9. Conclusions

The IRP model, extensively applied to different case studies in Piemonte region, demonstrated to be a suitable model to risk and damage estimation, either for the aims of the implementation of flood directive or for the design of countermeasures. The model aims at expressing an "index," where estimation is based on a scientific approach (i.e., on the definition of damage and of risk) and on the basis of available databases at the regional scale (Piemonte region) and national scale (Italy).

The usability of the model to compute an "index" has been proven elsewhere, and it is confirmed on the present application to the 2016 case study, to Bormida, Tanaro, and Chisola rivers.

The comparison between the computed "index" and the *collected* residential and productive damages proves that if the former should be used to estimate the real damages, an *over-* or *under*estimation of the latter could be done. Moreover, collected damages can be very different with respect to real damages. This is due to the many factors, including the attitude of privates, or legislation. Application to Bormida river also showed a strong variability in the total amount of indemnification requested by economic activities.

For this reason, it should be considered that, at the present state, a real calibration of the model is not possible and the use of the term *index* should be maintained. However, the IDP can be a useful index to estimate the order of magnitude of the total indemnification requests by privates or to estimate the total flood costs. Available data on 2016 flood show that, for Alessandria and Asti provinces, the total costs are between 1.6 and 3.9 times the private requests.

The adoption of the IRP allows the risk quantification and its ranking; in spite of the fact that, at present, risk quantification in EFD is not compulsory, in this frame, IRP can be a useful instrument to (i) improve risk ranking and mapping and to (ii) estimate damages for the application of Re.N.Di.S. procedures.

Obviously, over/underestimations by the model should be taken into account by decision makers and public administration, especially in Re.N.Di.S. procedures.

Acknowledgements

Conflict of interest

The authors declare that there are no existing or possible conflicts of interest, including financial, personal, or any other relationship which could influence their scientific work, at the time of manuscript submission.

List of acronyms

DPCM   Decree of the President of the Ministry council

EFD   European Flood Directive

IDP   index of damage risk

IRP   Index of Proportional Risk

ISPRA   Superior Institute for Protection and Environmental Research

MATTM   Ministry for the Environment, Land and Sea

OMI   Estate Market Observatory

PAI   Hydrogeological Asset Plan

PGRA   Management Plan for Flood Risk

Re.N.Di.S.   National Repository for Soil defense

Author details

Luca Franzi[1]*, Gennaro Bianco[2], Alessandro Pezzoli[3] and Angelo Besana[4]

*Address all correspondence to: luca.franzi@regione.piemonte.it

1 Soil Defence Department, Regione Piemonte, Torino, Italy

2 DIATI - Politecnico di Torino and Turin University, Torino, Italy

3 DIST - Politecnico di Torino and Turin University and R3C – Politecnico di Torino, Torino, Italy

4 DIST - Politecnico di Torino and Turin University, Torino, Italy

References

[1] European Commission, Directive 2007/60/EC of the European Parliament and of the Council of 23 October 2007 on the assessment and management of flood risks. 2007. Available from: http://ec.europa.eu/environment/water/flood_risk/index.htm [Accessed: 2018-06-01]

[2] PBDA. Piano per l'assetto idrogeologico - Relazione generale. Interventi sulla rete idrografica e sui versanti. 2001. Available from: http://www.adbpo.it/PAI/1%20-%20Relazione%20generale/1.1%20-%20Relazione%20generale/RelGenCap_1_2.pdf [Accessed: 2018-06-01]

[3] MATTM. Indirizzi operativi per l'attuazione della direttiva 2007/60/ce relativa alla valutazione ed alla gestione dei rischi da alluvioni con riferimento alla predisposizione delle mappe della pericolosità e del rischio di alluvioni. 2013. Available at: http://www.minambiente.it/sites/default/files/archivio/allegati/vari/documento_definitivo_indirizzi_operativi_direttiva_alluvioni_gen_13.pdf [Accessed: 2018-06-01]

[4] PBDA, Piano per la valutazione e la gestione del rischio di alluvioni. II Mappatura della pericolosità e valutazione del rischio. 2016. Available at: http://pianoalluvioni.adbpo.

it/il-piano-di-gestione-alluvioni/progetto-di-piano-di-gestione-del-rischio-alluvioni/ [Accessed: 2018-06-01]

[5] Cox LA Jr. What's wrong with risk matrices?, Risk Assessment. 2008;**28**(2):497-512

[6] Department of Defense Risk Management Guide for Defense Acquisition Programs. 7th ed. (Interim Release). Washington, D.C.: Office of the Deputy Assistant Secretary of Defense for Systems Engineering. 2014

[7] Kent DW. The trouble with risk matrices. Naval Postgraduate School (DRMI); 2001. Available at: https://www.researchgate.net/publication/267992252_THE_TROUBLE_ WITH_RISK_MATRICES [Accessed: 2018-06-01]

[8] EXCIMAP, European exchange circle on flood mapping: Hand-book on good prac-tices for flood mapping in Europe. EXCIMAP. 60 p. Available at: http://ec.europa.eu/ environment/water/flood_risk/flood_atlas/pdf/handbook_goodpractice.pdf [Accessed: 2018-06-01]

[9] European Commission, Guidance for Reporting under the Floods Directive (2007/60/ EC), Guidance document n. 29. Technical report 2013-071; 2013

[10] Cox LA Jr. What's wrong with hazard-ranking systems? An expository note. Risk Assessment. 2009;**29**(7):940-948

[11] Barbano A, Braca G, Bussettini M, Dessì B, Inghilesi R, Lastoria B, Monacelli G, Morucci S, Piva F, Sinapi L, Spizzichino D. Proposta metodologica per l'aggiornamento delle mappe di pericolosità e di rischio—Attuazione della Direttiva 2007/60/CE relativa alla valutazione e alla gestione dei rischi da alluvioni. Rome: ISPRA; 2012. 70 p. ISBN: 978-88-448-0571-5

[12] Italiasicura, The national plan of works and interventions and the financial plan for the reduction of the hydrogeological risk. 2017. Available at: italiasicura.governo.it/site/ home/dissesto/piano/documento1041.html. [Accessed: 2018-06-01]

[13] Huizinga J, Moel H, de Szewczyk W. Global flood depth-damage functions. Methodology and the database with guidelines. EUR 28552 EN. 2017. DOI: 10.2760/16510

[14] Franzi L, Bianco G, Bruno A, Foglino S. Flood risk assessment and quantification in Regione Piemonte. In: Tiepolo M, editor. Planning to Cope with Tropical and Subtropical Climate Change. DeGruyter; 2016. ISBN: 978-3-11-048079-5. (e-book) Available at: https:// www.degruyter.com/view/product/473515 (e-book) [Accessed: 2018-06-01]

[15] Franzi L, Pezzoli A, Besana A. Flood Lamination Strategies for Risk Reduction. In: Bucur D, editor. River Basin Management. InTech; 2017. DOI: 10.5772/63553. Available at: http://www.intechopen.com/books/river-basin-management/flood-lamination-strate gies-for-risk-reduction (ebook) [Accessed: 2018-06-01]

[16] PBDA. Torrente Orco da Cuorgnè a confluenza Po -Analisi idraulica. 2012. Available at: www.adbpo.it/on-multi/ADBPO/Home/documento13535.html

[17] OMI, Manuale della Banca Dati Quotazioni dell'Osservatorio del Mercato Immobiliare Istruzioni tecniche per la formazione della Banca Dati Quotazioni. 2018. Available at: http://www.agenziaentrate.gov.it/wps/file/Nsilib/Nsi/Schede/FabbricatiTerreni/omi/ Manuali+e+guide/Il+manuale+della+banca+dati+OMI/Manuale+2016_vers_2.0+modific ata+in+data+02-01-2018.pdf [Accessed: 2018-06-01]

[18] Civil Protection, Technical annex to the ordinances for the recognition of the needs. 2018. Available at: http://www.protezionecivile.gov.it/jcms/it/allegati_tecnici.wp

[19] Regione Piemonte - Direction of Public Works, Soil Defense, Mountain, Forests, Civil Protection, Transportation and Logistics. L'evento alluvionale del 21-25 novembre 2016 in Piemonte. 2016. Available at: www.regione.piemonte.it/alluvione2016/dwd/rap-porto_evento_nove2016.pdf [Accessed: 2018-06-01]

[20] Regione Piemonte - Direction of Public Works, Soil Defense, Mountain, Forests, Civil Protection, Transportation and Logistics, L'evento alluvionale del 21-25 novembre 2016 in piemonte - nota integrativa sugli effetti lungo le aste Tanaro e Bormida (Province di Asti e Alessandria). 2017. Available at: www.regione.piemonte.it/alluvione2016/dwd/ rapporto_evento_nove2016_nota.pdf [Accessed: 2018-06-01]

[21] Albano R, Mancusi L, Sole A, Adamowski J. FloodRisk: A collaborative, free and open-source software for flood risk analysis. Geomatics, Natural Hazards and Risk. 2017;**8**(2):1812-1832. DOI: 10.1080/19475705.2017.1388854

Flood Events: Impacts, Sensitivity Analyses and Mitigation Measures

Insight into the Correlation between Land Subsidence and the Floods in Regions of Indonesia

Heri Andreas, Hasanuddin Z. Abidin, Irwan Gumilar,
Teguh P. Sidiq, Dina A. Sarsito and Dhota Pradipta

Additional information is available at the end of the chapter

Abstract

Land subsidence by definition is the lowering of ground level from certain elevation references. The rates of subsidence can commonly vary between 1 and 20 centimeters per year and even more in certain places. Subsidence produces impacts such as infrastructure damage, problems with drainage, wider expansion of flood water, as well as tidal inundation (flooding by sea water at coastal areas experiencing land subsidence). These impacts are quite costly. All this is disastrous. In a number of regions of Indonesia, land subsidence and negative impacts in the shape of flooding and tidal inundation clearly exist. In Jakarta and Bandung we can see that the subsiding areas close to rivers frequently suffer from flooding. Tidal inundation is a regular feature at subsiding coastal areas such as Jakarta, Blanakan, Semarang, and Demak. Since these negative impacts are clearly formed a disaster while mitigation and or adaptation is still a big homework, in this case for better adaptation and mitigation in the future, understanding deeply the correlation of land subsidence and flooding is necessary as discussed in this chapter. We conclude that the correlation is quite tremendous and indeed producing a disaster.

Keywords: land subsidence, impact, flood, correlation, adaptation and mitigation

1. Introduction

Land subsidence is quite a well-known phenomenon in some regions of Indonesia, especially around urban areas such as Jakarta, Bandung, and Semarang. Rates of about 1–20 centimeters per year can be found at these regions from geodetic measurements such as Global Navigation Satellite System Global Positioning System (GNSS GPS) surveys, InSAR, and leveling. After

some decades a magnitude of 3–4 meters of subsidence has taken place in Jakarta and Bandung, and probably in other unsurveyed areas. The impacts or consequences from land subsidence can be seen in several forms such as infrastructure damage, wider expansion of flood water, as well as tidal inundation (flooding by sea water at coastal areas experiencing land subsidence).

In certain regions of Indonesia, the impact of land subsidence in the form of flooding and tidal inundation clearly exists. In Jakarta and Bandung we can see that the areas close to rivers, which suffer significant subsidence, are frequently being flooded. Tidal inundation is also a regular feature in the coastal areas of Jakarta, Blanakan, Semarang, and Demak, which are also experiencing large magnitudes of subsidence. This is inevitable when lowland coastal areas are lower than the level of the sea after experiencing subsidence; this leads to sea water flooding these areas.

This chapter will explain in detail the impact of land subsidence on flooding (in other words, the correlation of land subsidence and flooding) in regions of Indonesia. The way this is achieved is mostly descriptive using available data. Nevertheless, descriptive datasets would provide new insights into what is going on in these regions regarding the correlation, and will hopefully give a detailed understanding of these two phenomena so one can better adapt to or mitigate these disastrous situations. These impacts also give rise to the future risk of global climate change and its consequences.

2. Land subsidence and its impacts

Land subsidence by definition is a lowering of the ground level from a reference height system such as geoids or the level of the sea. The rates of subsidence can commonly vary between 1 and 20 centimeters per year and even more in some places. Over decades a magnitude of 4 to even 10 meters of subsidence can be found in some places in the world [1–9]. Capital or big cities, industrial areas, peatland areas, oil and gas fields, geothermal fields, and underground mining areas are the most common places where significant land subsidence may occur.

Geodetic measurements such as GNSS GPS surveys, InSAR, and leveling can reveal the rate and magnitude of land subsidence accurately. Other geotechnical approaches also commonly used are the extensometer and tilting measurement. **Figure 1** shows how to monitor subsidence using GNSS GPS and InSAR survey methods, while **Figure 2** illustrates the use of GPS data acquisition in the field. With GPS, several points, which are placed on the media (e.g. benchmarks) covering the area of investigation, are accurately positioned using GPS survey relative to a certain reference (stable) point. The precise coordinates of the benchmarks are periodically or continuously determined. By simply evaluating the rate of changes of the height coordinates from time to time, subsidence characteristics can be revealed. With InSAR, by using two or more synthetic aperture radar (SAR) images of an area, surface movements over time can be identified. The phase signal of InSAR records information on the distance between the satellite and the Earth's surface. By differential InSAR, where we use two SAR images of the same area acquired at different times, subsidence can be revealed if the distance between the ground and the satellite has changed.
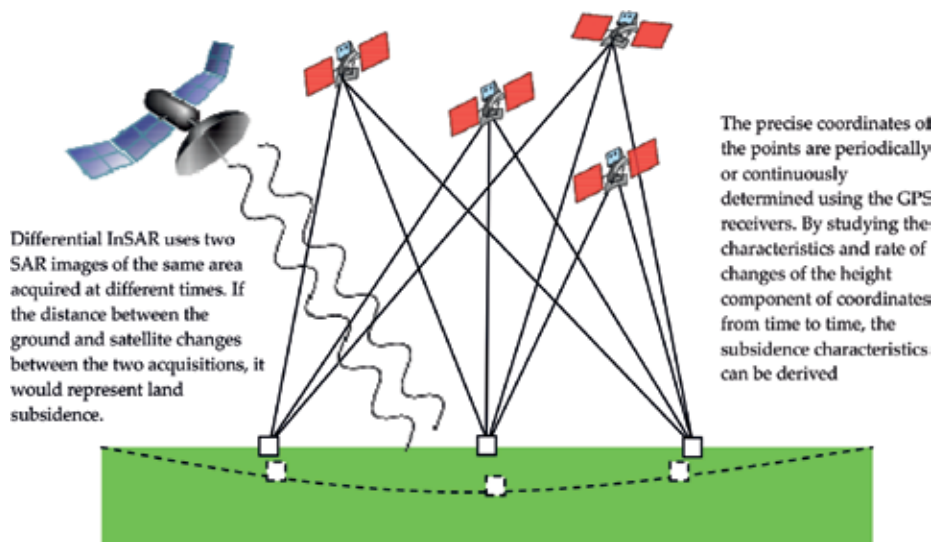
Figure 1. Principle of monitoring land subsidence by geodetic measurements (source: authors).

Figure 2. Field survey GPS observation to derive land subsidence (source: authors).

Infrastructure and building cracks, problems with drainage, the wider expansion of flooding areas, and tidal inundation as mentioned earlier are several impacts from subsidence (**Figure 3**). Surprisingly, many capital cities in the world (e.g. Jakarta, Tokyo, Osaka, Venice, Bangkok, and Ho Chi Mien) have suffered from land subsidence. The consumption of huge amounts of groundwater has led each city to subside significantly over many decades [1, 5–8, 10, 11]. Increased stress followed by compaction in an aquifer will result in subsidence of the surface of the ground. Some research has concluded that impact or the consequence of land subsidence is a disaster that takes place over time. However, over time impacts such as cracks on infrastructure or floods are worsening and will result in a real disaster. These infrastuctural cracks will eventually become a real danger. Road or bridge damage can be a danger for transport. The wider expansion of flooded areas is also due to continuing subsidence. Economically, huge amounts of money are needed to fix the problems of land subsidence.

In many places, short-term measures have been created to mitigate these disasters such as building temporary dykes, fixing or elevating roads, repairing houses and land, including

Figure 3. Example of documentation of the impact of subsidence such as cracks in buildings and infrastructures, and tidal inundation (sources: [12, 13]).

building up mangrove areas. Long-term measures include either building giant sea walls around some coastal areas or stopping land subsidence. Giant sea walls are recognized in places such as New Orleans, Tokyo, and Osaka.

3. Land subsidence in regions of Indonesia

Indonesia is shaped from the interaction of several major plates (e.g. Australia and Eurasia). As a consequence, Indonesia has many sediment areas. Flat sediment areas are the best places for urban and city development, especially around coastal sediment areas. Jakarta and Semarang are examples of coastal sediment cities in Indonesia. Interestingly, sediment areas are places where land subsidence generally exists. Based on our investigation of at least 17 sediment areas in Indonesia, cities, farms, fishpond areas, or peatlands, these regions are experiencing land subsidence with rates varying between 1 and 20 centimeters per year [3–5, 8, 9, 12, 14, 15] (**Figure 4** and **Table 1**).
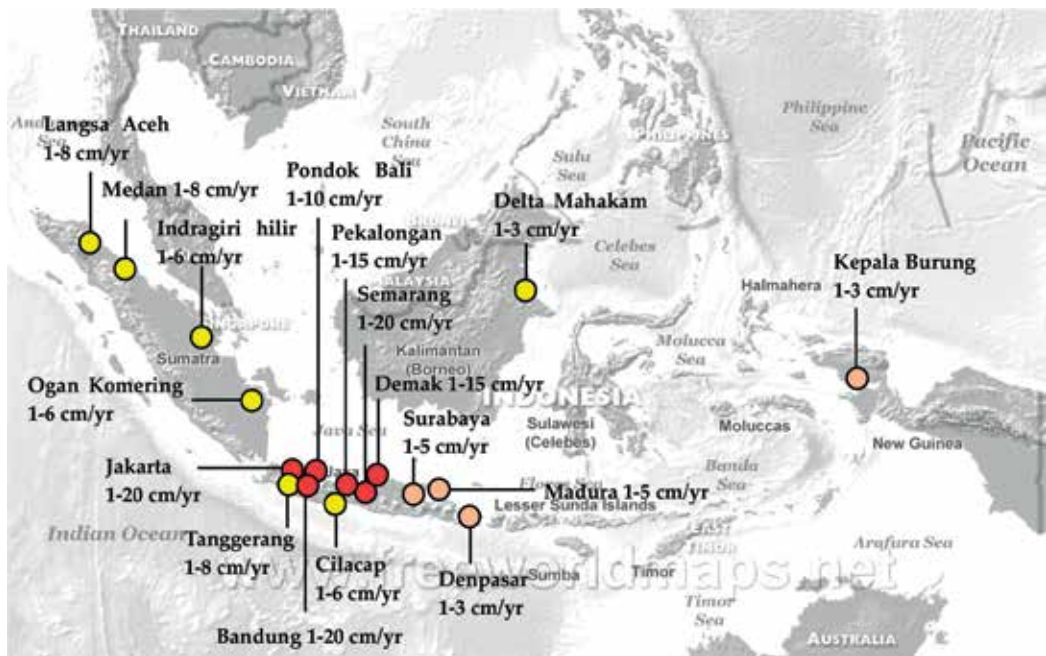
Figure 4. Places of land subsidence in Indonesian regions (sources: [3–5, 8, 9, 12, 14, 15]).

Jakarta city is a well-known place for land subsidence in Indonesia. According to some publications (e.g. [3, 5, 8]) the rates of subsidence in Jakarta generally range from 1 to 10 centimeters per year and may reach 20–26 centimeters in certain places, especially in the northern part of the city (**Figure 5**). Subsidence will continue since mitigation is beyond the priority program. The linear trend of subsidence can be seen as an indicator.

Bandung is another well-known city for land subsidence in Indonesia. According to some publications (e.g. [2, 3, 8, 14]) the yearly amount of Bandung's subsidence generally ranges from 1 to 20 centimeters per year. The highest rate existed around Cimahi district in the northwestern part of the city (**Figure 5**). Generally, a linear trend can be seen, which means that subsidence may continue for quite sometime.

Semarang is also quite well known for land subsidence in Indonesia. According to some reports, subsidence in Semarang has been predicted to continue for more than 100 years. Based on some publications (e.g. [8, 9]) the yearly amount of Semarang's subsidence generally ranges from 1 to 17 centimeters per year, and in certain places, especially in the northeastern part of Semarang, it may reach 20 centimeters (**Figure 5**).

Excessive groundwater extraction in combination with natural compaction of sediments and probably tectonic deformation, land setting/reclamation, loading from the construction of new buildings, oil and gas extraction, underground mining, drainage of peatlands, etc. are considered possible causes of land subsidence in regions of Indonesia, including Jakarta, Bandung, and Semarang.

The consequences of land subsidence in Jakarta, Bandung, Semarang, and other places in Indonesia can be seen in several forms such as cracking of buildings and infrastructures,

Regions	Rate subsidence (cm/year)	Notes
1. Langsa Aceh	1–8	Possible main cause oil and gas extraction
2. Medan	1–8	Possible main cause groundwater extraction
3. Indragiri Hilir	1–6	Possible main cause peatland draining
4. Ogan Komering	1–6	Possible main cause peatland draining
5. Tanggerang	1–8	Possible main cause groundwater extraction
6. Jakarta	1–20	Possible main causes groundwater extraction and load of building
7. Bandung	1–20	Possible main cause groundwater extraction
8. Pondok Bali	1–10	Possible main cause oil and gas extraction
9. Cilacap	1–6	Possible main cause oil extraction
10. Pekalongan	1–15	Possible main cause groundwater extraction
11. Semarang	1–20	Possible main causes groundwater extraction and land reclaimed
12. Demak	1–15	Possible main cause groundwater extraction
13. Surabaya	1–5	Possible main cause groundwater extraction
14. Madura	1–6	Possible main cause oil and gas extraction
15. Denpasar	1–3	Possible main cause groundwater extraction
16. Delta Mahakam	1–3	Possible main cause oil and gas extraction
17. Kepala Burung	1–3	Possible main cause gas extraction

(Sources: [3–5, 8, 9, 12, 14, 15]).

Table 1. Land subsidence information in Indonesian regions.

problems with drainage, the wider expansion of flooding areas, tidal inundation, and increased inland sea water intrusion (**Figures 6** and **7**). The coastal area of Semarang city regularly suffers from tidal inundation at high tide. The same situation was happening in Jakarta before the sea dyke was established. Within this chapter we will look at the impact of land subsidence in the shape of flooding, including its wider expansion. More specifically, we will see how they are significantly correlated with each other in deriving disaster.

The consequences of land subsidence in the affected areas also badly influence the quality and amenity of the living environment, e.g., sanitation and public health. Indeed, some villagers in coastal areas have been evacuated from their homes due to permanent land sinking into the sea. The dispute as to who is responsible for these impacts is ongoing. People are spending their own money to stem these impacts, while the government is spending money on elevating roads and bridges, road repairs, and other consequences of subsidence. It is possible that there are some who contribute to subsidence along with its consequences and they should be responsible for compensating for any damage. Nevertheless, the government should have overall responsibility regarding any disaster.
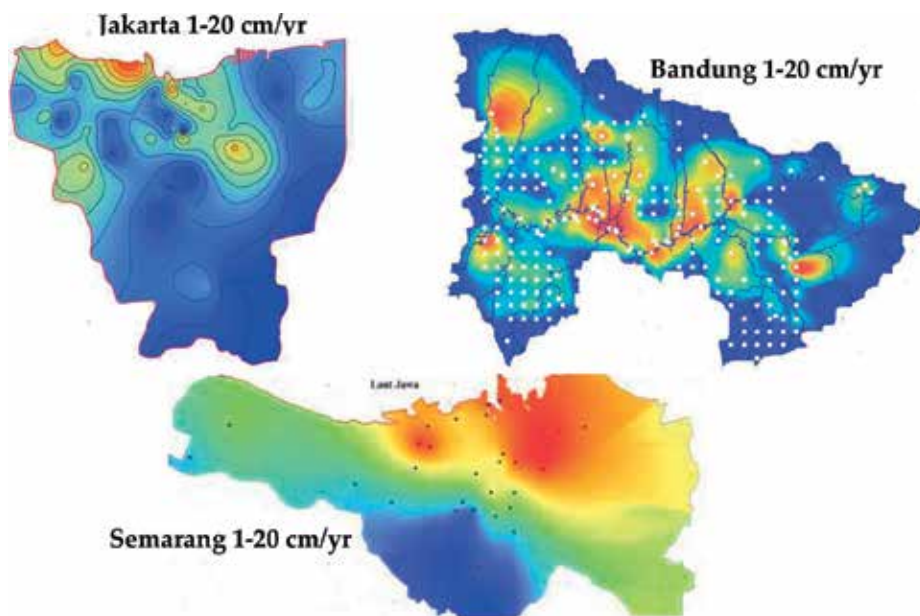
Figure 5. Map of land subsidence in Jakarta, Bandung, and Semarang. Highest rate of 20 centimeters per year is represented by the red color. North Jakarta and northeastern Semarang areas are experiencing the highest rate. Meanwhile the highest rate in the Bandung area is in the industrial areas (modified from [5, 9, 14]).

Figure 6. Pictures of the impact of subsidence (e.g. cracks in buildings and infrastructures and tidal inundation) in Jakarta, Bandung, and Semarang (source: authors).

Figure 7. Pictures of the impact of subsidence (e.g. cracks in buildings and infrastructures and tidal inundation) in other regions of Indonesia (source: authors).
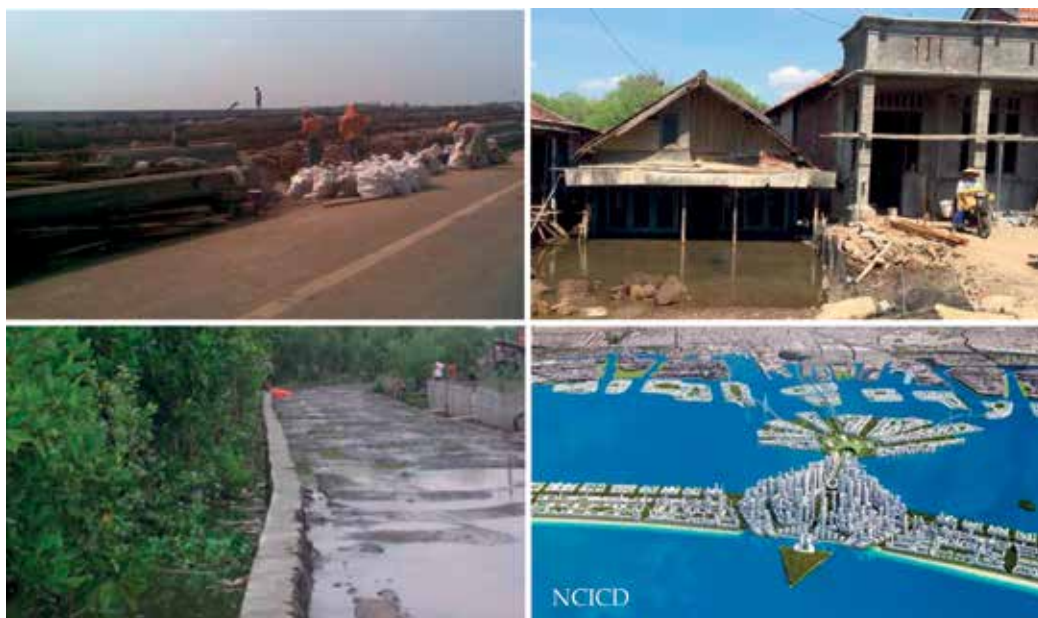
Figure 8. Short- and long-term mitigation and adaptation against the consequences of land subsidence (e.g. elevating roads and housing, and building dykes, mangrove areas, and giant sea walls) (sources: authors, [12, 16]).

Comprehensively collecting information on the characteristics of land subsidence (e.g. rate, magnitude, places, causes, and impacts) in regions of Indonesia or elsewhere is appropriate for short- and long-term adaptation and mitigation (**Figure 8**). Respectively for Indonesia, short-term mitigation has been created against disasters that result in building temporary dykes, elevating the land, roads, housing, etc., including building up mangrove areas in many places along the subsiding coastal area. Long-term mitigation includes building giant sea walls around some coastal areas in an effort to stop subsidence by artificial recharge and/or stopping groundwater extraction.

4. Land subsidence and flooding insight correlation

As mentioned earlier we will look at the impact of land subsidence in the shape of flooding in some regions of Indonesia. More specifically, we will see how these are significantly correlated with each other and what the consequences of disaster would be. Fortunately, we can see quite clearly the qualitative and quantitative expected correlation between land subsidence and flooding using databases. Below is a detailed explanation of what is happening in Jakarta, Bandung, Semarang, Demak, and Pondok Bali Blanakan, which can best highlight the correlation examples. We will see clearly that the correlation is producing many problems.

Where a lowland area is experiencing land subsidence as a result of a cone of subsidence or there is a subsidence bowl, water will directly flow into it and create a flood zone. If the subsidence continues over time, in this case the cone of subsidence would become larger. As a consequence, wider expansion of flooding will likely occur as well. From all parameters that may create a flood (rain intensity, retention capacity, run-off, infiltration, land subsidence, land use, etc.), the subsidence parameter will likely influence a deeper and wider flood over time.

When we speak of a disaster from subsidence and flooding, we are likely to face economic and other losses. Millions of dollars have to be spent fixing problems from both land subsidence and flooding, and millions more will be spent in the future [17] (**Table 2**). With these kinds of losses, therefore, mitigation and/or adaptation are necessary. One key point regarding better mitigation and/or adaptation is to understand insight correlation between land subsidence and flooding. If flooding is proven to be influenced significantly by land subsidence, in this case reducing or even stopping the subsidence might be the best mitigation.

Geologically speaking, Jakarta is a lowland flood basin area. Thirteen rivers run across the area. Therefore, Jakarta is prone to frequent flooding. When a river is beyond its capacity to retain water from heavy rainfall, then flooding will occur. On the other hand, many places in Jakarta and the surrounding area experience land subsidence. With this situation, Jakarta is even more prone to frequent flooding. Spatially, the correlation between subsidence area and flood-prone area is very clear in Jakarta. Places that are experiencing high rates of subsidence are coincidentally those places most prone to flooding, such as Pluit, Sunter, Kamal Muara, and Joglo (**Figure 9**). In Pluit and Sunter, based on people's experience, floods seem to be

Problems to fix	Cost	Notes
1. Elevated roads	$1 million for 1 kilometer	Spent
2. Elevated bridges	$1 million for one long bridge	Spent
3. Fixing drainage	$200,000 for 1 kilometer	Spent
4. Social cost	$100 million/year	Estimated
5. Temporary dyke	$5 million for 1 kilometer	Spent
6. Giant sea wall	$600 million for 40 kilometers	Estimated
(Source [17]).		

Table 2. Cost of fixing problems from land subsidence and floods.

Figure 9. Map of land subsidence in Jakarta (modified from [5]) correlated with a model of existing flooding in the area. Some pictures show flooding in the field (sources: authors, [18]). We can see that a significant area suffering from subsidence is also constantly suffering from flooding.

wider and deeper over time. Generally, this is one of the indicators of true spatial correlation between land subsidence and flooding.

Jakarta is one of the biggest coastal cities in Indonesia and even in the southeast of Asia. It is quite remarkable how the city has rapidly grown through the decades. Nevertheless, the coastal area of this city is a place where the highest rate of subsidence exists. The lowering of coastal land due to subsidence will result in tidal inundation. Continuing land subsidence in combination with the rise in sea level has made the city prone to significant tidal inundation. We use the LiDAR Digital Elevation Model to look at the subsidence over time and create a projection of tidal inundation in Jakarta. Surprisingly, based on the model we found that around 26.86% of Jakarta would be below sea level in 2025 and potentially suffer from
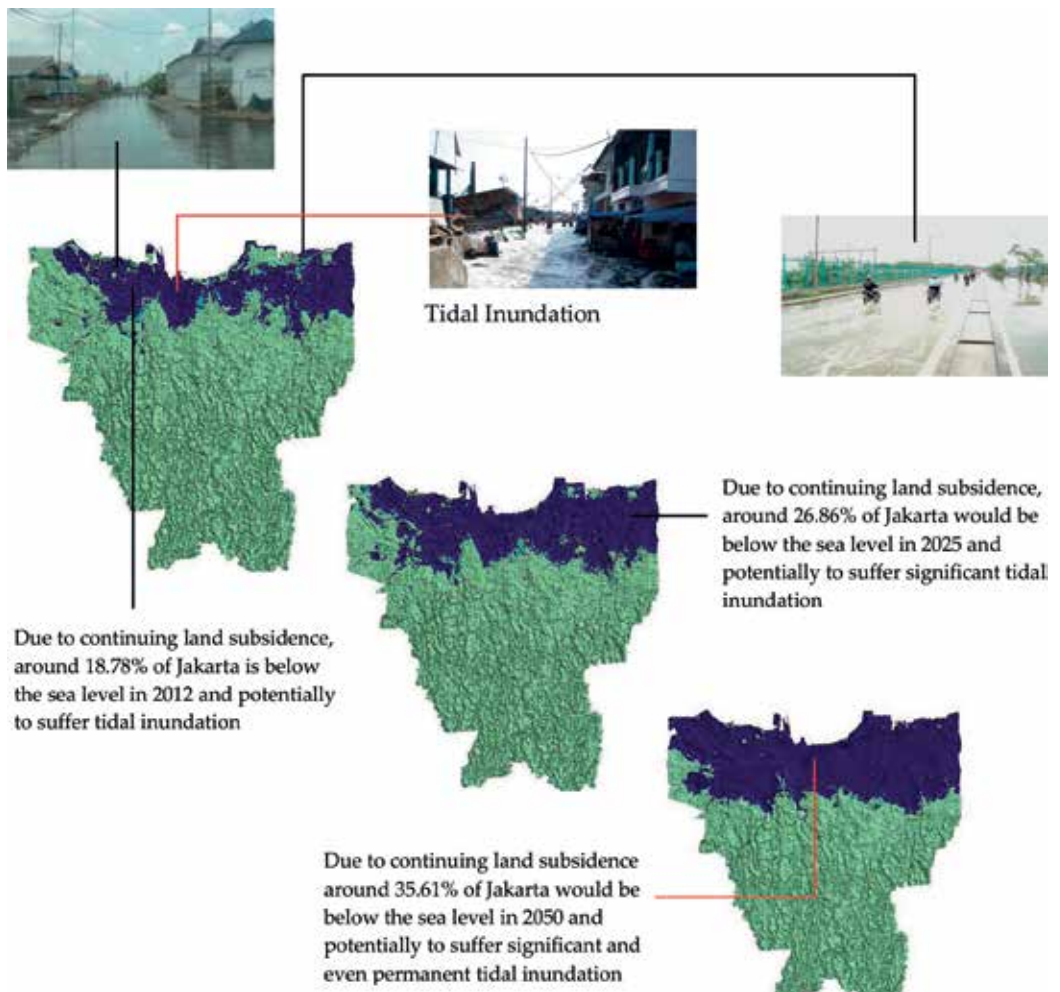
Figure 10. Map of tidal inundation in the area of Jakarta and the future tidal inundation projection as a consequence of continuing land subsidence in the area. Some pictures are given here to describe the existing tidal inundation in the field (source: authors).

significant tidal inundation, and around 35.61% of Jakarta would be below sea level in 2050 and potentially suffer from significant and even permanent tidal inundation (**Figure 10**).

The city of Bandung and its suburbs is located on a high land basin formed from the ancient crater of Gunung Sunda (super volcano). Thick sediment is overlaid below this area. Lying across the basin is the Citarum River. Land subsidence exists in Bandung Basin at a very significant rate per year. In certain places it may reach 20 centimeters per year. If we take a close look, subsidence mostly takes place around the industrial area, which is mainly located near the Citarum River and its tributaries (e.g. Dayeuh Kolot, Gedebage, Majalaya). When industry takes large amounts of groundwater, subsidence occurs in the area and creates a subsidence bowl. When heavy rain comes and the river cannot hold the water, then the surrounding area, including the subsidence bowl, is flooded (**Figure 11**). This clearly shows that the area suffering from land subsidence is constantly suffering from flooding.

Semarang is the biggest coastal city in Indonesia after Jakarta. Half of the city unfortunately is experiencing land subsidence, especially around the northeastern part. As a consequence of
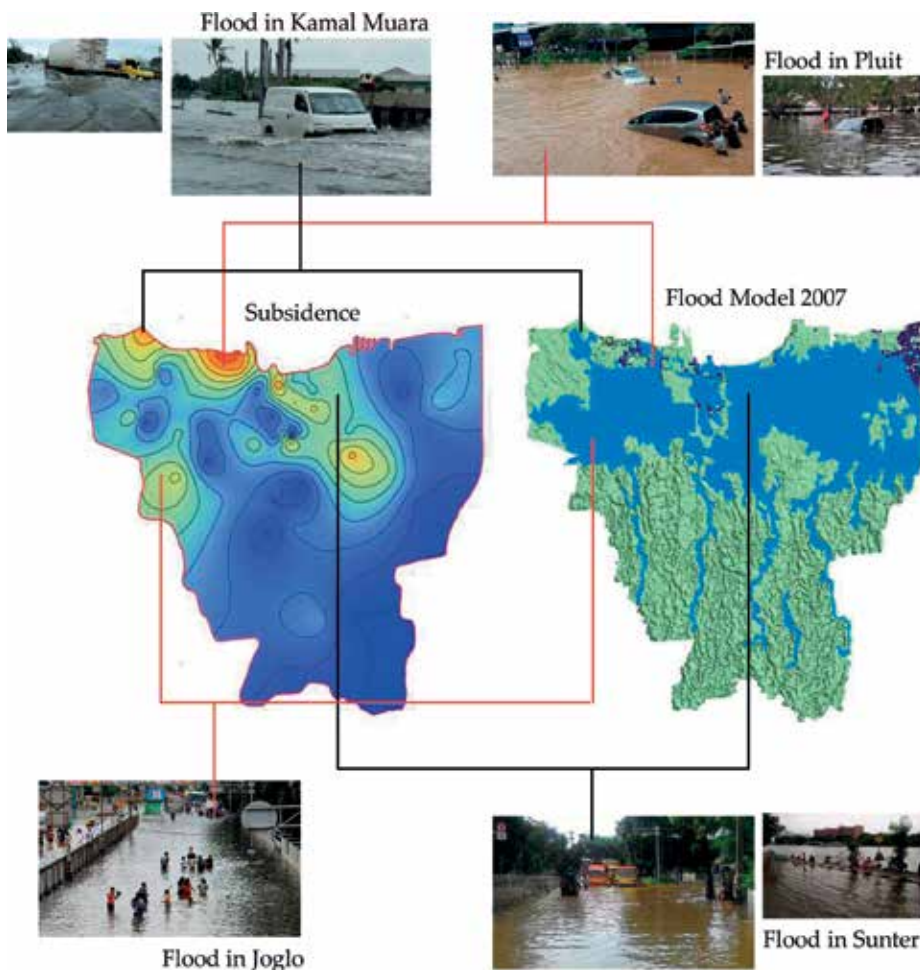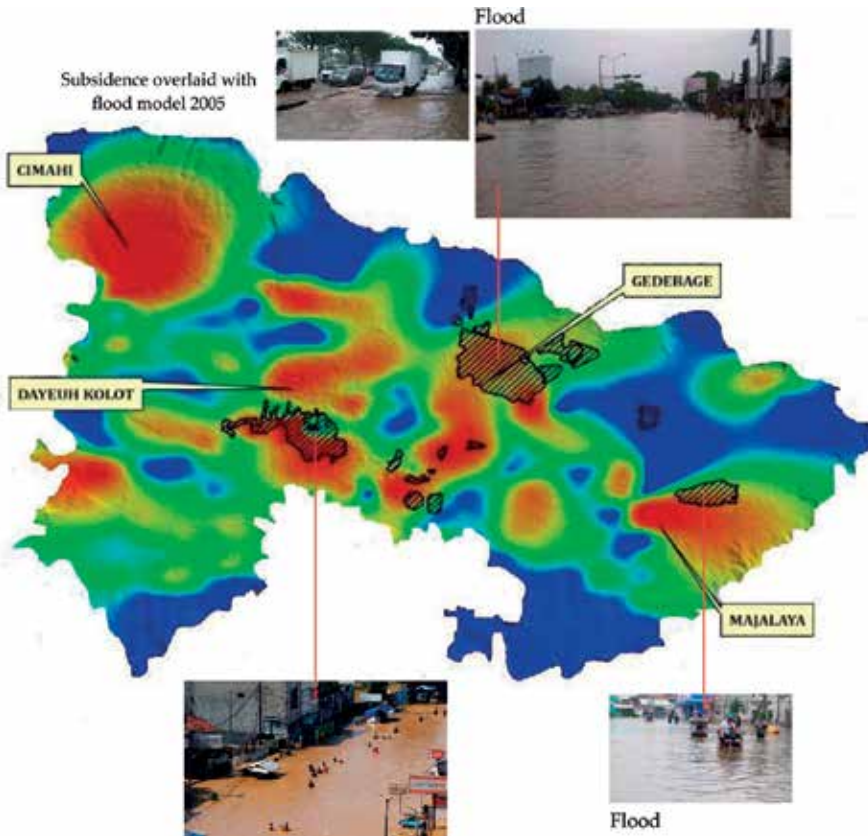

Figure 11. Map of land subsidence in Bandung (modified from [14]) correlated with the model of existing flooding in the area. Some pictures are given to describe flooding in the field (sources: authors, [18]). The area suffering from subsidence is constantly suffering from flooding.

lowering land due to subsidence, this place is prone to either flooding from rainfall or flooding from the sea or tidal inundation (**Figure 12**). When the high tide comes at the same time as heavy rainfall, what happens in northeastern Semarang is a real disaster. The place is drowning in the sea. Indeed, some parts of the area are permanently drowning as endorsed by analysis using the time series of high-resolution satellite image data as depicted in **Figure 12**. It is an undoubted fact of correlation between subsidence and flooding creating a real disaster. Sometime in the future this problem may worsen if we see a significant linear rate of subsidence in this area; on the other hand, attempts to mitigate or adapt to this situation are still not a priority.

Moving a little further east from Semarang we find a district called Demak. It is a coastal area used mostly for farming and fishing. At the southern part of the district are many industrial areas. It is not surprising that these industrial areas have taken huge amounts of groundwater; what is also surprising is that farming and fishing have also taken huge amounts of groundwater from deep aquifers. As a consequence, the Demak area is suffering from a significant rate of land subsidence. While the low land of the coastal area is sinking, over time more frequent tidal inundation will make things worse and in certain places it has already become permanently inundated. Based on high-resolution satellite image analysis, it is surprising that 3000 hectares of the Demark area are suffering from
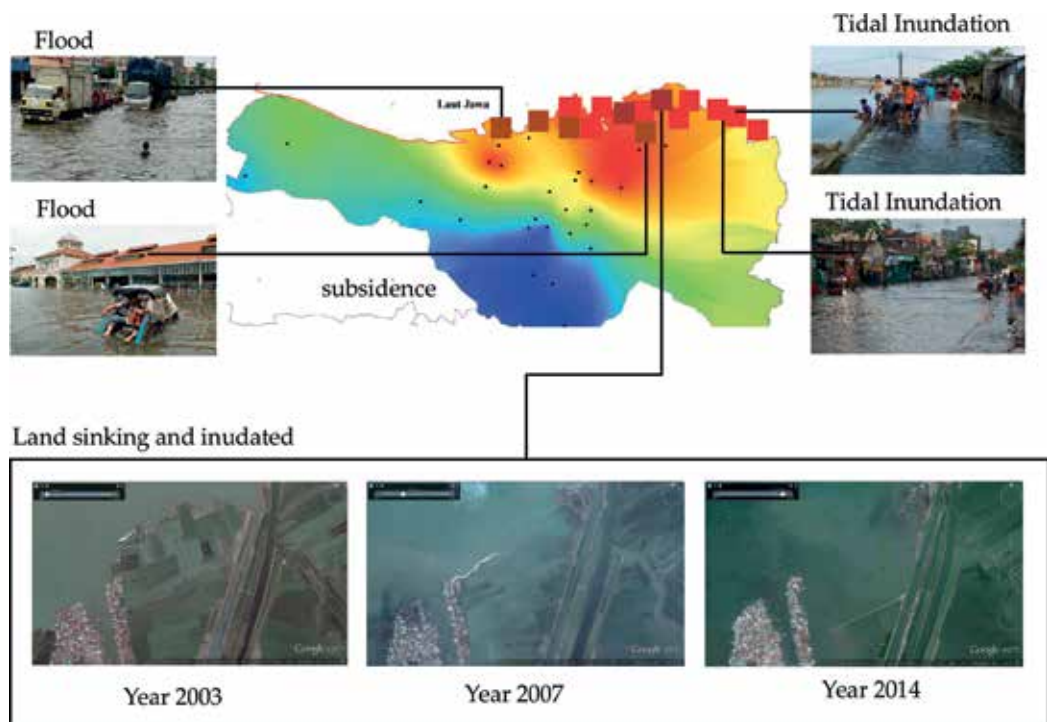
Figure 12. Map of land subsidence in Semarang (modified from [9]) correlated with existing flooding and tidal inundation in the area and also with satellite images of the land sinking (sources: authors; [18, 19]). We can see that the significant area suffering from subsidence is also constantly suffering from both flooding and tidal inundation.
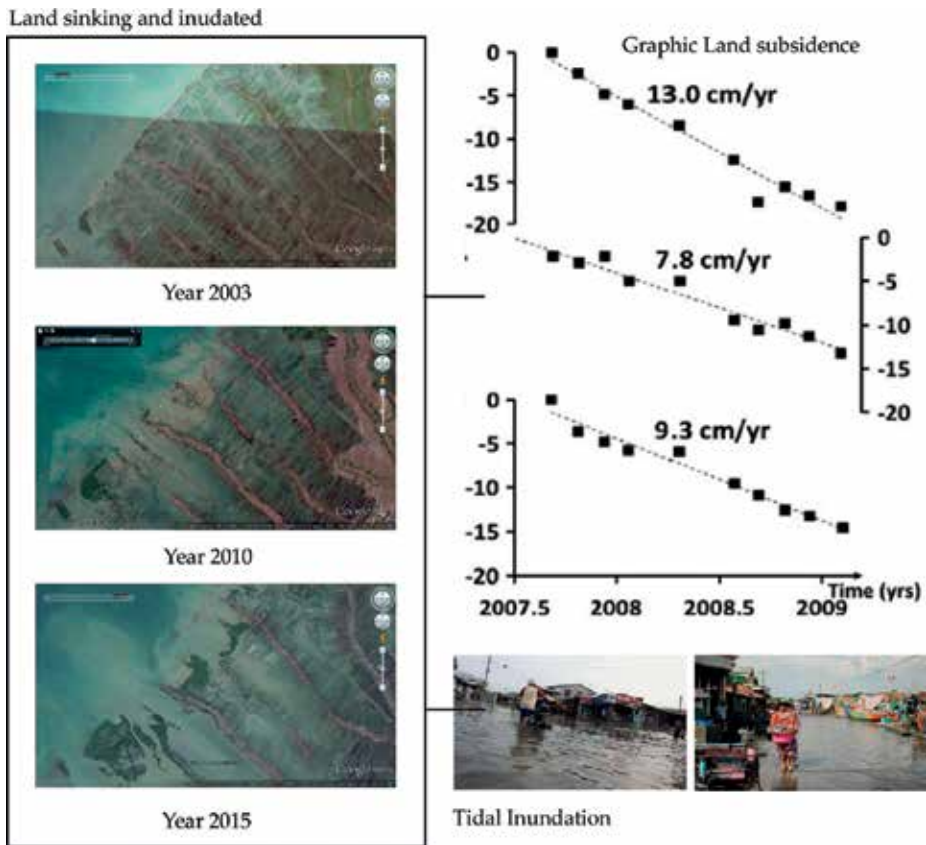
Figure 13. Graph of land subsidence in Demak (modified from [8]) correlated with pictures of existing tidal inundation and also with satellite images of land sinking (sources: authors, [18, 19]). We can see the general linear trend of subsidence indicating the sinking of the land.

inundation. **Figure 13** shows a graph of the subsidence in the Demak area along with a picture of tidal inundation in the field, as well as a depiction from a time series of high-resolution satellite image.

Pondok Bali Blanakan is a coastal area a few hundred kilometers east of Jakarta, and is mostly a farming and fishing area. First, it is quite surprising that this natural farming and fishing area is suffering from significant land subsidence. Nevertheless, after a detailed investigation we found that the area is an oil and gas exploitation area. The huge amount of oil and gas exploitation is causing subsidence. While the low land of the coastal area is sinking over time, more frequent tidal inundation is attacking the area and in certain places it has already become permanently inundated. Based on high-resolution satellite image analysis, it was found that a few hundred hectares of the Pondok Bali Blanakan area are suffering from inundation. **Figure 14** shows a graph of the subsidence in the area along with a picture of tidal inundation in the field, as well as a depiction from time series of high-resolution satellite image analysis. Again, we can see clear evidence of disaster.
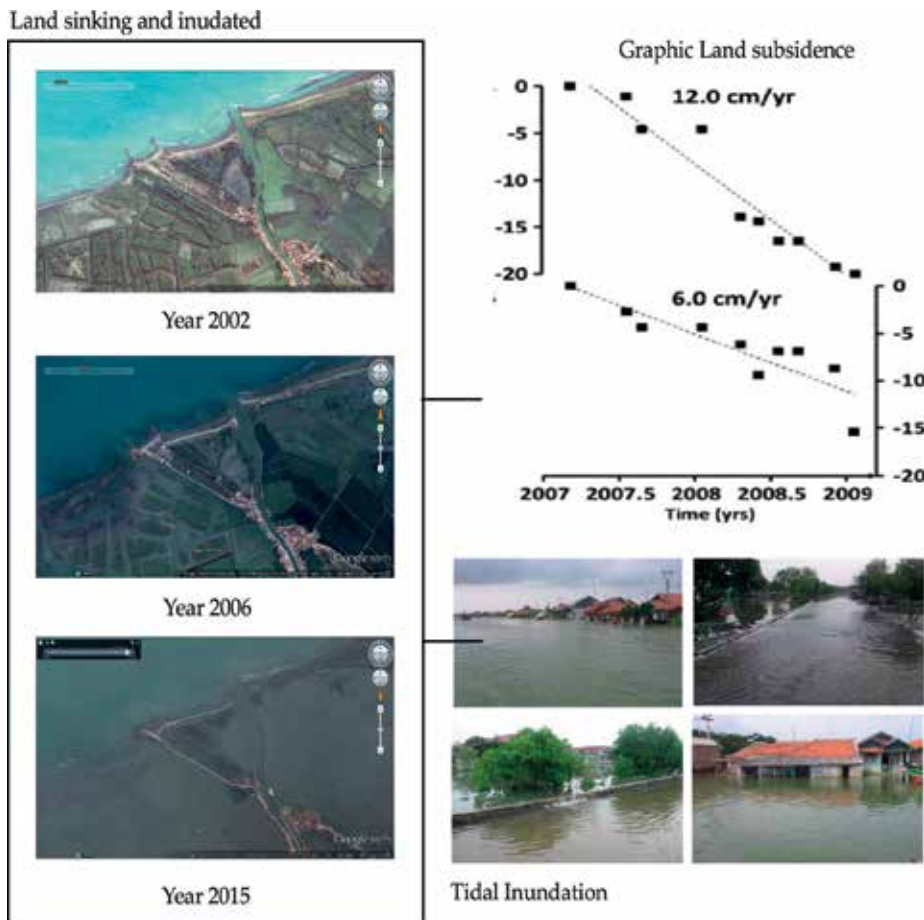
Figure 14. Graph of land subsidence in Pondok Bali Blanakan (modified from [8]) correlated with existing tidal inundation and also with the satellite images of land sinking (sources: authors, [18, 19]). We can see the linear trend of subsidence indicating the sinking of land and making it regularly inundated.

5. Discussion

Based on the correlation between land subsidence and flooding in some areas in Indonesia we can see clearly that the correlation between them is very strong and may result in disastrous situations. We can see that the significant area suffering from subsidence is also constantly suffering from flooding and tidal inundation. When we speak of disaster, we tend to think of economic loss. Indeed, millions of dollars have to be spent fixing problems from both land subsidence and flooding, and it seems more will be spent in the future. So, based on this fact we need better mitigation and/or adaptation. For example, if indeed flooding proves to be influenced significantly by land subsidence, in this case reducing or even stopping the subsidence might be the best mitigation. This fact shows that it is possible to stop land subsidence by stopping groundwater extraction and/or recharging artificially [8–10, 14, 20].

As far as we have seen, mitigation and/or adaptation are still beyond the best agenda in Indonesia. Only sporadic or short-term measures have been created against these problems such as building temporary dykes, elevating the land, roads, housing, etc., including building up mangrove areas in many places along coastal subsiding areas. Long-term measures such as building giant sea walls or stopping subsidence are still ongoing or are being planned and discussed. In fact, talking about stopping land subsidence is still an issue. Note that sometime in the future these problems may worsen if we see significant linear rate of subsidence in those areas; on the other hand, attempts to mitigate or adapt to this situation are still beyond the best agenda.

Indonesia is one of the fastest-growing countries in the world. In spite of this remarkable achievement, the ecological potential disaster from subsidence and flooding as explained in this chapter is quite serious. It is perhaps one of the mistake actions on growing the country. This descriptive chapter can be a lesson to learn for other growing countries. Do not make the same mistake. Do not let subsidence happen significantly. If possible do not let it happen at all. Singapore is a prime example for less subsidence. This country forbids the extraction of any groundwater.

We have been warned of global climate change consequences. Melting of ice caused by rising global temperatures is making the sea level rise. This sea level rise is projected to cause risk of flooding in coastal areas of the world. By this descriptive chapter we can see the risk is even multiple higher. The rates of sea level rise are generally a few millimeters per year [21, 22], while coastal subsidence can be up to a decimeter per year. This means that global climate change consequences may arrive earlier for coastal-subsiding areas such as Jakarta, Semarang, and probably others in the world.

6. Conclusions

Subsidence produces a number of impacts such as infrastructure damage, problems with drainage, wider expansion of flooding, as well as tidal inundation. The impacts can be quite costly. In some regions of Indonesia, land subsidence and the negative impacts in the shape of flooding and tidal inundation clearly exist. In Jakarta and Bandung we can see that subsiding areas close to rivers are frequently suffering from flooding. Tidal inundation comes regularly to subsiding coastal areas such as Jakarta, Blanakan, Semarang, and Demak. This typical situation can probably also be seen in other regions of Indonesia. Based on insight and looking at the correlation between land subsidence and flooding, we can conclude that the correlation between them is very strong and can be disastrous.

We need to perform mitigation and/or adaptation respectively. Nevertheless, as mentioned in the discussion, as far as we have seen, mitigation and/or adaptation are still beyond the best agenda in Indonesia. Only sporadic or short-term measures have been created against these disasters such as building temporary dykes, elevating the land, roads, housing, etc., including building up mangrove areas in many places along coastal-subsiding areas.

The descriptive explanation throughout this chapter can hopefully provide better mitigation and/or adaptation in Indonesia such as building giant sea walls or stopping subsidence. Note

once again that in the future these disastrous situations may even worsen if we see a significant linear rate of subsidence. This chapter will hopefully become a lesson learnt for other places around the world, especially those growing countries prone to subsidence and flooding.

Acknowledgements

Author details

Heri Andreas*, Hasanuddin Z. Abidin, Irwan Gumilar, Teguh P. Sidiq, Dina A. Sarsito and Dhota Pradipta

*Address all correspondence to: heriandreas49@gmail.com

Geodesy Research Division, Faculty of Earth Science and Technology, Institute of Technology Bandung, Bandung, West Java, Indonesia

References

[1] Bell J, Amelung F, Ramelli A, Blewitt G. Land subsidence in Las Vegas, Nevada, 1935-2000: New geodetic data show evolution, revised spatial patterns, and reduced rates. Environmental and Engineering Geoscience. 2002;**8**(3):155-174

[2] Abidin HZ, Djaja R, Andreas H, Gamal M, Hirose K, Maruyama. Capabilities and constraints of geodetic techniques for monitoring land subsidence in the urban areas of Indonesia. Geomatics Research Australia. 2004;**81**:45-58

[3] Abidin HZ. Suitability of levelling, GPS and INSAR for monitoring land subsidence in urban areas of Indonesia. GIM International. 2005;**19**(7):12-15

[4] Abidin HZ, Andreas H, Djaja R, Darmawa D, Gamal M. Land subsidence characteristics of Jakarta between 1997 and 2005, as estimated using GPS surveys. In: GPS Solutions. Berlin/Heidelberg: Springer; 2008. DOI: 10.1007/s10291-007-0061-0

[5] Abidin HZ, Andreas H, Gamal M, IGumilar I, Napitupulu M, Fukuda Y, et al. Land subsidence characteristics of the Jakarta Basin (Indonesia) and its relation with groundwater extraction and sea level rise. In: Taniguchi M, Holman IP, editors. Groundwater Response to Changing Climate, IAH Selected Papers on Hydrogeology, Chapter 10. Vol. 16. London: CRC Press; 2010. pp. 113-130. ISBN: 978-0-415-54493-1

[6] Cabral-Cano E, Dixon TH, Miralles-Wilhelm F, Diaz-Molina O, Sanchez-Zamora O, Carande RE. Space geodetic imaging of rapid ground subsidence in Mexico City. Geological Society of America Bulletin. 2008;**120**(11-12):1556-1566. DOI: 10.1130/B26001.1

[7] Meckel TA. An attempt to reconcile subsidence rates determined from various techniques in southern Louisiana. Quaternary Science Reviews. 2008;**27**(15-16):1517-1522. DOI: 10.1016/j.quascirev.2008.04.013

[8] Chaussard E, Amelung F, Abidin HZ, Hong SH. Sinking cities in Indonesia: ALOS PALSAR detects rapid subsidence due to groundwater and gas extraction. Remote Sensing of Environment. 2013;**128**:150-161. DOI: 10.1016/j.rse.2012.10.015

[9] Andreas H, Abidin HZ, Gumilar I, Sidiq TP, Yuwono B. Adaptation and mitigation of land subsidence in Semarang. AIP Conference Proceedings. 2017

[10] Holzer, Thomas L. Land subsidence caused by groundwater withdrawal in urban areas. GeoJournal. 1985;**11**(3):245-255. Reidel Publishing Company

[11] Andreas H, Usriyah HZ, Abidin H, Sarsito DA. Tidal inundation ("Rob") investigation using time series of high resolution satellite image data and from in situ measurements along northern coast of Java (Pantura). In: IOP Conference Series: Earth and Environmental Science; 2017. Vol. 71. p. 012005. DOI: 10.1088/1755-1315/71/1/012005

[12] Deltares. Personal Communication; 2018

[13] Marine and Fishery Department. Slide Presentation, Forum Group Discussion; 2009

[14] Gumilar I, Abidin HZ, Andreas H, Sidiq TP, Gamal M, Fukuda Y. Land subsidence, groundwater extraction, and flooding in Bandung Basin (Indonesia). In:International Association of Geodesy Symposia; 2014

[15] Susilo (2018). Personal Communication

[16] NCICD. Project Report, National Committee Integrated Coastal Development; 2014

[17] Government of Jakarta Province. Personal Communication; 2018

[18] Kompas Digital Image Gallery

[19] Google Earth

[20] JICA. Lesson learned from land subsidence in Tokyo, Japan. In: Presentation on "High Level Meeting on Subsidence." Balai Kota DKI, Jakarta, Indonesia; 2014

[21] Nurmaulia SL, Fenoglio-Marc L, Becker M. Long term sea level change from satellite altimetry and tide gauges in the Indonesian region. In: Paper presented at the EGU General Assembly; 2010, May 2-7; Vienna, Austria; 2010

[22] IPCC. In: Stocker TF, Qin D, Plattner GK, Tignor M, Allen SK, Boschung J, Nauels A, Xia Y, Bex V, Midgley PM, editors. Climate Change 2013. The Physical Science Basis. Contribution of Working Group I to the Fifth Assessment Report of the Intergovernmental Panel on Climate Change. Cambridge, United Kingdom and New York, NY, USA: Cambridge University Press; 2013

Assessing the Impact of Land Use Changes and Rangelands and Forest Degradation on Flooding Using Watershed Modeling System

Nafise Moghadasi, Iman Karimirad and
Vahedberdi Sheikh

Additional information is available at the end of the chapter

Abstract

Extensive flood damages all over the world necessitate flood risk mitigation. Land use changes affect hydrological characteristics such as total runoff and flood's peak flow. This study investigates the impacts of land use change on flooding of the Boostan dam catchment in Golestan province, Iran. For this purpose, watershed modeling system (WMS) is used to compare different types of land uses between 1996 and 2006 using corresponding maps. After calibration and validation of the model in each period of time, flooding of the catchment was evaluated using two representative parameters of peak flow and volume of flood. Comparison of land use maps in 1996 and 2006 revealed the total rangelands have been increased while good rangeland areas decreased, fair rangeland increased, and poor rangeland remained relatively constant. It means the region faces decrease in high-quality rangelands in the catchment. Also the forest areas decreased. Both degradation of rangeland and deforestation intensify flooding. But peak flow and flood volume of the whole catchment have been mitigated. Because in spite of negligible change in total curve number (CN) of the catchment, rangelands in downstream and near residential areas converted to agricultural lands and upstream agricultural lands transformed to high- and medium-density rangelands. This means that distribution of land use changes was in such a way, influential upstream areas in flooding, associated with reduced CNs. So the implemented biological measures have reduced the flooding potential of the catchment. Sensitivity analysis of the model showed that 5% decrease in CN can cause 40% decrease in peak flow of the catchment and in contrast and 5% increase in CN can enhance flood peak flow up to 60%.

Keywords: flood, sensitivity analysis, curve number, Boostan dam

1. Introduction

With the rapid population increase and the associated demand on land resources, it is now incumbent upon policy makers and land use planners to adopt preventive and restorative measures [1]. Land use is an indicator of human interaction with nature. Therefore, it is necessary to discover and monitor land use changes in order to either protect the environment or ensure sustainable development [2]. Hydrological response of a watershed is representative of a bunch of its conditions and characteristics, and so land use changes may affect the performance of watershed [3]. Hydrologic impacts of land use and land cover change appear in many ways, such as total runoff, base flow, flood's peak flow, soil moisture, and evapotranspiration [4].

Watershed is a complex open system that should be modeled to achieve the desired objectives such as assessment and forecasting. Through the modeling of complex systems, the cost of studies will reduce, and it will be possible to predict how to manage the watershed for the future. One of the applications that are capable of geometric and hydrological modeling of watershed is the watershed modeling system (WMS). WMS was developed by Brigham University researchers in 1999 in cooperation with the US army corps of engineers. Due to the variety of appropriate hydrologic and hydraulic models included in WMS, nowadays experts use it to assess the watershed management projects [5].

Checking the stats and information about annual damages due to flooding in Iran and the whole world indicates the impact of this phenomenon on human well-being. In Golestan province, over the past four decades, 71 major flood events have been reported that caused total 380 casualties. Therefore, developing integrated programs to curb, control, and utilize the flood using appropriate management measures is inevitable [6]. Our understanding about the effects of mechanical and biological measures on watershed response to rainfall is one of the key issues in the watershed management and flood control studies. Implementation of any treatment in the watershed associates with changes in Manning's roughness coefficient, time of concentration, vegetation, and permeability of the soil. So it can cause changes in rainfall-runoff relation of the watershed and eventually flood peak discharge [7].

Many researchers investigated land use changes in different places. Ariapour et al. [8] studied land use changes of Barabad-Darook district in Sabzevar City, Iran, during 1987–2007 using remote sensing. Results indicated that third-rated and first-rated rangelands have been decreased from 6.85 to 4.14% and from 0.35 to 0.01%, respectively. Also irrigated agricultural lands are to be decreased from 6.53 to 0.07%. Therefore first-rated rangelands and irrigated agricultural lands have been nearly disappeared in this 20-year period. Nasri et al. [9] in Ardestan, Iran, used GIS and showed that almost 31% of the total area of the region had undergone some changes during a 30-year studied period.

Several studies on WMS and the relationship between land use change and floods have been conducted in Iran and other countries that some of them are mentioned here. Khosroshahi and Saghafian [10] used WMS and, according to curve number (CN) parameter sensitivity analysis, introduce it as the most sensitive parameter for calibration. Githui et al. [11] studied River

Nzoia catchment, Kenya, in a time period with an increase in agricultural area from 39.6 to 64.3% and a decrease in forest cover from 12.3 to 7.0%. It caused difference in runoff ranging from 55 to 68%. Assessing the impacts of land cover change on hydrological regimes which has been done by Germer et al. [12] showed influence of land use change and proved that deforestation for pasture may increase runoff volumes over wide regions of Amazonia. Hosseini [13] studied the WMS model capability in determining the flood peak flow in the Khuzestan Province, Iran. The results showed that WMS models' computed flood has a good correspondence with empirical equations' calculated values in this Khuzestan Province.

Asharf et al. [14] assessed the impact of land use change on Rawal watershed, sub-Himalayan region hydrology. They observed a decrease of over 16% in the scrub forest coverage, while built-up land increased threefold during 1992–2010 period that resulted in an increase of about 6% in the water yield and 14.3% in the surface runoff of the watershed. Zadsar and Azimi [15] studied impact of land use changes on hydrological response Gorganroud catchment, Golestan, Iran, using SWAT. Accordingly, biomechanical measures can reduce runoff up to 20.7%.

Although flood is mainly a function of climatic conditions, especially the amount, intensity, and spatiotemporal distribution of rainfall, various features of watershed such as land cover and land use that consist of rangeland and forest degradation are other effective parameters. In this chapter, the effect of land use changes, especially rangeland and forest degradation, on peak flow of flood have been evaluated in Boostan dam catchment involving 14 watersheds.

2. Materials and methods

Boostan dam catchment is a part of Gorganroud basin in the east of Golestan province, Iran (**Figure 1**). It drains approximately 1562 km^2 and is situated within 37°23ʹ to 37°46ʹ north latitude and 55°26ʹ to 56°4ʹ east longitude.

In this chapter, impact of land use changes specially rangeland and forest degradation on runoff generation and flooding potential in Boostan dam catchment with 14 sub-basins was studied by employing WMS (version 7). For this purpose, digital elevation model (DEM) is prepared, and land use maps of the catchment in two time periods of 1996 and 2006 (**Figure 2**) are compared in GIS. This time interval was chosen due to major watershed management measures in the region performed in these years. The investigation involves amount of changes in land use as well as its spatial distribution. So areas of each land use types such as forest, rangeland, and agriculture are calculated and compared. Then distribution of the changes in upstream and downstream areas of each watershed was determined.

In general, watershed management measures in the Boostan dam catchment area can be classified in mechanical operations including construction of debris dams (61 items), rocky mortar structures (5 cases), and gabioning (55 items) and biological measures such as grazing plans, pitting along with seeding, and fertilizing. Also in Chenarly, Gharnave, and Karim ishan sub-basins' extensive forestation has been carried out.
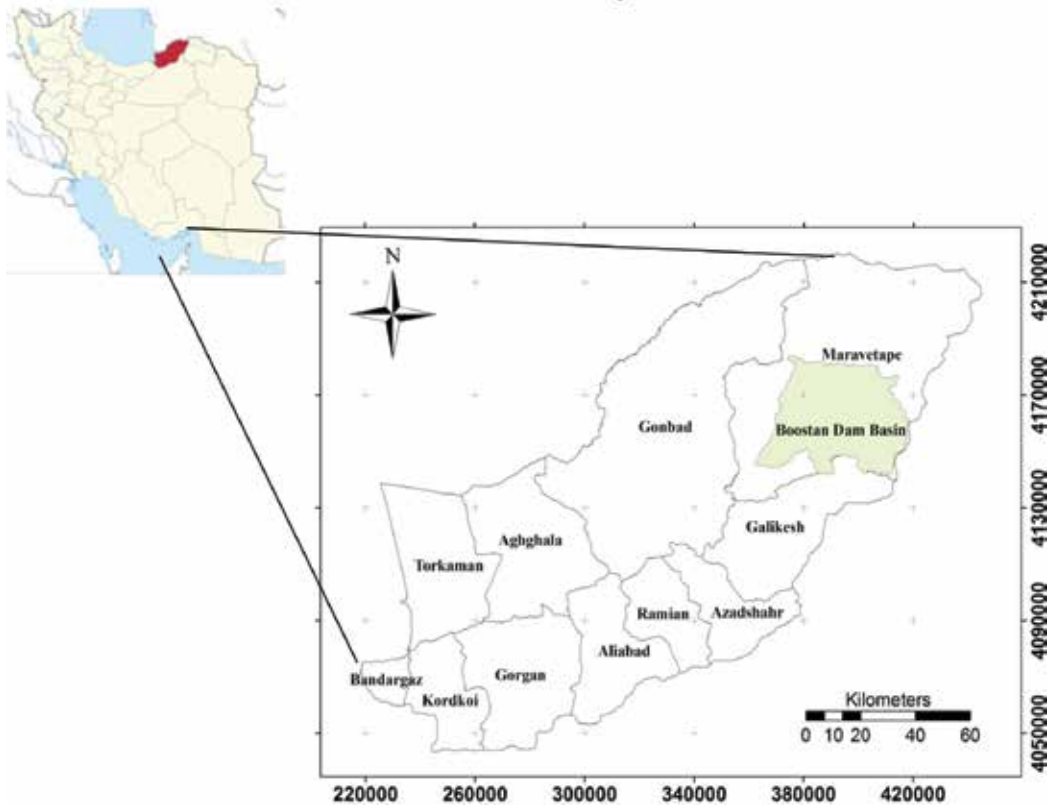
Figure 1. The situation of Boostan dam catchment in Golestan province, Iran.
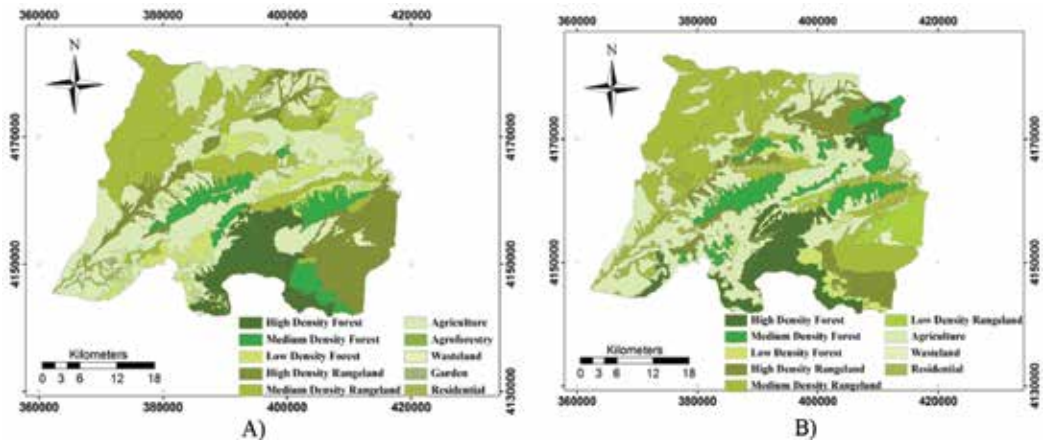
Figure 2. Boostan dam catchment land use map: (A) 1996 and (B) 2006.

In order to incorporate spatial distribution of land use changes, the catchment was divided into 14 watersheds using WMS. Runoff curve number values were obtained and rainfall-runoff modeled according to soil conservation service (SCS) method. The runoff curve number (also called a curve number or simply CN) is an empirical parameter used in hydrology for predicting direct runoff caused by rainfall. CN is a dimensionless number that relates to soil and covers conditions of the catchment and has a range of 0–100. CN = 0 means no runoff, and CN = 100 means no infiltration, and it is documented by SCS [16]. The soil conservation service (SCS) model estimates precipitation excess as a function of cumulative precipitation, soil cover, land use, and antecedent moisture. This method generates CN values integrating land use/land cover and hydrologic group of soil to determine precipitation lost [17]. S in this method is potential maximum retention after runoff begins (Eq. 1). On the other hand, R indicates total runoff (Eq. 2). This equation is only valid for P > 0.2S; if P is less than or equal to 0.2S, there is no runoff. In this section, the lag time is calculated using the SCS method, which is done separately for each sub-basin. The SCS CN method relationships are as follows (Eq. 3 to Eq. 6):

$$S = \frac{25400}{CN} - 254 \tag{1}$$

$$R = \frac{(P - 0.2S)^2}{(P + 0.8S)} \tag{2}$$

$$T_{lag} = \frac{L^{0.8}(S+1)^{0.7}}{1900\sqrt{Y}} \tag{3}$$

$$T_P = \frac{\Delta t}{2} + T_{lag} \tag{4}$$

$$U_P = 2.08\frac{A}{T_P} \tag{5}$$

$$T_c = 1.67\,T_{lag} \tag{6}$$

where P = accumulated rainfall depth at time t; T_{lag} = the basin lag, defined as the time difference between the center of mass of rainfall excess and the peak of the unit hydrograph (UH); L = hydraulic length (the longest flow path in the watershed); Y = average watershed slope in percent; T_P = time to peak; Δt = the excess precipitation duration (which is also the computational interval in the run); U_P = peak of standard UH; A = watershed area; and T_c = time of concentration.

The model calibration performed by optimizing estimated curve number and efficiency of optimized model is evaluated by comparing observed and simulated hydrographs of real flood events. Some other flood hydrographs used to indicate validity of the model. After validating the hydrological model of Boostan dam catchment, the effect of land use changes that caused changes in curve numbers was examined in several rainfall events. It should be noted that to investigate the impact of rangeland and forest degradation on flooding of the catchment, two representative parameters of peak flow and volume of flood were considered.

Watershed modeling system (WMS) is equipped with automatic calibration in a feasible range. In this approach changing of some parameters continues until the best matching of the observed hydrograph and simulated one is achieved, and the most suitable values of calibration parameters are obtained. In calibration phase, due to the importance of peak discharge of flood, maximum discharge is considered as the fitting index. Regarding the use of SCS method, the curve number (CN) is considered as calibration parameter.

Physiographic characteristics are main inputs of hydrological modeling software WMS. In order to calculate physiographic characteristics of the catchment, 1:250,000 topography maps of national cartographic center of Iran in 2006 have been used. Calculated values for each watershed of Boostan dam catchment are shown in **Table 1**.

Soil hydrologic group map is another input data for SCS model, and the amounts of runoff depend on it. Map of soil hydrologic group of the catchment is presented in **Figure 3**. In **Figure 3**, B and C represent soil hydrologic groups with permeability in range of 3.8–7.5 and 1.3–3.8, respectively.

As the next step, each of land use maps of 1996 and 2006 was integrated with soil hydrologic group map in WMS, and then using the table of CN (**Table 2**), curve numbers per watershed were determined. **Figure 4** represents curve number map of Boostan dam catchment in 1996 and 2006.

To simulate the catchment in WMS, flood hydrographs recorded in Tamar hydrometric station at the catchment's outlet were investigated. To determine the corresponding rainfalls, daily

Watersheds	Area (km^2)	Slope (m/m)	Average altitude (m)	Length of main stream (m)	Slope of main stream (m/m)
Kalshor	116.65	0.118	414.90	32580.5	0.013
Shordare	123.23	0.181	461.21	24668.4	0.015
Aghemam	143.02	0.192	548.49	20832.1	0.015
Chenarli	69.04	0.165	756.52	12495.7	0.022
Gharnave	94.97	0.239	934.82	19967.9	0.034
Karimishan	128.40	0.208	675.61	25972.3	0.026
Ghopan	46.19	0.174	396.39	13068.8	0.029
Azizabad	112.87	0.188	375.25	25304.3	0.011
Zav	135.01	0.245	906.04	17861.9	0.025
Golidagh	190.20	0.221	860.51	38121.7	0.015
Yelcheshme	265.01	0.161	1333.48	30862.5	0.028
Sub-basin 1	55.64	0.129	307.54	10875.7	0.017
Sub-basin 2	45.34	0.067	212.55	14189.6	0.011
Sub-basin 3	41.41	0.082	174.94	9477.4	0.015

Table 1. Physiographic characteristics of Boostan dam catchment.
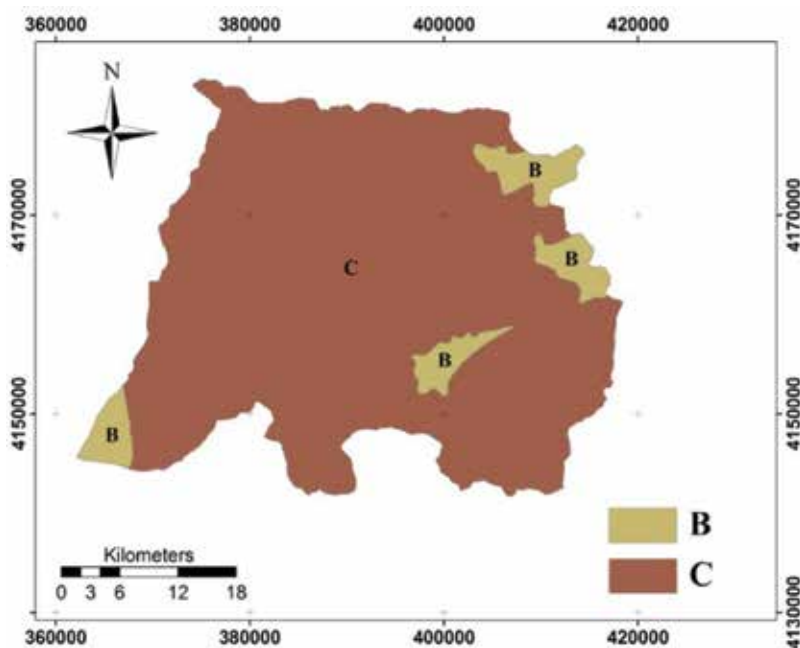
Figure 3. Soil hydrologic group map of Boostan dam catchment.

Cover description		Curve number for hydrologic soil group			
Cover type	Hydrologic condition	A	B	C	D
Pasture, grassland, or range-continuous forage for grazing	Poor	68	79	86	89
	Fair	49	69	79	84
	Good	39	61	74	80
Woods	Poor	45	66	77	83
	Fair	36	60	73	79
	Good	30	55	70	77
Farmstead building, lanes, driveways, and surrounding lots	—	59	74	82	86

Table 2. Runoff curve number for some land use types.

rainfall records of rain-gauge stations in and around Boostan dam catchment provided by Golestan Regional Water Authority are used. **Table 3** shows some information about these stations.

It should be noted that in this chapter, to analyze the model's results, observed and simulated hydrographs of three flood events are compared using four statistics including root mean square error (RMSE), coefficient of determination (R^2), Nash Sutcliffe efficiency index (E), and index of agreement (d). RMSE indicates the error rate, and zero is the best value for it [18]:
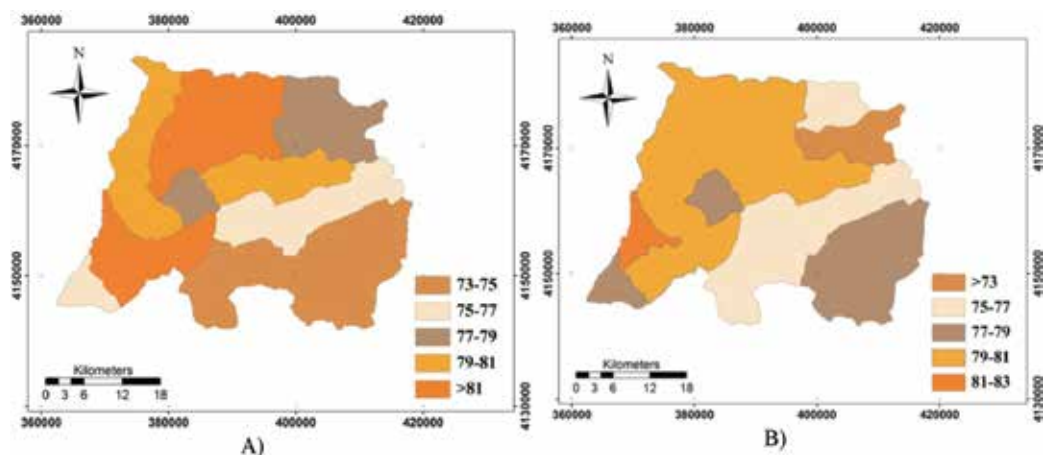
Figure 4. The curve number map of Boostan dam catchment: (A) 1996 and (B) 2006.

Station name	Date of establishment	Altitude (m)	Geographical coordinates	
			Latitude	Longitude
Tamar	1965	132	37°28'	55°29'
Park meli Golestan	1997	460	37°24'	55°49'
Gharnagh	1996	500	37°43'	55°43'
Golidagh	1996	1000	37°39'	56°00'
Pishkamar	1970	250	37°36'	55°35'
Zavebala	1997	700	37°31'	55°45'

Table 3. Some information about rain-gauge stations in and around Boostan dam catchment.

$$\text{RMSE} = \sqrt{\frac{\sum_{i=1}^{n} \left(O_i(t) - P_i(t)\right)^2}{n}} \tag{7}$$

in which O_i (t) is observed discharge at time t, Pi (t) is calculated discharge at time t, and n is the number of observations.

Coefficient of determination is a number between 0 and 1 and the number closer to 1; the correlation between the observed data and computed values is better [19]:

$$R^2 = \left(\frac{\sum_{i=1}^{n} \left(O_i - \overline{O}\right)\left(P - \overline{P}\right)_i}{\sqrt{\sum_{i=1}^{n} \left(O_i - \overline{O}\right)^2} \sqrt{\sum_{i=1}^{n} \left(P_i - \overline{P}\right)^2}} \right)^2 \tag{8}$$

Nash Sutcliffe efficiency index ranges from negative infinity to 1 that means observation data and calculated ones are entirely corresponded [20]. An efficiency of 1 (E = 1) corresponds to a perfect match between model and observations. An efficiency of 0 indicates that the model predictions are as accurate as the mean of the observed data, whereas an efficiency less than zero ($-\infty < E < 0$) occurs when the observed mean is a better predictor than the model. Essentially, the closer the model efficiency is to 1, the more accurate the model is:

$$E = 1 - \frac{\sum\limits_{i=1}^{n} (O_i - P_i)^2}{\sum\limits_{i=1}^{n} (O_i - \overline{O})^2} \tag{9}$$

Finally index of agreement is between 0 and 1; the values closer to 1 show higher accordance between the observed and computed data [19]:

$$d = 1 - \frac{\sum\limits_{i=1}^{n} (O_i - P_i)^2}{\sum\limits_{i=1}^{n} \left(|P_i - \overline{O}| + |O_i - \overline{O}|\right)^2} \tag{10}$$

Sensitivity of the model to CN was analyzed to assess effectiveness of this variable factor on floods in the region. In this chapter, the sensitivity of flood peak flow at the catchment's outlet to the curve number was determined. For this purpose, the parameter changed from -10 to $+10\%$, and its impact on the flood discharge was determined.

3. Results

Land use changes were assessed using GIS in ArcMap 9.3 framework. Land use maps have been prepared by the Department of Natural Resources and Watershed Management in Golestan province. The results are presented in **Table 4**. Accordingly the whole area of forests and rangelands decreased from 1060.36 to 1027.67 km^2 in 10 years. Although the total area of rangeland increased by 17.24 km^2, high-density rangeland decreased by 78.47 km^2, medium-density rangeland increased by 93.24 km^2, and low-density rangeland area remained relatively constant. This represents a decrease in rangeland quality of the catchment, which has a negative impact on its flooding.

Result also revealed that rangelands in downstream and near residential areas changed to agriculture. On the other hand, upstream agriculture areas in 1996 changed to high- and medium-density rangeland probably due to lack of precipitation. Also some areas located in Golestan National Park territory changed from medium-density forest to medium-density rangeland that can be caused by natural or anthropogenic factors that have a great importance from environmental point of view.

Land use	1996		2006		Percent of change
	Total catchment (%)	Area (km^2)	Total catchment (%)	Area (km^2)	
Agriculture	32.20	508.31	33.76	533.02	4.84
Agroforestry	0.14	2.14	0.01	0.20	−92.86
Garden	0.05	0.81	0.02	0.30	−60.00
High-density forest	9.21	145.36	10.24	161.73	11.18
Semi-density forest	7.39	116.58	9.66	152.46	30.72
Low-density forest	9.07	143.19	2.60	41.01	−71.33
High-density rangeland	14.22	224.39	9.24	145.92	−35.02
Semi-density rangeland	23.48	370.44	29.56	466.68	25.89
Low-density rangeland	3.83	60.40	3.79	59.87	−1.04
Residential	0.10	1.51	0.74	11.65	640.00
Wasteland	0.31	4.83	0.38	6.01	22.58

Table 4. Land use distribution of Boostan dam catchment.

The other land use changes occur in this region are change from medium-density forest to low-density forest. Moreover, some high-density forests and low-density forests have been cultivated. Of course in few cases low-density forest changed to medium-density forest.

Determined curve numbers using calibrated Boostan dam catchment model before and after the implementation of watershed management measures are presented in **Table 5**. As demonstrated the total catchment's CN decreased from 78.21 to 78.05 that is ignorable.

Soil moisture retention, lag time, and time of concentration are calculated using SCS method and CN values. These calculations are performed by WMS software for each 14 watersheds. These parameters before and after implementation of watershed management measures are shown in **Table 6**.

Calibration and validation of WMS models are performed using three and two flood events in Tamar hydrometric stations, respectively. These flood hydrographs are shown in **Figures 5** and **6**.

The results of model verification indicate that there was a good coincidence between observed data and computed hydrographs in WMS. For example, coefficients of determination values were between 0.87 and 0.92 which suggests a high correlation. **Table 7** shows calculated statistics for the flood events used in model validation.

Table 8 demonstrates the impacts of land use changes due to rangeland and forest degradation on peak flow, and volume of flood in different return periods is shown. The mentioned results show that, for example, the mean 25-year peak flow decreased 15% between 1996 and 2006.

Table 9 shows different impacts of land use change due to rangeland and forest degradation on peak flow and volume of flood in all 14 watersheds of the catchment in 25-year return period.

Watersheds	1996	2006	Percent of change
Kalshor	80.06	79.66	−0.50
Shordare	81.51	80.52	−1.21
Aghemam	8170	79.94	−2.15
Chenarli	78.83	76.99	−2.33
Gharnave	78.04	70.29	−9.93
Karimishan	82.13	79.58	−3.10
Ghopan	78.94	78.07	−1.10
Azizabad	82.47	79.68	−3.38
Zav	73.44	75.14	2.31
Golidagh	74.48	75.73	1.68
Yelcheshme	74.42	78.82	5.91
Sub-basin 1	80.95	80.50	−0.56
Sub-basin 2	82.10	82.31	0.26
Sub-basin 3	74.80	77.15	3.14
Total	78.21	78.05	−0.20

Table 5. Curve number values of the watersheds in 1996 and 2006.

Watersheds	1996			2006		
	Soil moisture retention (mm)	Lag time (h)	Time of concentration (h)	Soil moisture retention	Lag time (h)	Time of concentration (h)
Kalshor	12.65	3.23	5.39	12.97	3.27	5.46
Shordare	11.52	2.56	4.28	12.29	2.64	4.41
Aghemam	11.38	2.19	3.66	12.75	2.31	3.86
Chenarli	13.64	1.89	3.16	15.18	1.99	3.32
Gharnave	14.29	2.10	3.51	21.47	2.62	4.38
Karimishan	11.05	2.40	4.01	13.04	2.61	4.36
Ghopan	13.55	1.78	2.97	14.27	1.83	3.06
Azizabad	10.80	2.49	4.16	12.96	2.72	4.54
Zav	18.37	2.23	3.72	16.81	2.13	3.56
Golidagh	17.41	3.86	6.45	16.28	3.72	6.21
Yelcheshme	17.46	3.92	6.55	13.65	3.44	5.74
Sub-basin 1	11.95	1.73	2.89	12.31	1.75	2.92
Sub-basin 2	11.08	2.83	4.71	10.92	2.80	4.68
Sub-basin 3	17.11	2.53	4.23	15.05	2.36	3.94

Table 6. Soil moisture retention, lag time, and time of concentration before and after implementation of watershed management measures.
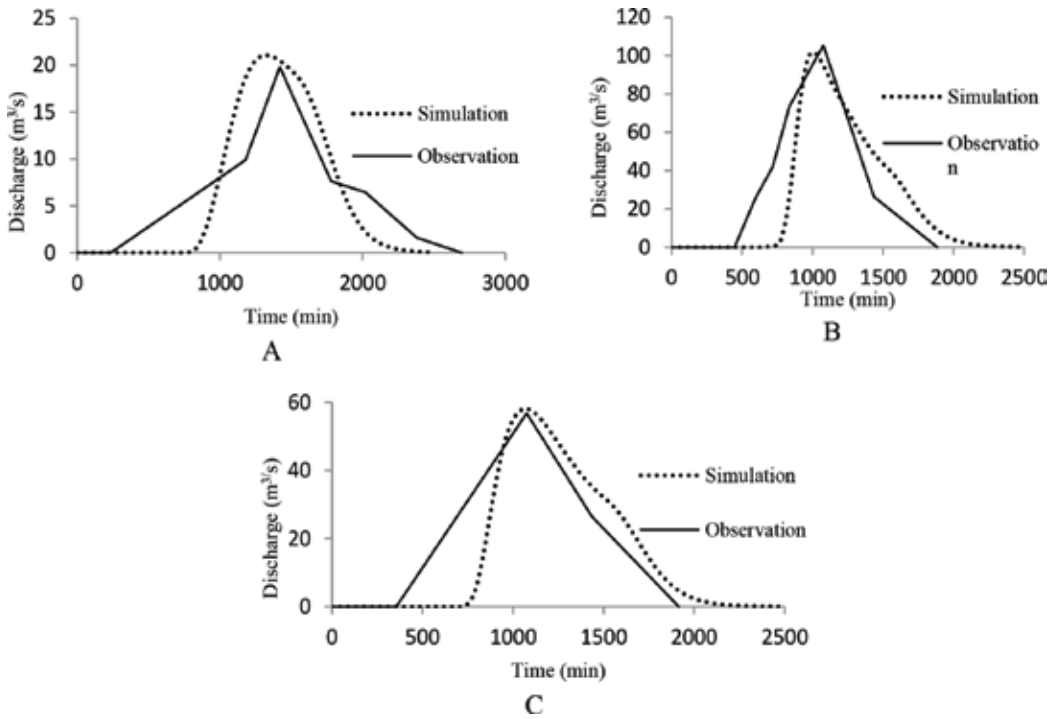
Figure 5. Observed and simulated flood hydrographs in Tamar station (used for calibration): (A) 11/6/1997, (B) 5/30/1998, and (C) 9/11/1998.
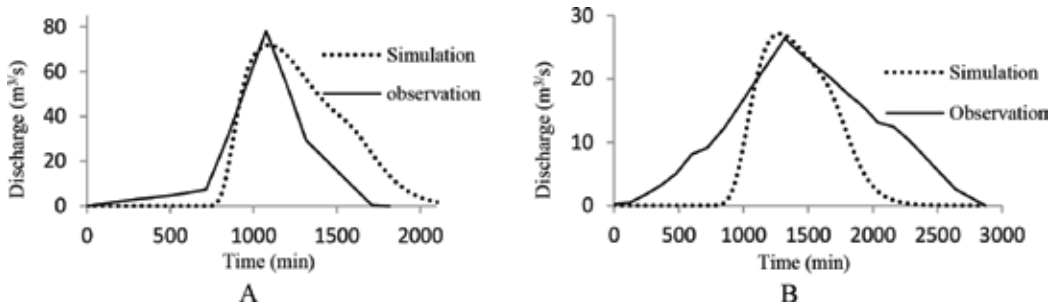
Figure 6. Observed and simulated flood hydrographs in Tamar station (used for validation): (A) 7/25/1998 and (B) 4/10/1999.

Sensitivity analyses investigate the model's sensitivity to changes in CN of watersheds of Boostan dam catchment. **Figure 7** shows flood's peak flow sensitivity to changes in curve number. Accordingly, 10% decrease and increase in CN values can cause up to −50 and 150% change in peak flow, respectively.

Date of event	Index of agreement	Nash Sutcliffe efficiency index	Coefficient of determination	Root mean square error
1997/11/6	0.92	0.54	0.92	0.58
1998/5/30	0.93	0.74	0.87	0.66
1998/7/25	0.92	0.63	0.88	0.88
1998/9/11	0.93	0.75	0.87	0.64
1999/4/10	0.87	0.32	0.89	0.57

Table 7. Statistics for model performance evaluation in different flood events.

Return period (years)	1996		2006	
	Peak flow (m^3/s)	Volume flood (1000m^3)	Peak flow (m^3/s)	Volume flood (1000m^3)
2	324.64	11213.59	283.72	11203.49
5	617.42	20424.06	531.52	20402.26
10	819.08	26579.50	701.29	26514.12
25	1076.05	34309.64	917.60	34188.83
50	1262.85	39820.19	1074.23	39668.44
100	1448.11	45265.43	1229.64	45075.48
200	1633.98	50697.64	1385.87	50473.60

Table 8. The impacts of land use change on peak flow and volume of flood in different return periods.

4. Discussion

According to statistics, simulated hydrographs are modeled properly compared to observe ones, so that the index of agreement ranges from 0.87 to 0.93, coefficient of determination (R^2) from 0.87 to 0.92, and root mean square error from 0.66 to 0.58 and Nash Sutcliffe efficiency indices are between 0.32 and 0.75. So the model showed good performance that it corresponds with results of Hosseini [13].

In spite of abovementioned land use changes that all had negative impact on flooding, the peak flow of modeled floods reduced. For example, the 25-year peak flow was decreased 15% that is in contrast with results of Githui et al. [11] as well as Asharf et al. [14]. The reason seems to be the distribution of changes that can be represented as the key achievement of this study. There were rangelands in downstream and near residential areas that changed to agriculture and upstream agriculture areas changed to high- and medium-density rangeland. So despite negligible change in total CN of the catchment, changes were in such a way that curve numbers of high slope areas in upstream lands that are effective in generating flood have been reduced that had decreasing impact on flood characteristics. Results of the sensitivity analysis

Watersheds	1996		2006	
	Peak flow (m^3/s)	Volume flood (1000m^3)	Peak flow (m^3/s)	Volume flood (1000m^3)
Kalshor	112.84	2823.06	114.04	2815.06
Shordare	140.76	2883.78	130.29	2739.41
Aghemam	179.70	3299.65	156.97	3011.69
Chenarli	91.14	1529.22	78.70	1384.95
Gharnave	118.74	2150.82	55.78	1321.51
Karimishan	163.52	3320.00	144.14	3003.88
Ghopan	66.51	1073.54	64.64	1044.43
Azizabad	152.88	3103.46	127.56	2734.36
Zav	113.04	2244.08	130.35	2468.34
Golidagh	122.40	3038.27	132.45	3750.61
Yelcheshme	163.48	4875.48	245.94	6348.19
Sub-basin 1	98.41	1533.42	102.71	1549.30
Sub-basin 2	56.35	1234.12	58.91	1261.53
Sub-basin 3	34.24	703.30	38.26	770.34

Table 9. The impacts of land use change on peak flow and volume of flood in different watersheds in 25-year return period.
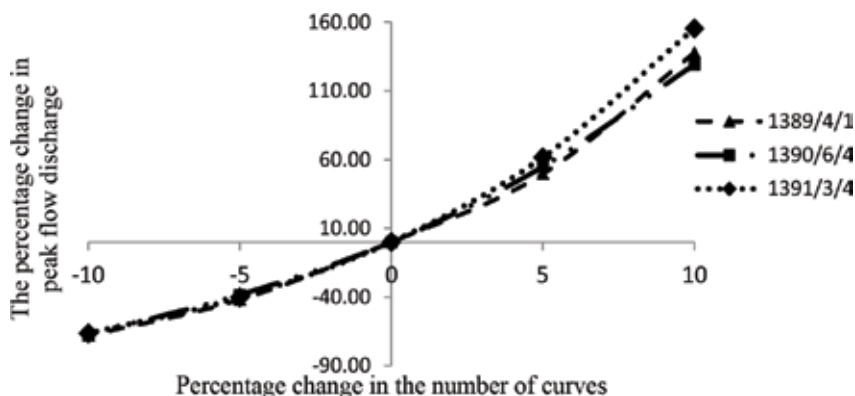
Figure 7. Flood peak flow sensitivity analysis to changes in CN.

emphasize on the importance of curve number parameter that is used to calibrate the model, and it corresponds with Khosroshahi and Saghafian [10]. The sensitivity analysis showed that if CN reduce 5%, peak flow of the catchment would decrease 40%, and on the other hand, 5% increase in CN will increase flood peak flow up to 60% that prove the importance of biological watershed management measures and prevention of forest and rangeland degradation.

5. Conclusions

In this chapter, hydrologic response of Boostan dam catchment in 1996 and 2006 simulated using WMS. Land use map investigation showed that the study area has 11 types of land uses. Assessment of changes in land use of Boostan dam catchment in the period 1996–2006 indicates that due to deforestation, more than 1.56% of the area is added to the farm lands. According to the results during the 10-year period, the total forest area has decreased, from 25.67 to 22.50%, and in contrast the rangeland area has increased from 41.53 to 42.63%. So the total forest and rangeland land uses in the catchment decreased almost 3%. Moreover in this period of time, high-density rangeland decreased 78.47 km^2 in other words 35.02% of its initial area; semi-density rangeland increased 96.24 km^2 that means 25.89% of its initial area, and low-density rangeland area remained relatively constant. This represents a decrease in rangeland quality of the catchment, which has a negative impact on its flooding. On the other hand, residential area increased more than seven times that has a negative impact on flooding too. It can be concluded that the implemented biological measures during this period of time have been effective to mitigate floods of the catchment.

It can be suggested that forestation in high lands as the main factor to mitigate flooding of a reign should continue and amplify. On the other hand, land management plans should focus on not only changes in main land uses (forest, rangeland) but also degradation in a particular land use, such as decline in quality of rangelands in the current study.

Author details

Nafise Moghadasi[1]*, Iman Karimirad[2] and Vahedberdi Sheikh[1]

*Address all correspondence to: nafisehmogadasi@yahoo.com

1 Department of Watershed Management, Gorgan University of Agricultural Sciences and Natural Resources, Gorgan, Iran

2 Deptartment of Irrigation and Reclamation Engineering, Faculty of Agricultural Engineering and Technology, College of Agriculture and Natural Resources, University of Tehran, Tehran, Iran

References

[1] Sakieh Y, Salmanmahiny A, Jafarnezhad J, Mehri A, Kamyab H, Galdavi S. Evaluating the strategy of decentralized urban land-use planning in a developing region. Land Use Policy. 2015;**48**:534-551

[2] Pandian M, Rajagopal N, Sakthivel G, Amrutha DE. Land use and land cover change detection using remote sensing and GIS in parts of Coimbatore and Tiruppur districts, Tamil Nadu, India. International Journal of Remote Sensing & Geoscience. 2014;**3**(1):15-20

[3]   Miller SN, Kepner WG, Mehaffey MH, Hernandez M, Miller RC, Goodrich DC, Devonald KD, Heggem T, Miller WP. Integrating landscape assessment and hydrologic modeling for land cover change analysis. Journal of the American Water Resources Association. 2002;**38**(4):915-929

[4]   Sikka AK, Sarma JS, Sharda VN, Samraj P, Lakshmanam V. Low flow and high flow responses to converting natural grassland into Bluegum (*Eucalyptus globulus*) in Nilgiris watersheds of South India. Journal of Hydrology. 2003;**2**(70):12-26

[5]   WMS. Watershed Modeling System v7.0, Reference Manual. Environmental Modeling Research. Utah, USA: Laboratory of Brigham Young University; 1999

[6]   Brouwer R, Van EK. Reintegrated ecological, economic and social impact assessment of alternative flood control policies in the Netherlands. Ecological Economics. 2004;**50**:1-21

[7]   Simonovic SP. Two new non-structural measures for sustainable management of floods. Water International. 2002;**27**:38-46

[8]   Ariapour A, Dadrasi Sabzevar A, Toloee S. Estimation of vegetation and land use changes using remote sensing techniques and geographical information system (case study: Roodab plain, Sabzevar City). Journal of Rangeland Science. 2013;**4**(1):1-13

[9]   Nasri M, Sarsangi A, Yeganeh H. Detection of land use changes for thirty years using remote sensing and GIS (case study: Ardestan area). Journal of Rangeland Science. 2013; **4**(1):23-33

[10]   Khosroshahi M, Saghafian B. Routing Role of the River in the Identification and Resolution of Flood- Prone Areas in the Watershed. Presented at the Fifth Conference on Hydraulic, Shahid Bahonar University of Kerman, Iran (in Persian); 2005

[11]   Githui F, Mutua F, Bauwens W. Estimating the impacts of land-cover change on runoff using the soil and water assessment tool (SWAT): Case study of Nzoia catchment. Journal of Hydrological Sciences. 2009;**54**(5):899-908

[12]   Germer S, Neill C, Krusche AV, Elsenbeer H. Influence of land-use change on near-surface hydrological processes: Undisturbed forest to pasture. Journal of Hydrology. 2010;**380**(3): 473-480

[13]   Hosseini Y. WMS model assessment in determining the maximum flood discharge in Khuzestan province. Presented at the First National Conference on Strategies for Achieving Sustainable Development in Agriculture, Natural Resources and the Environment, Tehran (in Persian); 2012

[14]   Asharf A, Naz R, Wahab A, Ahmad B, Yasin M, Saleem M. Assessment of Landuse change and its impact on watershed hydrology using remote sensing and SWAT modeling techniques—A case of Rawal watershed in Pakistan. International Journal of Agricultural Science and Technology. 2014;**2**(2):61-68

[15] Zadsar M, Azimi M. Using SWAT model to investigate the impact of rangeland management practices on water conservation (case study: Gorganroud watershed, Golestan, Iran). Journal of Rangeland Science. 2016;**6**(4):309-319

[16] SCS. National Engineering Handbook, Section 9: Hydrologic Soil-Cover Complexes. Washington, D.C: Soil Conservation Service, USDA; 2004

[17] Cronshey R, McCuen R, Miller N, Rawls W, Robbins S, Woodward D. Urban hydrology for small watersheds—TR–55: Washington. DC, US Dept. of Agriculture, Soil Conservation Service, Engineering Division, Technical Release 55. 1986. p. 164

[18] Willmott CJ. On the validation of models. Physical Geography. 1981;**2**(2):184-194

[19] Legates DR, McCabe GJ Jr. Evaluating the use of "goodness-of-fit" measures in hydrologic and hydro climatic model validation. Water Resources Research. 1999;**35**(1):233-241

[20] Nash JE, Sutcliffe JV. River flow forecasting through conceptual models. Discussion of principles. Journal of Hydrology. 1970;**10**(3):282-290

Extent of 2014 Flood Damages in Chenab Basin Upper Indus Plain

Shakeel Mahmood and Razia Rani

Additional information is available at the end of the chapter

Abstract

This chapter analyzes the extent of flood damages in the Chenab basin upper Indus plain. The upper Indus plain is a fertile area and supports millions of human population and diverse economic activities. Every year in summer, the combined action of monsoon rain water and meltwater (melting of snow and glaciers) augment rivers discharge leading to damaging flood. The study region is prone to floods. The upstream areas of Chenab basin are mountainous and experiences characteristics of flash floods, whereas riverine floods dominate the lower reach. In wake of observed climate change, there is a rising trend in temperature, which indicates the early and rapid melting of snow and glaciers in the catchment areas. The analysis reveals that the spatial and temporal scales of violent weather events have also been grown during the past three decades. The substantial increase in heavy precipitation events and rapid melting of snow in the headwater region, siltation in river channels, human encroachments on the active flood plain and bursting of embankments have further escalated the flooding events. Analysis further reveals that in the study region, almost every year, the floodwater overflows the levees and cause damages to standing crops, infrastructure and sources of livelihood, and incurs human casualties.

Keywords: flood, Chenab basin, damages, Indus plain

1. Introduction

Flood is destructive hydrometeorological hazard causing damages to life, infrastructure, and services [1–3]. Globally, flood disaster claims over 20,000 human lives and reflective property loss annually [4]. Various natural and anthropogenic factors generate riverine floods [5, 6]. The catchment characteristics including vegetation cover, shallow soil and

steep slope, and high intensity rainfall generate sharp peaks in short span of time which results in flood in the low-lying areas [7, 8]. Similarly, in the current scenario of climate change, the frequency and intensity of violent weather events and floods might become more prevalent. This has further increased vulnerability of the communities spatially distributed in the proximity of rivers [9].

Pakistan is exposed to devastating natural hazards including floods, earthquake, landslides, and droughts because of diverse topography and climatic conditions [10]. Floods have been common and disastrous in Pakistan [11]. Rainfall in monsoon period and melting of snow/glaciers in northern Pakistan are flood generating factors [12]. Monsoon is the major source of summer rainfall which contributes 50–75% of the total rainfall [13]. Monsoon season temporally extends from June to September in South Asia, but it brings more rain during July and August which results in disastrous floods [14]. Pakistan has faced flood events of various magnitude since 1950 but the catastrophic were in 1988, 1992, 2010, and 2014 [15]. The hydrometeorological conditions, geography, and lack of standard structural measures in the Indus watershed are the main factors of flood genesis [16]. In 2010, Pakistan was hit century worst flood and anthropogenic activities in the fertile Indus plain further intensified its damaging nature. This destructive nature of flood has damaged buildings, infrastructure, and agricultural activities with huge economic loss [14]. About 1900 people died, affecting more than 20% of the total area and more than 14 million people with economic losses of tens of billions US$. The spatial extent, depth, duration, and direct effect of flood were variable because of the spatial diversity in relief features and landforms, human land uses, population density, and anthropogenic activities. This was the most calamitous flood in Pakistan's flood history [15]. Similarly, high flood in river Chenab and Jhelum has been observed in September 2014 in which Chenab has attained peak of 0.45 million m^3/s [16]. The purpose of this study is finding the extent of 2014 flood damages in Chenab basin.

In Pakistan, flood is one of the devastating natural hazards causing damages to lives, properties, agriculture, and infrastructure [15]. So far, 23 major flood events have been hit the country since its inception with disastrous consequences (**Table 1**). In September 2014, a heavy late monsoon wet spell further increased water discharge in the eastern tributaries of Indus river particularly Chenab river and generated an unprecedented flood in Azad Jammu & Kashmir (AJ&K) and Punjab both in terms of discharge and spatial extent. This flood damaged standing crops, physical infrastructure, and human settlements. As consequence, the national economy was affected adversely in direct and indirect ways [17]. The total human life losses were 368, affected population was above 2 million, and more than 120 thousands houses have been damaged partially or completely.

Agriculture sector was also severely affected by this flood by affecting over 4000 km^2 of arable land and 250 thousands farmers. The standing crops were damaged with an estimated recovery cost of 440 million US$ [19].

Geographically, the study area extends from 73°43′40.8″E to 74°57′3.6″E longitude and 30°36′7.2″N to 32°49′40.8″N latitude (**Figure 1**). Administratively, the study area encompasses the districts of Sailkot, Gujrat, Jhang, Hafizabad, Mandibahudin, Sargodha and Gujranwala from Head Marala to Head Trimum along Chenab river. Chenab river is the main eastern

Sr. no.	Year	Life losses	Affected villages	Affected area
1	1950	2190	10,000	17,920
2	1955	679	6945	20,480
3	1956	160	11,609	74,406
4	1957	83	4498	16,003
5	1959	88	3902	10,424
6	1973	474	9719	41,472
7	1975	126	8628	34,931
8	1976	425	18,390	81,920
9	1977	848	2185	4657
10	1978	393	9199	30,597
11	1981	82	2071	4191
12	1983	39	643	1882
13	1984	42	251	1093
14	1988	508	100	6144
15	1992	1008	13,208	38,758
16	1994	431	1622	5568
17	1995	591	6825	16,686
18	2010	1985	17,553	160,000
19	2011	516	38,700	27,581
20	2012	571	14,159	4746
21	2013	333	8297	4483
22	2014	368	4065	9779
23	2015	238	4634	2877
Total		**12,178**	**197,203**	**616,598**

Source: [18].

Table 1. Major floods in Pakistan.

tributary of Indus river draining the basin [20]. In Pakistan, the total length of Chenab river is 274 km with catchment area of 41,656 km^2. It enters Pakistan at Marala Headwork. The annual average discharge of the river is 1.52 million m^3.

Climatically, the study region is located in the monsoon region. The amount of winter rainfall is low, where in summer rainfall is maximum (**Figure 2**). From May onward, the amount of rainfall increases, and July-August receives the highest rainfall from monsoon, and then from September onward, the rainfall decreases. The temperature conditions are also variable across the year. December and January are the months with lowest temperature 21 and 16°C,
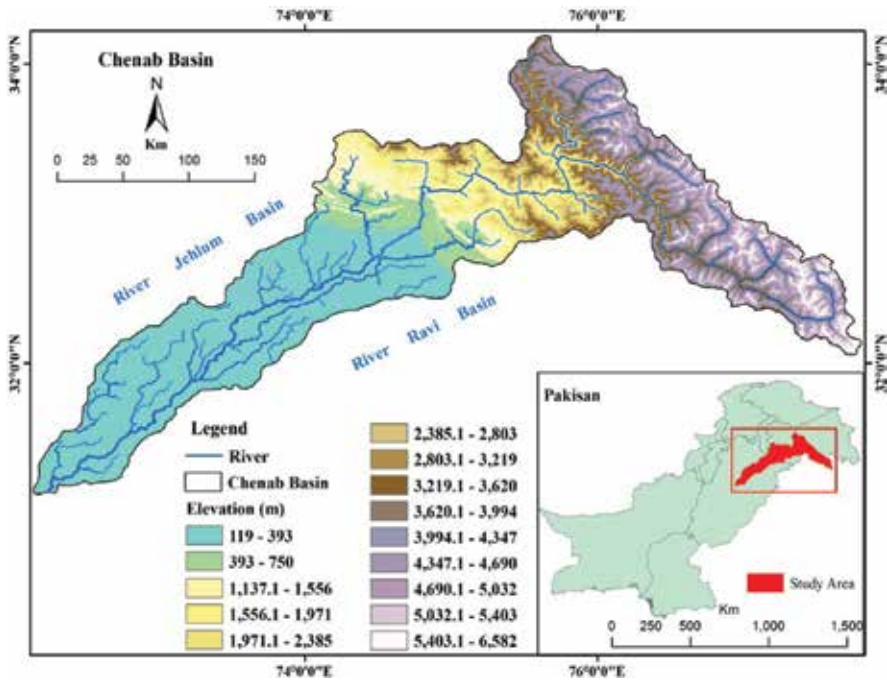
Figure 1. Location of the study area. Source: authors.
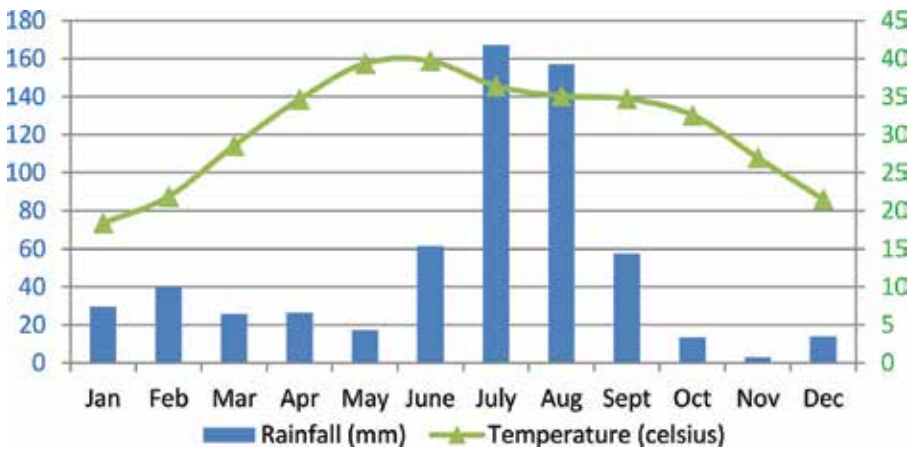
Figure 2. Mean monthly temperature and rainfall. Source: [21].

respectively. The temperature gains momentum from March onward and attains its maximum peak in May (40°C) and June (42°C). In July and August, the temperature falls due to monsoon rainfall.

The main activity of the people in the study area is agriculture because of the availability of fertile soil deposited by the river and water for irrigation through canals from the same river. The main cultivated crops are rice, sugarcane, maize, cotton, fodder, and beans. The local residents are earning their livelihood from agriculture. In most of the target area, houses

are made of bricks and mud which are nonresilient to flood. Similarly, on average monthly income of the surveyed household is less than 200 US$. This situation has made the people more vulnerable living in the river proximity.

2. Data acquisition and analysis

The study is based on mixed approach. Primary data regarding the depth and spatial extent of flood were acquired in the field using community perception. Similarly, Global Positioning System (GPS) survey was conducted simultaneously to acquire the geolocation of places having different flood depth. Secondary data were collected from concerned government departments. Monthly temperature and rainfall data (2000–2015) and discharge data (1925–2015) were collected from Pakistan Meteorology Department (PMD). Flood damage data were collected from Provincial Disaster Management Authority (PDMA). The Shuttle Radar Topographic Mission (SRTM) Digital Elevation Model (DEM) having 30 m spatial resolution was downloaded from United States Geological Survey (USGS), which is a open source geodatabase.

Watershed modeling approach was applied to delineate Chenab basin in geographic information system (GIS) environment by using SRTM DEM as input data. Buffer analysis was implemented in GIS environment to delineate the flood minimum and maximum extent. The flood depth was geo-visualized by applying inverse distance weighted (IDW) techniques.

Similarly, descriptive statistical analysis was applied on temperature, rainfall, and discharge data to visualize the temporal trend and past flood events. Maps and tables were used to visualize the results.

3. Results and discussion

The study area is located in flood prone area. Every year flood caused huge economic loss due to direct damages in agricultural sector, housing sector, and infrastructure sector. Flood inundation has the potential to cause human fatalities, displacement of people, and environmental damage putting pressures on country's economy and economic development [22].

Flood is the abnormal behavior of river flow which results in the breaching of embankments and inundates the low-lying areas on both sides of the river. Heavy rainfall in summer season in the upstream areas together with meltwater (melting of snow and glaciers) increases discharge in the river and generate flood. The Chenab river has been showing such abnormal behavior, and in the 80 years many times its flow has crossed the magnitude of 20,000 m^3/s (**Figure 3**).

3.1. 2014 flood event

In the first week of September 2014, unprecedented rainfall was recorded in Kashmir, Gilgit Baltistan, and many other parts of Pakistan, which has resulted heavy floods in Neelum river at Muzaffarabad, Hunza river at Gilgit, Chenab river at Marala and Jhelum river at Mangla. Parallel to this high discharge, India has also released 5600 m^3/s in Chenab river, which has
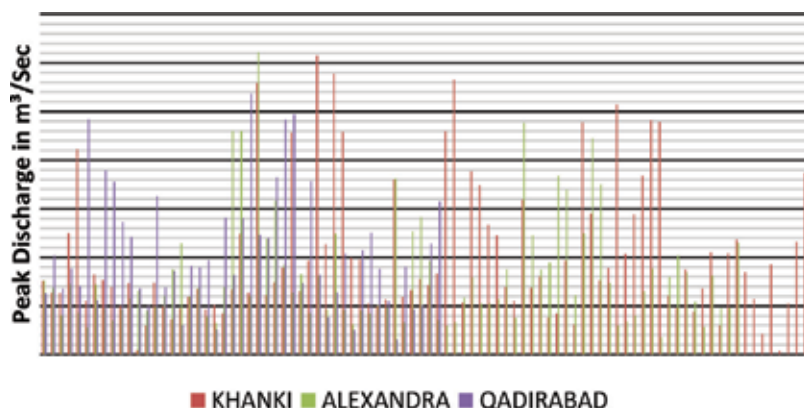
Figure 3. Peak discharge at Khanki Headwork's, Alexandra Headwork's, and Qadirabad Headwork's (1925–2014). Source: [21].

brought devastating flood in the floodplain of Chenab. As a consequence, it has incurred 185 human losses and approximately 40,000 km^2 cropped land was inundated. During field survey, it was found that on 6th September high floods was reported in the upper part of Punjab especially in the districts of Jhelum, Gujrat, and Sialkot, and in the lower Indus plain, the severely affected districts were Jhang and Muzaffargarh Punjab province comprising vast plain areas, therefore, the flood inundated the adjacent areas.

The discharge in normal flood condition remains less than 2800 m^3/s, whereas above 17,000 m^3/s are exceptionally high flood. In the year 2014, peak discharge in river Chenab at Marala was 15,300 m^3/s, at Qadirabad 16,000 m^3/s, and at Khanki above 18,000 m^3/s. Therefore, based on the PMD defined criteria, this flood was declared as high flood in Chenab basin after the disastrous flood in 1992.

The spatial extent of flood was variable in the selected reach of the river. The spatial extent of flood was demarcated on the map on both sides of the river on the bases of community perception. The maximum extent was 20 km, whereas the minimum extent was 10 km in the upper Indus plain (**Figure 4**). Similarly, the depth of flood was also spatially variable. The maximum depth (5 m) was found in district Jhang located in the lower reach of the study area. The extent and depth of flood has caused severe damages to standing crops, livestock, houses, and infrastructure.

The 2014 flood has affected most of the social and economic sectors including community physical infrastructure, housing, agriculture, and flood combating system. Community physical infrastructure sector was the leading affected sector (39.09%) with estimated economic damage of 0.17 billion US$, followed by housing sector (28.67%) with estimated rehabilitation cost of 0.13 billion US$. The standing crops were also severely affected by floodwater with estimated economic loss of 0.11 billion US$ (**Table 2**).

3.2. Extent of damages

The study area is fertile agricultural land and canals are the main source of irrigation. Agriculture is the leading affected sector after infrastructure and housing. During flood,
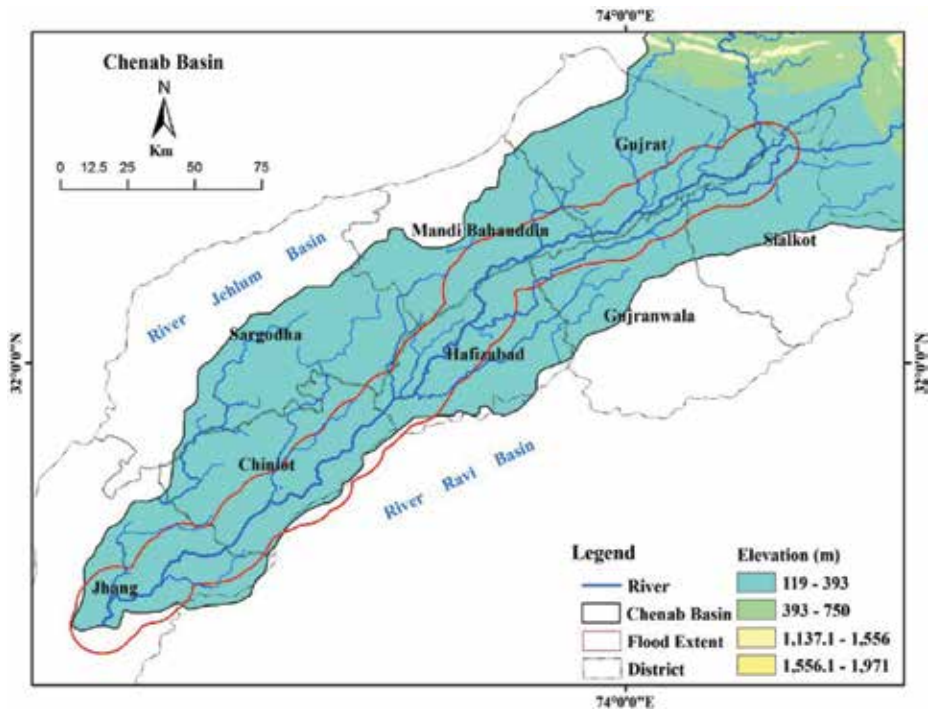
Figure 4. Spatial extent of 2014 flood. Source: authors.

Sectors	Damages (PKR billion)	Damages (US$ billion)	Damages (in percentage)
Physical infrastructure	17.16	0.17	39.09
Housing	12.59	0.13	28.67
Agriculture	10.91	0.112	25.20
Livelihoods	11.14	0.03	6.24
Flood combating system	0.35	0.003	0.80
Total	**52.15**	**0.445**	**100**

Source [23].

Table 2. Sectors wise flood damages.

especially the standing crops of cotton, rice, and sugarcane were ready to harvest but the spatial extent floodwater into the crops left no choice for farmers rather than to protect their lives. According to an estimation of National Disaster Management (NDMA), the standing crops on about 4000 km^2 area were inundated by flood and damaged it completely. Extensive damages were reported in the districts of Jhang, Muzaffargarh, Multan, and Sargodha.

Damages to standing crops not only affected the farmer's livelihood but also have negative consequences on overall agricultural production. The 2014 flood has caused reduction in crop production particularly in rice around 0.217 million ton, in sugarcane 0.726 million tons, and

0.25 bales of cotton were lost. Beside this, seed stocks were lost, agricultural tools and equipment got damaged, irrigation channels were breached by flood or blocked by siltation and land erosion over some places further caused damages to land and standing crops affecting the agricultural sector [18].

Livestock is one of the important components of agricultural sector, considered as a secondary source of earning livelihood, and also fulfills the needs of food and nutrition of households. Significant losses of livestock were also observed due to the floods. In the study region, about 2000 of livestock were lost in the upstream areas, whereas buffalos (303), cows (256), and goats (381) were lost in low-lying areas in upper Indus plain.

In the study area, 2014 flood has also damaged the housing sector. The total number of completely damaged houses was higher than the partially damaged houses. According to the estimate of PDMA, approximately 9872 houses were completely damaged and 2894 houses were partially damaged. The damaged houses were higher in the districts of Jhang followed by Chinot.

Analysis reveals that most of the houses in the flood zone were made of (mud) non-resilient material. Flood surge has damaged directly the houses and its content, while the duration of floodwater has further intensified the impact of floodwater on houses. This is a time for disaster management authorities to rethink and plan again on sustainable way to protect human life and property by strengthening the flood combating system. Flood risk zonation is very important to highlight the high risk areas.

4. Findings and conclusions

The study shows that the 2014 flood was destructive in Pakistan and clearly depicts incapacity of disaster dealing machinery at the Federal, Provincial, and district level. This flood was caused by heavy rainfall over the Chenab basin particularly in upstream areas.

This study found the extent of 2014 flood damages in agricultural housing and infrastructure sectors. The 2014 flood was one of the devastating disasters and affected the socioeconomic setup in 16 districts in Punjab province. Out of the total affected districts eight were selected in this study located in upper Indus plain.

In the study region, the severely affected districts were Jhang, Sargodha, Gujranwala, and Hafizabad due to damages in agricultural and housing sector. Analysis reveals that the flood has damaged the social and economic life of people. Houses were damaged which not only cause social negative impact but economic as well. On the other hand, study area mostly comprises agriculture, and flood has destroyed completely all crops. Rice, sugarcane, and fodder are mostly affected. The damages to agricultural equipments and loss of livestock further increased the economic losses. To avoid the socioeconomic damages, it is necessary to build embankments along river, develop effective flood warning system, and develop a management cell based on community perception to combat flood.

Pakistan is a disaster prone developing economy and does not have sufficient resources and infrastructure to deal with and recover from devastating disasters. This situation has increased the exposure and vulnerability of communities. The strengthening of the disaster

risk management system is highly required in order to reduce exposure and vulnerability by capacity building. In this regard, expansion of structural and nonstructural mitigation measures is vital to enhance the efficiency of the flood risk management system. Flood hazard and risk zonation are also extremely important to identify high risk areas. Similarly, flood forecasting and early warning system are also required to be enhanced by increasing the weather radar network.

This is a time for disaster management authorities to rethink and plan again on sustainable way to protect human life and property by strengthening the flood combating system. Flood risk zonation is very important to highlight the high risk areas.

Author details

Shakeel Mahmood* and Razia Rani

*Address all correspondence to: shakeelmahmoodkhan@gmail.com

Department of Geography, Government College University, Lahore, Pakistan

References

[1] Ahern M, Kovats RS, Wilkinson P, Few R, Matthies F. Global health impacts of floods: Epidemiologic evidence. Epidemiologic Reviews. 2005;**27**:36-46

[2] Ali A. Indus basin floods: Mechanisms, impacts, and management. Mandaluyong City, Philippines: Asian Development Bank. 2013

[3] Arslan M, Tauseef M, Gull M, Baqir M, Ahmad I. Unusual rainfall shift during monsoon period of 2010 in Pakistan: Flash flooding in northern Pakistan and riverine flooding in southern Pakistan. Academic Journals. 2013;**7**(9):882-890

[4] Rahman A, Khan AN. Analysis of flood causes and associated socio-economic damages in the Hindukush region. Natural Hazards. 2011;**59**(3):1239-1260. DOI: 10.1007/s11069-011-9830-8

[5] Collins MJ, Kirk JP, Pettit J, DeGaetano AT, McCown MS, Peterson TC, Zhang X. Annual floods in New England (USA) and Atlantic Canada: synoptic climatology and generating mechanisms. Physical Geography. 2014;**35**(3):195-219

[6] Douben KJ. Characteristics of river floods and flooding: A global overview, 1985-2003. Irrigation and Drainage. 2006;**55**:9-21

[7] Houze R a, Rasmussen KL, Medina S, Brodzik SR, Romatschke U. Anomalous atmospheric events leading to the summer 2010 flood in Pakistan. Bulletin of the American Meteorological Society. 2011;**92**(3):291-298

[8] Hussain MS, Lee S. Long-term variability and changes of the precipitation regime in Pakistan. Asia-Pacific Journal of Atmospheric Sciences. 2014;**50**(3):271-282

[9] Mahmood S, Khan AH, Mayo SM. Exploring underlying causes and assessing damages of 2010 flash flood in the upper zone of Panjkora River. Natural Hazards. 2016;**83**(2): 1213-1227

[10] Gaurav K, Sindha R, Panda PK. The Indus flood of 2010 in Pakistan: a perspective analysis using remote sensing data. Natural Hazards. 2011;**59**:1815-1826. DOI: 10.1007/s11069-011/9569-6

[11] Khan AN. An assessment of floods hazard causes for efficient flood plain management: A case of Neelam-Jehlum Valley. Pakistan Geographical Review. 2005;**60**(1):42-53

[12] Kazi A. A review of the assessment and mitigation of floods in Sindh, Pakistan. Natural Hazards. 2014;**70**(1):839-864

[13] Kelly DJ, Garvin SL. European flood strategies in support of resilient buildings. In: Ashley R, Garvin S, Pasche E, Vassilopoulos A, Zevenbergen C, editors. Advances in Urban Flood Management. Balkema, London: Taylor & Francis; 2007

[14] Manzoor M, Bibi S, Manzoor M, Jabeen R. Historical Analysis of Flood Information and Impacts Assessment and Associated Response in Pakistan (1947-2011). Research Journal of Environmental and Earth Sciences. 2013;**5**(3):139-146

[15] Mahmood S, Khan AH, Ullah S. Assessment of 2010 flash flood causes and associated damages in Dir Valley, Khyber Pakhtunkhwa Pakistan. International Journal of Disaster Risk Reduction. 2016;**16**:215-223

[16] Rehman S, Shah MA. Rainfall trends in different climate zones of Pakistan. Pakistan Journal of Meteorology. 2012;**9**:37-47

[17] Shamshad A. The south Asiatic monsoon and flood hazard in the Indus River basin. Journal of Basic & Applied Science. 2011;**7**:101-115

[18] Annual flood report. Federal flood commission. Government of Pakistan Ministry of Water & Power. Office of the chief engineering advisor & chairman federal flood commission islamabad. 2015

[19] Wang SY, Davies RE, Huang WR, Gillies RR. Pakistan's two-stage monsoon and links with the recent climate change. Journal of Geographical Research. 2011;**116**:1-15

[20] Zaman Q, Afzal M. Temporal Trends in the Peak Monsoon Precipitation Events over Northeast Pakistan. Pakistan Journal of Meteorology. 2013;**10**(19):19-30

[21] Pakistan Meteorological Department (PMD). Pakistan: Regional Office Lahore; 2016

[22] Gaurav K, Sindha R, Panda PK. The Indus flood of 2010 in Pakistan: A perspective analysis using remote sensing data. Natural Hazards. 2011;**59**:1815-1826. DOI: 10.1007/s11069-011/9569-6

[23] Government of Pakistan (GoP). Damages & Recovery Needs Assessment Report. Islamabad, Pakistan: National Disaster management Authority; 2014

Climate Change and Reconstruction of Natural Hazard Events

Towards the Reduction of Vulnerabilities and Risks of Climate Change in the Community-Based Tourism, Namibia

Selma Lendelvo, Margaret N. Angula,
Immaculate Mogotsi and Karl Aribeb

Additional information is available at the end of the chapter

Abstract

Climate change is one of the contemporary issues in the world that has proven to have direct impact on the development of different nations. Community-based tourism has been identified as a potential contributor to household security. In this chapter, the analyses were derived from regional consultations in the two regions with community members, traditional leaders, and key stakeholders. In Namibia and particularly Kunene and Zambezi regions, community-based tourism has expanded, providing employment to the residents of these communities. Similarly, there has been an increase in joint venture agreements between local communities and external investors in areas such as constructions of lodges, tented camps and tour guiding. The community-based tourism sectors in Zambezi region and Kunene region are prone to climatic hazards, in particular, frequent floods and prolonged drought. This chapter recommends inclusive climate change adaptive strategies that promote climate proof infrastructure for tourism establishment. An effective community-based tourism intervention for the Zambezi region is necessitated by a well-informed and consultative planning and execution to reduce the effects of flood. For Kunene region, community-based tourism interventions should be aimed at addressing the risks resulting from drought. It should, therefore, prioritise sustainable water security and environmental management practices.

Keywords: tourism, gender, women, climate change, vulnerability

1. Introduction

Climate change is one of the contemporary issues in the world that has proven to have direct impact on the development of different nations. Established evidence through literature and research indicates that climate change poses socio-cultural, economic and environmental threats on the continent; these impacts remain experienced at spatial and temporal scales [1, 2]. Geographic impacts of climate changes have resulted in diverse approaches for mitigation and adaptation strategies to climate change. Intergovernmental Panel on Climate Change (IPCC) also have played a role in providing crucial information for execution of well-informed planning, global policy formulation and implementation processes, aiming to address climate change [1]. The global work on climate change does not only differentiate spatially but also reflects that climate change impacts are gendered owing to the different vulnerabilities between men and women.

Climate change adaptation is more a societal than a technical issue [3]. As a result, across the globe, particularly among developing nations, studies were conducted to develop reforms for gender mainstreaming [4–12]. Gender-differentiated climate change impacts and adaptive capacity is pronounced in Namibia and is considered an important factor in a vulnerability assessment research done at local level or communal areas. However, challenges to effectively address gender-differentiated impacts continue to occur. In most cases, the impediment behind addressing these gender imbalances arises from socio-cultural systems that traditionally favoured men. Gender inequalities in many societies were not only contributed by unequal benefits from different available opportunities but also have contributed to recurrent socio-economic disadvantages among women, making them more vulnerable to disaster [12]. It is evident that the poorest nations or components of the society are most disadvantaged during variable climatic conditions, because their livelihoods are heavily depended on climate-sensitive sectors such as agriculture. In addition, women- and children-headed households also form part of the poorer segment of most developing nations. Poor households in developing nations are expected to face tougher risks due to climate change over the coming decades, especially in the form of water and food shortages as well as other key human necessities and this will lead to increased vulnerabilities [13].

Livelihood strategies among the Namibian people have also been affected by climate change over the past decades. Agriculture is so far the most important livelihood activity in the country and has been severely affected by the variable climatic conditions. Unstable yields from agriculture have resulted in various livelihood diversification approaches gaining momentum to reduce climate change risks at household and community levels. The emergence of community-based natural resources management (CBNRM) in most rural communities of Namibia broaden the utilisation of land to buffer climate change-related hazards. Most specially, rural tourism advanced from the efforts of CBNRM to uplift the local economy and consequently assist to support households and community resilience to climate change. Being a semi-arid country, climate change affects different sectors and a greater part of the Namibian population; hence, it receives high priority and support at national level. The Namibian government ensured the accreditation of a local institution, the Environmental Investment Fund (EIF), with the Green Climate Fund (GCF) to enable the country to benefit from the GCF funding packages [12, 14].

Furthermore, the government ensured that a National Policy on Climate Change outlines the need for different institutions to develop programmes and initiatives to improve adaptations and reduce exposure of men and women to climatic change impacts. In addition, climate change adaptations should be mainstreamed in legislations and legal frameworks. For instances, Namibia has successfully developed a mainstreaming strategy for the disaster risks management programmes to enable the government to respond proactively to climate hazards. Sensitivity of a community to climate change risks can be reduced considerably by improving the adaptive capacity.

The global climate change frameworks are provided by the United Nations Framework Convention on Climate Change (UNFCCC) (which Namibia is a party to) that allow for global and local engagement efforts to address climate change mitigation and adaptation programmes. The global framework has also resulted in the development of the Namibia National Climate Change Policy in 2001 to provide a framework for addressing the resilience to risks resulting from climate change in the country [14]. The capacity of both men and women to adapt and cope with climate change has been reduced over time, and this has also been shaped by the gender relations. Climate change impacts have a potential to change gender and social relations at local level either positively or negatively. In most African cultural communities, duties and responsibilities are divided among husband, wife and siblings based on stereotypes of what men and women should do and how women should behave and not necessarily based on skills or ability [15, 16].

The majority of Namibian women have limited or no decision-making power within households and community. Women's lack of decision-making, gender-power imbalance and limited control of resources has direct bearing on how they respond to climate-change impacts [17]. Up until now, most of the policies and strategies aimed at developing and strengthening climate resilience of men and women continually fail to incorporate gender mainstreaming [18] or incorrectly formulate gender risks in policy development [19]. There is still insufficient understanding of the different adaptive strategies that men and women apply in order to secure their livelihoods in the face of climate change. Understanding gendered vulnerability, coping and adaptation strategies are vital for equitable interventions that are benefiting men, women and youth.

The results of this chapter are depended on regional consultations with community members and key stakeholders. In addition, secondary information in the form of government reports and publications, baseline studies on the communities of the targeted regions and also other relevant documentation on the subject of climate change and community-based tourism in the Kunene and Zambezi regions in Namibia were reviewed. The data and documentations were obtained from various offices in Namibia. In order to understand who influences what, where, how and why, and how activities in conservancies and community forests are implemented, the Harvard Gender Analytical Framework was used. The social relations approach framework helped the authors to analyse focus group workshop findings in order to understand the existing inequalities in distribution of responsibilities and power within conservancies and community forests in Namibia. Finally, the vulnerability framework was applied to identify the exposure and sensitivity of communities on impacts of climate change as well as their adaptive capacity to respond to these impacts. As a result, the multistakeholder

consultations yielded an in-depth understanding of gender, culture, climate change vulnerability and adaptation as well as developmental challenges among communities residing in conservancies and community forest areas.

2. Study area

Namibia is a sparsely populated country situated in the south-western part of Africa (**Figure 1**) with a total population of 2,113,077 of which 57% resides in rural areas [20] with a land area of 825,615 km^2. The 14 administrative regions in Namibia present landscape, economic and socio-cultural diversity. The sex-disaggregated population of Namibia is 1,091,165 females and 1,021,912 males. The percentage of female-headed households in Namibia is 44% with the three northern regions of Ohangwena, Omusati and Oshana having more female-headed households compared to male-headed counterparts [20]. The socio-economic status of households in rural areas differs significantly compared to urban areas. For instance, per capita income of households is differentiated by headship US$ 595 for female-headed and US$ 969 for male-headed households [21]. Likewise, unemployment rates are higher for women in rural areas (41%) than in urban areas (26%). These indicators illustrate low adaptive capacity in rural Namibia in general and female-headed households in particular.

The chapter will focus on the Kunene and Zambezi regions of Namibia. The Kunene region is located on the north-west of Namibia, bordering Angola in the north and the Atlantic Ocean in the west, with a land area of 115,260 km^2 [2]. The Zambezi region on the other hand is on the far north-east of Namibia. Zambezi region borders with Angola, Zambia, Zimbabwe and Botswana. The land area of Zambezi region is 14,784 km^2 [2]. Wildlife is the main tourism product in both Kunene and Zambezi regions [22]. Tourism enterprises are generally lodges, up-market safari camps, campsites, and the associated service enterprises [22–24]. Kunene and Zambezi regions have the highest number of registered conservancies with 36 and 17, respectively [25]. **Table 1** presents the description of the climate, tourism, and natural resources profiles of the two regions derived from secondary literature.

The implementation of community-based natural resources management (CBNRM) approach in Namibia has given birth to a growing local natural resources management and tourism establishments. The first four conservancies (covering about 16,821 km^2) were gazetted by the Ministry of Environment and Tourism (MET) in 1998, namely, the Nyae Nyae Conservancy (Otjozondjupa region), Salambala Conservancy (Zambezi region), and Torra and #Khoadi //Hôas Conservancies (Kunene region). Five years later, the number of conservancies in Namibia had expanded to 70,995 km^2 after a further 29 conservancies were gazetted by the MET by the end of 2003 [34]. The number of conservancies continued to increase in the country and by the end of 2013, a total of 79 registered conservancies had been established in different regions on communal land. In total, 43.5% of the country's surface area was under wildlife conservation by 2013, consisting of which 16.8% are state-protected areas, 6.1% freehold conservancies, 0.8% tourism concession areas, 19.4% communal conservancies and 0.4% of community forests outside conservancy areas. By the end of 2016, there were 82 communal conservancies covering 161,900 km^2, registered in Namibia [25, 34].
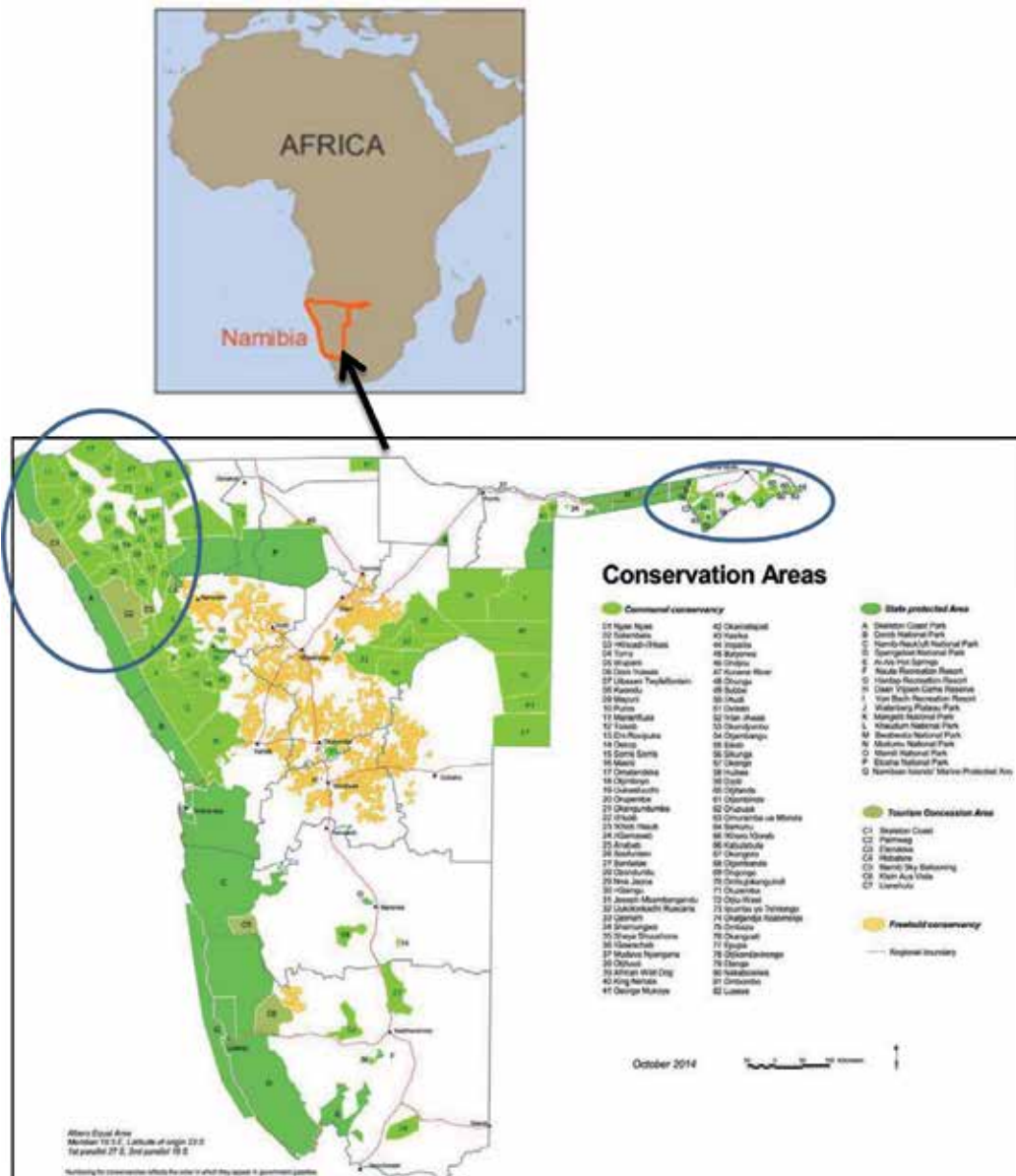
Figure 1. Namibian map showing conservation areas including communal conservancies. Circled parts represent the two study regions, Kunene and Zambezi regions [35].

In addition, the conservancy development in Namibia has also advanced community-based tourism, which benefits many rural households. By the end of 2016, conservancies had engaged in about 53 joint-venture enterprises, over a 1000 indigenous plant harvesters and also about 500 local craft producers, benefiting approximately 4000 inhabitants of the conservancies through employment and trading opportunities. In monetary terms, a combined income of US\$ 7,469,137 was generated by the conservancies and their private sector partners from the community-based tourism enterprises during 2016 [25].

Kunene region	Zambezi region
• Hosts Skeleton Coast Park as its entire western boundary with the Atlantic Ocean [26].	• One of the smallest regions in the country (14,785 km²) with a his population density of over 90,000 people live in this region, about 4% of the total Namibian population [30, 31].
• Home to 86,856 inhabitants, representing 4% of the Namibian population [26, 20].	• Have 'a fertile wilderness of riverine forests, flood plains, swamps and open woodland created by a complex network of rivers and relatively high summer rainfall' [30, 32].
• Home to OvaHimba and Damara Ethnic groups of Namibia.	• The average rainfall in Zambezi is about 700 mm and this makes it the wettest region in the country.
• Rainfall in this region increases from north-west to north-east ranging from less than 50 to 400 mm, and is very sporadic [26].	• People in this region are subsistence farmers, mostly fisheries who make their living on the river bank of the Zambezi, Kwando, Linyanti and Chobe rivers.
• Possess 36 registered conservancies (44% of all registered conservancies in the country) [25].	• Possess 17 registered conservancies (21% of all registered conservancies in the country) [25].
• Boasts mountainous landscapes, semi-precious and precious minerals, underground water and springs.	• Tourist attractions include the transboundary rivers, unique culture and craft of people.
• 'Prides itself as the most ethnically and demographically diversified region because the OvaHimba lifestyle, tradition, values and culture have never transitioned to modernity even after centuries of colonialism' [27].	• The conservancies in the region benefits from the high number of tourists that frequent the area.
• There are wildlife species such as 'black rhinoceros, elephant, black-faced impala and Hartmann's mountain zebra' [29] and a large population of lions roaming outside National Parks' fence [28].	• Popa Game Park and Bwabwata National Park are opposite to each other and have similar species of birds and animals. Furthermore, Bwabwata is a home to more than '35 large game species, including elephant, buffalo, impala, reedbuck, red lechwe, sitatunga, hippo, giraffe, zebra, and wildebeest' [33]. There are 400 recorded bird's species including 'kingfishers, herons, cormorants, African skimmers, wattled cranes, pygmy geese and African fish-eagles' [33]. All these ecosystems and their biodiversity beauty make Zambezi region an outstanding tourism destination [30, 33].
• Tourist attractions of value to visitors include 'unique desert dwelling large mammals [29] traditional cultures, quality of Kunene remoteness, and sense of isolation and perception of uncrowded 'exclusivity' [28, 29].	• High tourism potential in the region has attracted both domestic and international tour operators in the area who have established accommodation facilities.
	• The conservancies in the region benefits from the high number of tourists that frequent the area.

Table 1. Description of the regional profiles for the Kunene and Zambezi regions in Namibia.

Figure 1 illustrates the location and sizes of all registered conservancies in Namibia as at December 2016. This map also indicates conservancies from (see circles inserted) Kunene and Zambezi regions, the main focus areas for this chapter [35].

3. Projected climate change and existing vulnerabilities

3.1. Projected changes in temperature and rainfall for Namibia

According to the adaptation at scale in semi-arid regions (ASSAR) project, 'Average temperature trends in the semi-arid areas of Southern African have increased by 0.25°C per decade since 1960. Combined model results indicate a warming rate of between 0.32 and 0.38°C per decade to 2050, depending on future greenhouse gas emissions being either moderately reduced or not reduced at all. Very hot days are projected to occur about 20 times more per year in the 2030s than today. The total rainfall and rainfall extremes, projections for future rainfall are far less certain than those for temperature. However, it is likely that the rainfall variability of the recent past will continue into the future. Projections suggest that dry spells will increase in the future—the longest dry period in a year is projected to increase by about seven days in 2030 compared to today' [36, 2].

Other studies argue that projections for Namibia indicate that Namibia is exposed to the impacts of climate change. These studies further argue that mean temperatures in Namibia have increased by up to 0.5°C over the past half century and are expected to increase by a 5°C by 2100. Namibian rainfall extremes have become more frequent, and rainfall is projected to become more variable with a general trend towards decreased rainfall over the coming century [37].

The climatic and geographic climate of southern Africa, including Namibia, is prone to extreme weather and high annual rainfall variability [38]. It is projected that rainfall in southern African countries might show a decline by −0.6 mm/day with even greater annual variations by the end of the twenty-first century [39]. Recently, northern Namibia experienced long-lasting rainfalls during 2008/09 and 2010/11, which caused devastating floods [40]. On the other hand, the severe drought that Namibia experienced in 2013 had detrimental effects on many people [41].

3.2. Vulnerabilities to climate change for the community-based tourism in Kunene and Zambezi regions

Livelihoods of communities and farmers in northern Namibia have been predominantly depended on rain-fed subsistence agriculture augmented with the natural products. However, with the emergence of the community-based natural resources management approach introduced in Namibia since 1996, the benefits from wildlife, forest products and local tourism contributed to diversification of livelihoods among rural communities in the northern Namibia. The effects of climatic hazards in Namibian rural areas are severe because of the low socio-economic development and poor infrastructure. For instance, the flooding that was experienced in the neighbouring countries of South Africa, Mozambique and Zimbabwe during the year 2000 had disastrous affects, with 600 human fatalities,

200 bridges and 1000 km road damaged [38, 42]. High levels of poverty and dependency on the traditional agricultural systems also contribute to vulnerabilities towards climatic risks [41].

There are limited reports of flooding affecting the livelihoods of communities in the Kunene region, and it seems that drought may be the greatest climatic hazard. Severe drought events that were experienced in the country occurred during 1981, 1990, 1995, 1998, 2001, 2002, 2013 [41] and 2016 [42]. On the 24 June 2016, the Namibian President, Dr. Hage Geingob made a declaration and was quoted by a local newspaper, declaring a state of emergency due to severe drought experienced in the country: 'I declare that a state of emergency exists in Namibia on the account of the persisting national disaster of drought that exists in all regions of the Republic of Namibia' [43]. Another declaration of emergency due to drought was done by the Former President of the Republic of Namibia, Dr. Hifikepunye Pohamba in 2013.

> *'The year 2013 will always be remembered by Namibian farmers as one of the toughest and most challenging periods in 30 years due to the debilitating and devastating drought still threatening the agricultural sector and the country's food security'* [44, 45].

The dependence on natural resources makes communities sensitive to climate variability, such as the extensive droughts experienced in Kunene region and annual floods in Zambezi region [46]. According to Schlechter [47], the effects of severe conditions such as drought and flood impact animal life in a negative manner, especially in conservancies where livestock and wildlife share resources. Species like hartebeest, gemsbok and the endangered black rhino were dying in the northern-west Kunene because of severe water scarcity. Migration of wildlife species to other areas in search for water is common during droughts, and this may lead to disruption of tourism activities in the region [48, 49].

The IPCC categorised the Zambezi basin as exhibiting the 'worst' potential effects of climate change risks among 11 major African basins [50, 51]. Unlike Kunene region in the far north-west, flood is by far the most common hazards in the Zambezi region involving the flooding of flood plains. In the dry season, most areas in the region can be reached by road, but after the rains, 80% of their surface area becomes flooded, cutting them off from the mainland [30, 32]. Long-term productivity of nature-based activities in the Zambezi region is affected by the frequent and heavy floods experienced. Flooding in the Zambezi region fluctuates in intensity depending on the annual rainfall received (**Figure 2**). Rainfall received during the season of 2009 resulted in the rising of the upper Zambezi River, causing severe floods that resulted in several casualties, fatalities and damage to property [52]. **Figure 2** shows that since 2007, the rainfall records indicate more frequent high rainfall followed by a below-average rainfall in 2010/2011 season.

The flood and drought hazards not only affect the agricultural livelihoods but also the nature-based tourism or ecotourism from which communities in communal conservancies earn a living. Tourism is an emerging economic activity in most communal areas of Namibia and is susceptible to natural disasters. The complexity of climate-related risks, coupled with the capacity of people in rural areas reduces the effectiveness of mitigation efforts, resulting in greater losses should a natural disaster occur. For example, developmental activities are likely to be affected by climatic events due to high water demand, poor or limited infrastructure,
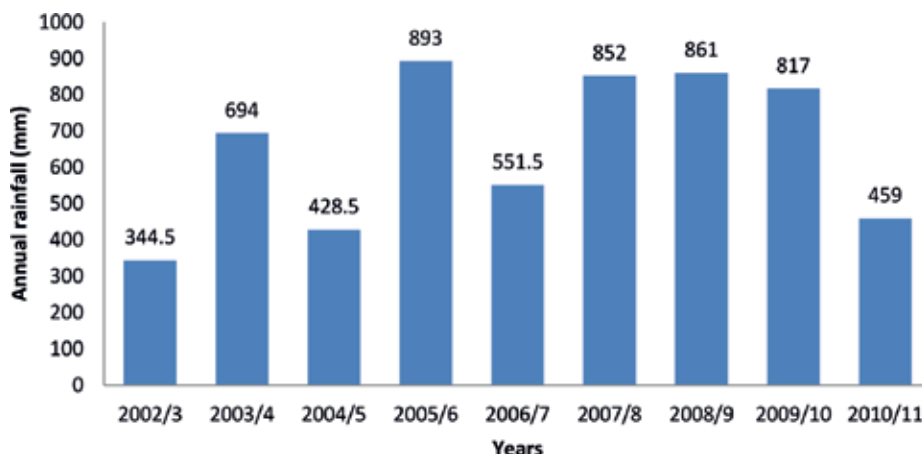
Figure 2. Annual rainfall of the Zambezi region during 2002/2003–2010/2011 rainy season [40].

degradation and disruption of land and environmental resources and human settlement patterns. Tourism in the two northern regions (Kunene and Zambezi) is primarily based on wildlife biodiversity, landscapes and cultural factors, despite the contrast of these aspects and scenery.

During the regional consultations, participants indicated climate risks that are affecting their conservancies and community forests and how these risks are affecting the tourism sector. The tourism sector and ecosystem services were indicated to be sensitive to climatic risks. Drought risks, for instance, lead to water scarcity impacting the tourism businesses, as well landscape scenery and wildlife populations upon which local tourism is depended upon. In Kunene region, veld fires and water scarcity had led to reduced operations or closure of some tourism establishment due to losses of vegetation, migration of game and in few instances, veld fires that destroyed campsite properties. This resulted in job losses and also reduced tourist visit to the region. Severe droughts lead to cancellations, reduced booked holidays and consequently, decline in tourist visitations [53].

Seasonal flooding has been identified as another climate risk that affects the tourism sector, mainly in the northern regions of Namibia. It makes roads inaccessible and also destroys tourist establishments. Disease outbreaks, in particular malaria, have been associated with stagnant waters created during flooding. However, tourist activities in the Zambezi region have been planned around its flood history in order to reduce the impacts that flooding may have on tourism in the area. For example, February–April are the months during which flooding is known to occur in this area, and these are the off-season months, when tourism activity is on its minimum. Recent intensified floods in the Zambezi region had resulted in the loss of field crops and livestock. Flooding also causes damages to infrastructure that affected many people in the region and led to the displacement of many families, a result threatening food security and livelihoods [40, 52]. Bosch [40] gave examples of the vulnerabilities within the tourism sector resulting from flooding hazards. Flooding during the year 2009 had been the worst in

40 years and had more devastating effect in the region than in the year 1969 [40]. For example, local people and tourists had to travel to and from Zambezi lodge or other reachable parking areas by boat, similarly Kalizo, Island View Lodges and Kalimbeza Fishing Camp were all only accessible by boat. In 2008, several other tourism establishments in Zambezi region were affected by the floods such as the Malyo Wilderness Camp, Camp Kwando and Namushasha Lodge's Airstrip, while in 2007, the Mukusi River Lodge was closed as the buildings were submerged in water [40].

Tourism is the source of livelihood diversification of households in both regions. Livelihood diversification strategies are important in Namibia because of the sensitivity to climate change presented in the form of semi-arid conditions. In addition, the impact of climate change on tourism business affects women more or leads to vulnerability among women through reduced earnings. In Namibia, women enjoy an advantage in the tourism workforce as well as most local-level Small-and-Medium-Sized Enterprises (SMEs) owned by women in the CBNRM sector [54]. Despite dominating the workforce, women from Kunene and Zambezi regions generally receive low wages, which make them more vulnerable to the toll of climate change. Generally, women in rural areas have limited educational qualifications, capital and access to land or property to compete with their male counterparts [55]. Many rural-based tourism opportunities have assisted women to obtain employment locally and other economic gains because they are not mobile or better skilled to migrate elsewhere.

4. Implemented measures to mitigate climate change risks and emerging gaps that need decision-making

4.1. Existing responses to reduce climate risks in Kunene and Zambezi regions

The adaptive capacity for climate change is crucial for minimising the effects that climate change may have on the community. This involves adjustments of actions and attitudes within the community to better cope with the impacts of climate change experienced. During focus group workshops with communities, coping strategies and adaptations to boost the tourism sector during drought or flooding were highlighted at different levels. The conservancy programme is hailed as a local-based institutional framework that works closely with the Namibian government to promote natural resources management and development of local-based tourism in rural communities. Most international and established local investors have been working with conservancies in developing local tourism to ensure long-lasting impacts of tourism on communities.

The responses to climate change risks on the tourism sector include improving the benefits accrued from natural resources in the event of droughts and floods. The major responses for the Kunene region in the case of drought were to particularly ensure water security for drinking, farming, business and wildlife. Initially, the response of the government has been reactive rather than proactive and long-term due to the absence of early warning information. The government spent millions in reacting to emergencies, which still left people unprepared

for the future hazards. During the 2003/2004 drought, the government spent approximately US$ 21 million in provision of emergency relief [55]. However, recently, the responses have been geared towards adaptation and increasing the capacity among residents during such risks. The government has implemented projects in the Kunene region to drill boreholes and build earth dams in different constituencies of the region. Activities such as aquifer recharge and acquiring earth-moving equipment were among the responses suggested by communities for ensuring water security in the regions. Sustainable forest management strategies were also among the responses to prevent adverse impact of drought on tourism, emphasising mainly on the veld fire management such as putting up firebreaks and promoting sustainable harvesting of forest products through permits and capacity building. Women in the Kunene region harvest the *Commiphora* species products, which are used to produce perfumes for export and for sale to local tourists as a source of income to support their families. This initiative receives great support from government and some relevant stakeholders [56].

In terms of flooding in the Zambezi region, the Government spent about US$ 8,241,099 on flood emergency response during 2009 [55]. Conservancies and government have also been working on adaptation strategies to reduce the impact of flooding hazards on communities, mainly providing assistance for people in lowlands to move to higher grounds permanently and promoting the use of flood resilient materials for residential and business construction. In addition, the government budget was also mainly geared towards ensuring connection and accessibility, even during floods, to different services location such as schools, hospitals, tourism areas and connecting communities. In order to sustain the source of income from the tourism sector, several strategies are employed by communities. Women from Zambezi region diversify to more drought resistance crops in order to supply the tourism-sector business outlets with local fruits and vegetables, despite the climatic events. In other areas, women travel long distances to collect antique natural products, including handcrafts that they supply to local tourism businesses. Although some products such as grass and fibre crafts are sold only by men, both men and women use different strategies to ensure the supply chain of these products. In general, the efforts in the country to increase the adaptive capacity and reducing the sensitivity to climate change risks, for both men and women, are presented in **Figure 3**.

4.2. Identified gaps and problems for building resilience

The climate change adaptation programmes and initiatives implemented should ultimately contribute to resilience of local communities and structures. The combination of the adaptive capacity assessment and the gendered social relations frameworks was used to analyse the gaps for resilience building resulting from the community consultations in the two regions. Both men and women from Kunene and Zambezi regions indicated to be accruing benefits from community-based tourism in different ways as well as participating in several activities involving natural resources management. Community-based tourism was rated in most consultations to play a crucial role in employment, training, income generation and empowerment opportunities for different segments of the communities such as the poor, unskilled and lowly educated, women, men and also the youth. A representative of the Namibia EcoAwards facilitating and promoting community-based tourism reflected on the following
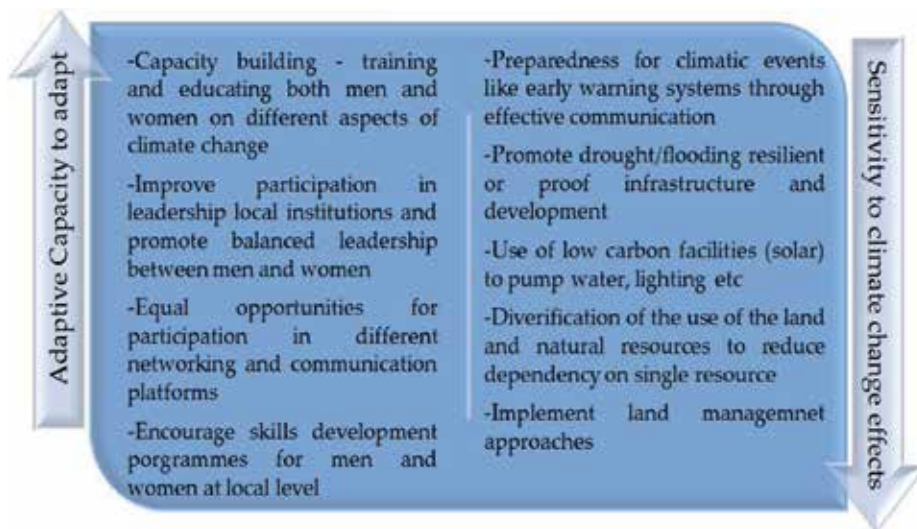
Figure 3. Key attributes for increasing the resilience of communities by increasing adaptive capacity and reducing exposure to climatic change impacts (source: authors).

Photo 1. A woman employed at a community-based tourism establish in the Zambezi region. Source: [25, 12].

'The pillars of tourism in Namibia are women, I have seen women growing from cleaners to a quality manager within the tourism sector'. There are several stories that can be told about women employment in community-based tourism enterprises: **Photo 1** shows a woman who is a receptionist at the Camp Chobe in the Salambala Conservancy situated in the Zambezi region. This illustrates women empowerment a factor that has a potential to enhance agency and strengthen adaptive capacity of women residing in patriarchal communities. Patriarchy is dominant in Kunene and Zambezi regions.

Gaps identified from the analysis during the community consultations:

a. Climate change risks and exposure affect both men and women: communities in the two regions face climate risks such as droughts, seasonal flooding, high temperatures, veld

fires and variable rainfall. The exposure to these climatic risks to the local people are also exacerbated by non-climatic factors involving population pressure, poverty levels of the people, cultural practices and belief systems and also governance-related aspects. Although men were likely to possess some levels of knowledge they use for leadership and acquiring better employment, communities in both the Kunene and Zambezi regions tend to be characterised by low levels of education and skills, which increase their exposure to these hazards.

b. Human wildlife conflicts affecting farming and tourism operations: men and women from both regions are at the receiving end of human-wildlife conflict (HWC), which is worsened during the occurrence of the climatic events. During droughts, the water-dependent elephants cause damages as a result of water scarcity; they overcrowd water points and causing damages to water infrastructures. A community member from the Puros conservancy in the Kunene region cited their encounter on human-wildlife conflict when elephants raided homes in search of food during the 2016 drought. Women were more vulnerable to such incidents because traditionally they stay at home while men have travelled to the field with the livestock in search of pasture. The flooding periods in Zambezi put men, women and children at risks as they have to use canoes to access schools, markets and also work places. Crocodile attacks on community members are the highest during floods in Zambezi region.

c. Gender division of labour within the tourism sector: men continue to dominate high-paying activities such as game-drive, tour-guiding and timber harvesting, while women mainly occupy low-paying jobs, such as cultural dance performers, cooks of traditional dishes, cleaners, waitresses and receptionists in the tourism accommodation establishment. Men's activities turn to be seasonal, resulting to short-term contract employment arrangements, while women's activities lead to permanent. Women are less engaged in negotiation of joint-venture deals in their communities, excluding their input on how to benefit from such ventures. Tourism joint venture negotiations remain the prerogative of men, resulting to women's views not taken into consideration. Generally, there exist lack of negotiation and legal skills among community members when entering into joint venture deals, making community member vulnerable in the process and unable to derive economic gains from these ventures. Conflict over the control over funds generated from joint ventures is a problem that is experienced and cause disruptions in the local leadership structures.

d. Gender parities decision-making and leadership in community-based institutions: although Namibia is historically a patriarchal society, great strides had been made in local-based institution and tourism initiatives to engage women in leadership position. The Kunene and Zambezi regions are generally the strongest regions in practicing traditional values, which support the male domination in leadership. There are still some scattered instances in the two regions where women prefer to rely on their husbands for information, thus perpetuating gender inequality. However, through empowerment efforts, women have started forming part of leadership structures in these two regions. On average, 35% of women are conservancy committee members and the majority of the

women are in treasurer or secretary positions? [44]. Despite, being reluctant to take up leadership positions, women tend to show high level of participation in several voluntary community initiatives.

  e. Cultural barriers to adaptations to building resilience in the community-based tourism: Kunene region experiences cultural myths and perceptions that emerged as one of the biggest obstacles in obtaining gender equality among the OvaHimba community. There is a tendency to frown upon men who do not participate in male-dominated activities and on women who talk openly in meetings.

In both Kunene and Zambezi regions, the gender division of labour is rigid, where women are expected to be nurturers and men to be providers. For example, women are expected to stay at home and look after the household and children, while men are working outside the home. Both men and women lack the desire to diversify their livelihood and engage in activities that are not common in their cultures. Culture and slow attitudinal changes remain the key challenges to adaptation and building resilience in people of the Kunene and Zambezi Regions. Women attend meetings but do not contribute constructively owing to cultural norms that inhibit women to dominate discussions in public or to specific in the presence of men. A greater gap still exists between men's and women's roles in the conservancy and tourism enterprises.

The adaptation strategies that are generated through the analysis are used in the Harvard Gender Analytical Framework and the Social Relations Approach Framework to analyse the complexities in building resilience among communities in these regions. There is a need to find mechanisms to address issues that are hindering resilience building among communities through various programmes to sustain adaptation measures to reduce the impacts of climatic events on the contribution of tourism on communities. Local institutions such as conservancies are evidently important arrangement to reduce the vulnerability to climate change impacts through collective capacity building, income generation, empowerment, social networking, and lobbying agent for community members. The active participation of women in local institutions, either by attending meetings or being voted into leadership position, allows them to be part of a collective voice, leading to strengthening of common identities and local democracy. It is also believed that this will lead to collective learning and equal accessing of information for both men and women. Although women's representation on committees and attendance during meetings is strong, the views of women are still often not taken as seriously as those of men at meetings and other important platforms such as negotiation and or review of tourism joint venture contracts.

5. Conclusion

To this end, the book chapter has presented an assessment of gendered vulnerabilities in CBNRM focusing on Kunene and Zambezi regions of Namibia. The National Climate Change Strategy and Action Plan (NCCSAP) clearly indicates that climate change adaptation in Namibia especially among rural communities is crucial. The approach to address

vulnerabilities should consider that our societies are facing inequalities that could hinder the effectiveness of climate change adaptation efforts, and therefore, there is a need for responses to climate change risks to be gendered. In order to ensure that adaptation efforts are sustained, gender-responsive actions/activities that address and strengthen the inclusion of all members of the society including the most vulnerable women and men in local-level natural resources management and tourism sector should be implemented. The gender-responsive actions/activities should be designed in association with gender performance indicators and sex-disaggregated targets linked to the results framework that would guide the Monitoring and Evaluation (M&E) of the initiatives.

Additionally, the involvement of men and women must also consider marginalisation, age and social status of individuals in a given community in order to be inclusive. The methods of consultation must recognise existing cultural barriers in order to ensure women are represented as well as collaborating with local NGOs that work with women and other marginalised communities. Where there are disparities in capacities, training is recommended in order to participate meaningfully. In order to build a resilient community, the gender disparity between men and women in accessing information and capacity building opportunities should be addressed through gender-responsive initiatives. They should provide community wide training on critical areas to ensure equitable sharing and benefit of resources. For instance, they should provide legal training or support to local communities to improve negotiations of joint-venture partnerships. Therefore, in order to address impacts of climate change in the community-based tourism in Namibia, there is a need to identify and enhance synergies between mitigation actions and the adaptive capacities of women and men to deliver long-term benefits.

List of acronyms

ASSAR	Adaptation at Scale in Semi-Arid Regions
CBNRM	Community-Based Natural Resource Management
EIF	Environmental Investment Fund
GCF	Green Climate Fund
IECN	Integrated Environmental Consultants Namibia
IFRC	International Federation of Red Cross and Red Crescent Societies
IPCC	Intergovernmental Panel on Climate Change
M&E	Monitoring and Evaluation
MET	Ministry of Environment and Tourism
MGECW	Ministry of Gender Equality and Child Welfare
NACSO	Namibian Association of CBNRM Support Organisations

NCCSAP	National Climate Change Strategy and Action Plan
NGOs	Non-Governmental Organisations
NSA	Namibia Statistics Agency
SDGs	Sustainable Development Goals
SME	Small-and-Medium-Sized Enterprises
UNAM/SARDC	University of Namibia/Southern Africa Research Documentation Centre
UNFCCC	United Nations Framework Convention on Climate Change

Author details

Selma Lendelvo[1]*, Margaret N. Angula[2], Immaculate Mogotsi[1] and Karl Aribeb[3]

*Address all correspondence to: slendelvo@unam.na

1 Multidisciplinary Research Centre, University of Namibia, Namibia

2 Faculty of Humanities and Social Sciences, University of Namibia, Namibia

3 Environmental Investment Fund of Namibia, Namibia

References

[1] IPCC. Climate change 2014: Synthesis report. In: Pachauri RK, Meyer LA, editors. Contribution of Working Groups I, II and III to the Fifth Assessment Report of the Intergovernmental Panel on Climate Change. Cambridge, UK: Cambridge University Press; 2014

[2] Namibia Statistics Agency (NSA). Namibia Census of Agriculture 2013/2014: Communal Sector Report. Windhoek: Ministry of Agriculture, Water & Forestry; 2015

[3] Petzold J, Ratter BMW. Climate change adaptation under a social capital approach—An analytical framework for small islands. Ocean & Coastal Management. 2015;**112**(112):36-43

[4] Dankelman I. Climate-change: Learning from gender analysis and women's experiences of organising for sustainable development. Gender and Development. 2010;**2**:21-29

[5] MacGregor S. Gender and climate change: From impacts to discourses. Journal of the Indian Ocean Region. 2010;**6**(2):223-238

[6] Babugura A. Gender and Climate Change: South Africa Case Study. Cape Town, Southern Africa: Heinrich Böll Stiftung; 2010

[7] Mogotsi I, Lendelvo S, Angula M, Nakanyala J. Forest resources management and utilization through a gendered lens in Namibia. Environment and Natural Resources Research. 2016;**6**(4):79-90

[8] Otzelberger A. Gender-Responsive Strategies on Climate Change: Recent Progress and Ways Forward for Donors. United Kingdom: University of Sussex, IDS & BRIDGE; 2011

[9] Goh AHX. A Literature Review of the Gender-Differentiated Impacts of Climate-Change on women's and men's Assets and Well-Being in Developing Countries. CAPRi Working Paper No. 106. Washington, DC: International Food Policy Research Institute; 2012. DOI: 10.2499/CAPRiWP106

[10] Moosa CS, Tuana N. Mapping a research agenda concerning gender and climate change: A review of the literature. Hypatia. 2014;**29**(3):676-694

[11] Angula MN, Menjono E. Gender, culture and climate change in rural Namibia. Journal for Studies in Humanities and Social Sciences. 2014;**3**(1&2):225-238

[12] Mogotsi I, Lendelvo S, Angula M. Gender Assessment Report for the EDA Project. Windhoek: Environmental Investment Fund; 2017b

[13] ASSAR (adaptation at scale in semi-arid regions). In: Gendered Vulnerabilities to Climate Change: Insights from the Semi-Arid Regions of Africa and Asia. ASSAR Information Brief. Ottawa: CARIAA; 2016

[14] Mogotsi I, Lendelvo S, Angula M. Gender Desktop Review for the EDA Project. Windhoek: Environmental Investment Fund; 2017

[15] Ambunda L, de Klerk S. Women and customs in Namibia: A research overview. In: Ruppel OC, editor. Women and Custom in Namibia: Cultural Practice Versus Gender Equality. Macmillan Education Namibia: Windhoek; 2008

[16] Babugura A. Gender and Climate Change: South Africa Case Study. Southern Africa: Heinrich Böll Foundation; 2010. Retrieved: https://www.boell.de/en/navigation/climate-energy-South-Africa-9074.html

[17] Iipinge EM, LeBeau D. Beyond Inequalities: Women in Namibia. Windhoek and Harare: UNAM/SARDC; 2005

[18] Alston M. Gender mainstreaming and climate change. Women's Studies International Forum. 2014;**47B**:287-294. DOI: 10.1016/j.wsif.2013.01.016

[19] Arora-Jonsson S. Forty years of gender research and environmental policy: Where do we stand? Women's. Studies International Forum. 2014;**47**(B):295-308

[20] Namibia Statistics Agency (NSA). Namibia 2011 Population and Housing Census Main Report. Windhoek: Namibia Statistics Agency; 2011

[21] Central Bureau of Statistics. A Review of Poverty and Inequality in Namibia, Windhoek: Central Bureau of Statics. Windhoek: National Planning Commission; 2008

[22] Ashley C. The Impacts of Tourism on Rural Livelihoods: Namibia's Experience. London: Chameleon Press; 2000

[23] Massyn PJ, Humphrey E, Grossman D. Tourism Scoping Report—Kunene people's Park. Windhoek: Ministry of Environment and Tourism; 2009

[24] NACSO. Namibia's Communal Conservancies: A Review of the Progress and Challenges in 2011. Windhoek: NACSO; 2013

[25] NACSO. The State of Community Conservation in Namibia—A Review of Communal Conservancies, Community Forests and Other CBNRM Initiatives (2016 Annual Report). Windhoek: NACSO; 2016. Retrieved from: http://www.nacso.org

[26] MET. Management Plan: Skeleton Coast National Park. Windhoek, Namibia: Ministry of Environment and Tourism; 2013. Retrieved: www.met.gov.na/Skeleton Coast Management Plan.pdf

[27] National Statistics Agency (NSA). Population and housing census: Kunene regional profile. In: Basic Analysis with Highlights from 2011 Census. Windhoek: NSA; 2014

[28] Massyn PJ, Humphrey E, Grossman D. Tourism scoping report—Kunene peoples park. Prepared for: Ministry of Environment and Tourism, Directorate of Parks and Wildlife Management; 2009. http://www.the-eis.com

[29] www.met.gov.na/about-met/wildlife-and-national-parks/272

[30] International Federation of Red Cross and Red Crescent Societies (IFRC). Cost-Benefit Analysis Study Zambezi Region: Livelihoods Preparedness Intervention. Switzerland: IFRC; 2016

[31] National Statistics Agency (NSA). Population and housing census: Zambezi regional profile. In: Basic Analysis with Highlights from 2011 Census. Windhoek: NSA; 2014

[32] www.travelnewsnamibia.com/destinations/kavango-and-zambezi/zambezi-region/

[33] www.travelnewsnamibia.com/featured-stories/another-form-paradise-nambwa/

[34] [Registered conservancies in Namibia] (n.d). Retrieved from: http://www.nacso.org

[35] [Namibian map showing conservation areas] (August 2017). Retrieved from: http://www.nacso.org.na/resources/conservation-areas-map-a3

[36] ASSAR (Adaptation at Scale in Semi-Arid Regions). Planning for climate change in the semi-arid regions of southern Africa. In: ASSAR Information Brief #1. Ottawa: CARIAA; 2015

[37] Spear D, Baudoin M, Hegga S, Zaroug M, Okeyo A, Haimbili E, Angula M. Vulnerability and adaptation to climate change in southern Africa. In: ASSAR Working Paper. Ottawa: CARIAA; 2014

[38] Fauchereau N, Trzaska S, Rouault M, Richard Y. Rainfall variability and changes in southern Africa during the 20th century in the global warming context. Natural Hazards. 2003;**29**:139-154

[39] Jury MR. Climate trends in southern Africa. South African Journal of Science. 2013; **109**(1/2):980

[40] Bosch N. Flooding Caprivi. 2011. Retrieved from: http://www.caprivi.biz/flooding.html

[41] Masih I, Maskey S, Mussá FEF, Trambauer P. A review of droughts on the African continent: A geospatial and long-term perspective. Hydrology and Earth System Sciences. 2014;**18**:3635-3649

[42] UNICEF Namibia Humanitarian Situational Report. 2017. Retrieved from: https://www.unicef.org/yemen/YEM_sitreps_Dec2017.pdf

[43] Kahiurika N. President Declares Drought an Emergency. The Namibian Newspaper. 2016. Dated: 2016-06-30

[44] Staff Report. The Worst Drought in Memory. New Era Newspaper; 2013

[45] https://reliefweb.int/report/namibia/worst-drought-memory

[46] Integrated Environmental Consultants Namibia (IECN). Dealing with climate change: A community information toolkit on adaptation. A Resource Package Developed for Farmers and Natural Resource Users in the Kunene Region, Namibia. Windhoek: Ministry of Environment and Tourism; 2011

[47] Staff Reporter. Drought kills rhino calf in Kunene. New era newspaper report. 2017, January 17. Retrieved from: https://www.newera.com.na/2017/01/17/drought-kills-rhino-calf-in-kunene/

[48] Turpie J, Midgley G, Brown C, Barnes J, Pallet J, Desmet P, Tarr J, Tarr P. Climate Change Vulnerability and Adaptation Assessment for Namibia's Biodiversity and Protected Area System. Windhoek: Ministry of Environment and Tourism; 2010

[49] Kapolo IN. Drought Conditions and Management Strategies in Namibia. Windhoek, Namibia; n.d

[50] Kaseke E. Zambezi basin strategic planning in the context of a changing climate overview. Presentation. Harare: Zambezi Watercourse Commission; May 2016

[51] Schlosser CA, Strzepek K. Regional climate change of the greater Zambezi River basin: A hybrid assessment. Climatic Change. 2015;**130**:9-19

[52] Long S, Fatoyinbo TE, Policelli F. Flood extent mapping for Namibia using change detection and thresholding with SAR. Environmental Research Letters. 2014;**9**(3):035002

[53] Thomas DSK, Wilhelmi OV, Finnessey TN, Deheza V. A comprehensive framework for tourism and recreation drought vulnerability reduction. Environmental Research Letters. 2013;**8**:8

[54] NACSO. Community Conservation in Namibia: A Review of Communal Conservancies, Community-Forests and Other CBNRM Initiatives. Windhoek: NACSO; 2015

[55] Ishila J, Zeidler J. Adaptation working group (AWG), investment and financial flows (I&FF) assessment. In: Climate Change Adaptation Viewpoints Namibia Series, Vol. 1(1). Windhoek: Ministry of Environment and Tourism; 2010

[56] Lendelvo S, Munyebvu F, Suich H. Linking Women's participation and benefits within the Namibian community-based natural resources management program. Journal of Sustainable Development. 2012;**5**(12):27-39

Using the Monoplotting Technique for Documenting and Analyzing Natural Hazard Events

Conedera Marco, Bozzini Claudio, Ryter Ueli,
Bertschinger Thalia and Krebs Patrik

Additional information is available at the end of the chapter

Abstract

Historical or present-day oblique terrestrial photographs documenting natural disasters are abundant in archives and may be easily taken nowadays. While in most cases they provide highly informative details, they can hardly be georeferenced, which prevents their systematic use for analyzing and documenting the events and any related signs of damage. In this chapter, we present a monoplotting software program developed at WSL (the WSL Monoplotting Tool) that allows the georeferencing of ordinary individual photographs in order to produce georeferenced vector data by drawing them directly on the photographs and exchanging them with traditional geographic information systems (GIS-Systems). We report on the application of the monoplotting tool on selected study cases of natural events or protection infrastructures in Switzerland.

Keywords: event documentation, avalanches, debris flow, landslides, terrestrial pictures, georeferencing, GIS

1. Introduction: Documenting natural hazards

Natural events such as avalanches, landslides, rockfall, debris flows, and floods are intrinsic to mountain regions. They become hazards when they impact infrastructures and human beings [1]. Increases in settlement and industrial areas, as well as the ever-increasing need for technology and mobility, make modern society highly vulnerable to natural events, and the resulting potential damage is correspondingly significant [2–5]. In addition, extreme natural events and related impacts are expected to further increase in future due to the ongoing

climate change [6–10]. This makes managing natural hazards and mitigating their impact a prerequisite for keeping mountainous areas suitable for inhabitation [11, 12].

Learning from past events represents a very efficient way to expand our knowledge and improve the institutional infrastructure for tackling natural hazards in a sustainable manner [4, 12–14]. This also includes the systematic recording, documentation, and post-processing of ongoing or past events [10, 15].

Based on these considerations, many initiatives have been generated in recent decades for developing methods and protocols for the comprehensive and professional documentation of natural hazards and their marks (see, for instance, the international initiative documentation of mountain disasters (DOMODIS) [16] or the Interreg-Project DIS-ALP—Disaster and Information Systems of Alpine Regions [17]). When trying to build such a systematic register, many difficulties, and bottlenecks may arise concerning both ongoing and past events.

In the case of current disaster events, priority must be given to people rescue and the reestablishment of possibly damaged communication and traffic connections. During such actions, the signs of significant damage may be erased precluding the possibility of subsequent and detailed collection of information documenting the event. Similarly, when there are many simultaneous small events or when events occur in remote and poorly accessible areas and no special devices such as small aerial drones (micro-unmanned aerial vehicles [UAVs]) are available [18, 19], only terrestrial pictures or aerial oblique pictures taken by rescue or technical teams may be available. Nowadays, they are easy to shoot and fairly good in terms of quality even when using portable phones.

Significant past disastrous events dating back to before the first half of the twentieth century are often documented through very detailed terrestrial photographs. They are, however, not georeferenced, and as a result, are not readily suitable for reconstructing the precise location of the event and the damage caused [20, 21]. A great number of historical photographs thus exist that could provide important details on areas under the risk of natural hazards [22, 23].

To make such existing and potential photographic documentation available to extract localized information on natural hazardous events, a user-friendly georeferencing tool for oblique pictures is needed. In this chapter, we report on the main features, needs, and handling of the WSL monoplotting tool (hereafter also referred to as MPT_2.0), a user-friendly software program we developed to orthorectify and georeference oblique pictures, and present some study cases related to past and present natural hazard events in Switzerland.

2. What is monophotogrammetry?

Since its appearance in the first half of the nineteenth century and until to the introduction of stereo pairs photography basically consisted of single oblique pictures. Most were produced on glass plates, films or other large-format capture mediums, making it possible to depict, and document detailed landscape features at very high resolutions and quality. Besides providing detailed views of historical landscapes, such single terrestrial photographs have the
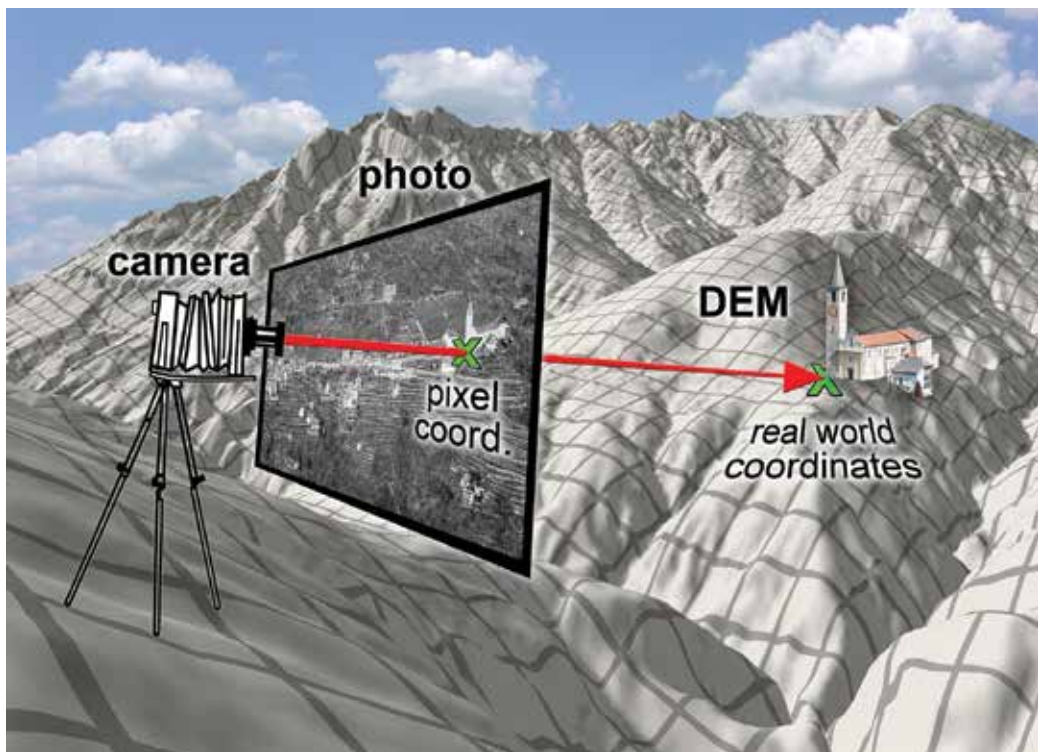
Figure 1. Main elements of the monoplotting system: Camera, image, and digital elevation model (DEM).

additional advantage of ease of interpretation as they represent people's everyday perception of the landscape [24]. Accurate georeferencing of such oblique pictures is, however, very difficult. This difficulty has so far prevented reliable quantitative geographical information from being obtained from such photographs.

To overcome this problem, the mono-photogrammetry or monoplotting idea was proposed in the early 1970s [25] wherein a photogrammetric system relates single unrectified, oblique terrestrial, or aerial images to a digital elevation model (DEM) of the corresponding landscape. As visualized in **Figure 1**, the basic idea is to relate to each other camera, picture, and DEM so that a ray from the camera center and going through a selected point in the picture will intersect the terrain DEM at the corresponding landscape point. Such a monoplotting system consists of the following main elements and input data:

• **One or more digital images** shot by digital cameras or resulting from the scanning of historical photographs (e.g., historic pictures on glass plates, postcards). Although the monoplotting system can handle any type of camera and lens (e.g., non-metric cameras), final system accuracy may be heavily influenced by their characteristics.

• **The digital elevation model (DEM),** which is usually structured as a regular data grid (e.g., geotiff raster data). The DEM may refer to the bare ground surface (i.e., Digital Terrain

Model: DTM) or may include vegetation, buildings, and other vertical objects (Digital Surface Model: DSM).

- **Control points (CPs)**, which are precisely and unambiguously identifiable locations (e.g., road and footpath intersections, rocky outcrops, and building corners) on both the image (pixel coordinates) and the landscape (real world coordinates, i.e., latitude, longitude, and altitude of the real-world coordinates). CPs should be at least four or more in number, preferably placed on the ground DTM, and possibly homogeneously distributed over the entire image. The corresponding real-world coordinates may be derived from georeferenced geographical information (e.g., orthophotos, maps, cadaster, DTM, and DSM) or can be directly surveyed in the field instrumentally (e.g., GPS).

Once calibrated in such a monoplotting system, single oblique pictures can also be interpreted three-dimensionally (3D). The main limitation of the monoplotting system is the fact that in mono-photogrammetry, only points on the terrain (DEM-surface) can be precisely located whereas stereo-photogrammetry enables the calculation of the position of any common pixel in the stereo pair.

3. The WSL monoplotting tool

The implementation of the monoplotting principle in a practical tool has been restricted by the lack of basic data (i.e., detailed digital elevation models [26]) or the inadequacy of the available computing power [27]. As a result, the pioneering work of Makarovič [25, 28] has long remained isolated. Only in the last 20 years have new software and tools been developed based on the monoplotting principle [29–32]. None of these products, however, really meet the needs of potential end users in terms of operational flexibility and user-friendliness, thus, greatly inhibiting their broad use.

Recently, improvements in digital photography (e.g., high-resolution digital cameras, digitalization of historical pictures in high-resolution) and advancements in computing science have opened new possibilities for developing a specific monoplotting tool with an interface that makes it easy to handle not only by specialized researchers, but also non-expert users for operational purposes [21]. To that end, we developed the WSL monoplotting tool (available at present in the 2.0 version) [24], which has the following main features and characteristics (see also https://www.wsl.ch/monoplotting for detail):

- A user-friendly, intuitive, and self-explanatory interface enabling the simultaneous visualization of one or more photographs of the target landscape as well as of related orthophotos, maps, or other georeferenced representation of the terrain surface (**Figure 2**).

- A computer-assisted, semiautomatic, and interactive calibration process for the camera, including the reconstruction of all elements in the monoplotting system (e.g., snapshot location).

- An immediate estimate of the error for each control point used for the calibration of the oblique photograph.

- A simple editor for defining and measuring features of particular interest (e.g., polygons, lines, points, and heights) on the photographs.

- The ability to handle native ERSI-shapefiles.

- Export–import routines allowing data exchange (e.g., CSV or shapefiles) between and from conventional geographic information systems (GIS).

The heart of the tool is the iterative process whereby camera calibration is achieved. This is done in order to precisely estimate and simulate the three intrinsic and the six extrinsic camera parameters. The three intrinsic parameters are the two-pixel coordinates (xc, yc) of the principal point (i.e., the image center), and the principal distance (perpendicular distance from the image to the projection center). The six extrinsic parameters are the three real-word coordinates of the lens pinhole and the three Euler rotation angles α (pan/z-axis), β (tilt/y-axis), and γ (roll/x-axis) of the camera (see [24, 33] for more details). The calibration routine generates a sequence of collinearity equations commonly used in photogrammetry [34] that estimates and approximates the unknown camera parameters [35] in order to progressively minimize the error of the camera model when applied to the input data. Once camera calibration is achieved, the tool implements a model of all the extrinsic and intrinsic camera parameters, which simulates the original camera setup when the picture was taken. The tool also
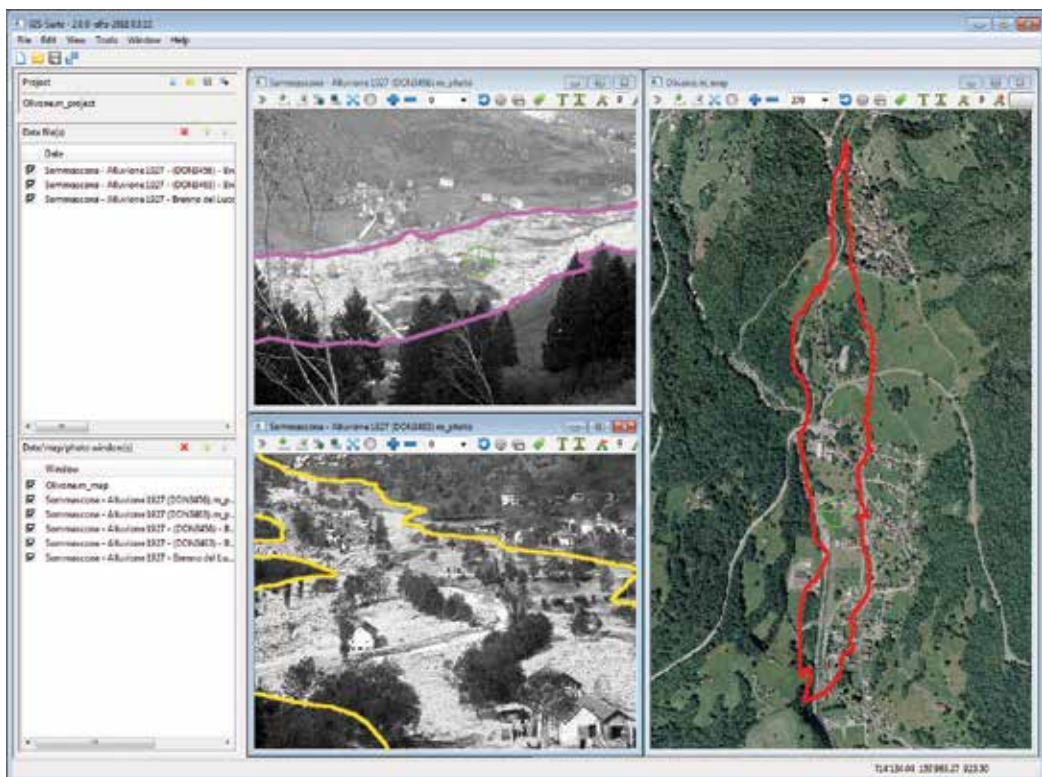

Figure 2. The MPT_2.0 applied to the Sommascona flood event (see Example 2). A major strength of the 2.0 release is the option of opening and processing more oblique images or maps of the same area to obtain a complete view of the event.

returns the theoretical 3D errors, which correspond to the deviation between the real-world coordinates of each control point and the corresponding coordinates as calculated from the calibration procedure of the monoplotting system.

It is important to note that shooting point reconstruction is implemented so as to optimize the overlap of the corresponding CPs in the image to be georeferenced and in the georeferenced map, respectively. Thus, the reconstructed theoretical shooting point may not necessarily correspond precisely to the real camera position, and the two may differ by a few centimeters to several meters.

4. Applications of the monoplotting tool

We present here selected examples of MPT applications in the field of natural hazards spanning from the reconstruction of historical and current damaging events to the verification of the efficiency of existent infrastructures as well as the related achieved precision and required workload.

4.1. Reconstructing historical natural events

A detailed reconstruction of past hazardous events may be of paramount importance for understanding related natural processes, defining danger zones, and planning protection infrastructures. Processing and evaluating pictures of past disastrous events by means of monoplotting is a highly efficient way of retrieving information contained in historical pictures, and transferring it to modern tools such as GIS.

4.1.1. Example 1: the Sasso Rosso slope failure: 1898, Airolo

The Sasso Rosso area above the village of Airolo (Canton of Ticino) turned into an unstable slope due to the decompression caused by post-glacial ice retreat. Local authorities were aware of this and put the area under surveillance. Initial significant slope movement began in the summer of 1898, followed by three slides of increasing size in December of the same year. Fortunately, the authorities decided at that time to close the school and evacuate the endangered part of the village. Just before midnight in the night of the December 27, 1898, a series of slides occurred, with a volume totaling 500,000 m^3, reaching part of the village and destroying a hotel, 11 houses, and 15 stables, while causing three deaths.

According to the reconstructed and digitalized perimeter of the debris deposit as reported in **Figure 3**, the area in question covered ca. 425,000 m^2. The MPT_2.0 also enables the projection of the digitalized deposit perimeter on a historical picture prior to the debris flow (**Figure 4**), clearly identifying the area and the buildings destroyed by the event.

4.1.2. Example 2: flood in Sommascona: 1927, Olivone

During the autumn of 1927, southern Switzerland and northern Italy experienced a period of heavy precipitation that caused several flood events of varying severity. The worst occurred
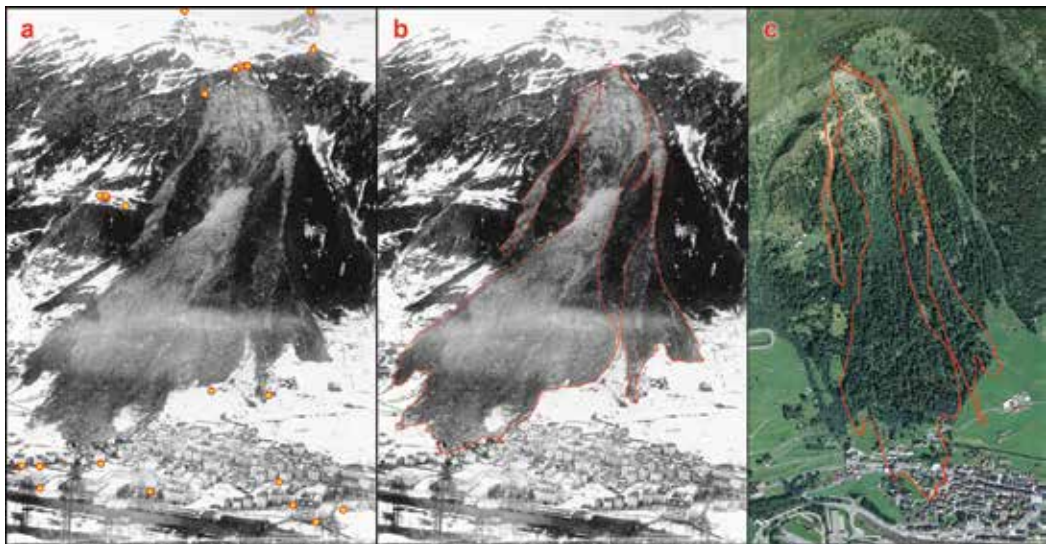
Figure 3. The Sasso Rosso slope failure (Airolo, 1898). (a) Original obliques images with control points. (b) Digitalization of the slide contour on the original obliques images. (c) Projection of the slide perimeter on a current orthophoto (modified from Conedera et al. [21]).

Figure 4. The Sasso Rosso slope failure (Airolo, 1898). Projection of the slide perimeter on an oblique terrestrial image of the area prior to the event (source: Conedera et al. [21]).

in Ticino (Switzerland) on Sunday afternoon on September 25, 1927, as a consequence of a strong and long-lasting waterspout above the mountain village of Olivone. This flood is still considered to be the most damaging natural event of the last century in the region. It destroyed part of the village of Campo Blenio and flooded the plain of Olivone over an area of at least 199,366 m^2 (ArcGIS computation of the perimeter as digitalized with the monoplotting tool), affecting two sawmills and several private buildings (**Figure 5**). Due to the favorable weekday, no fatalities were recorded.
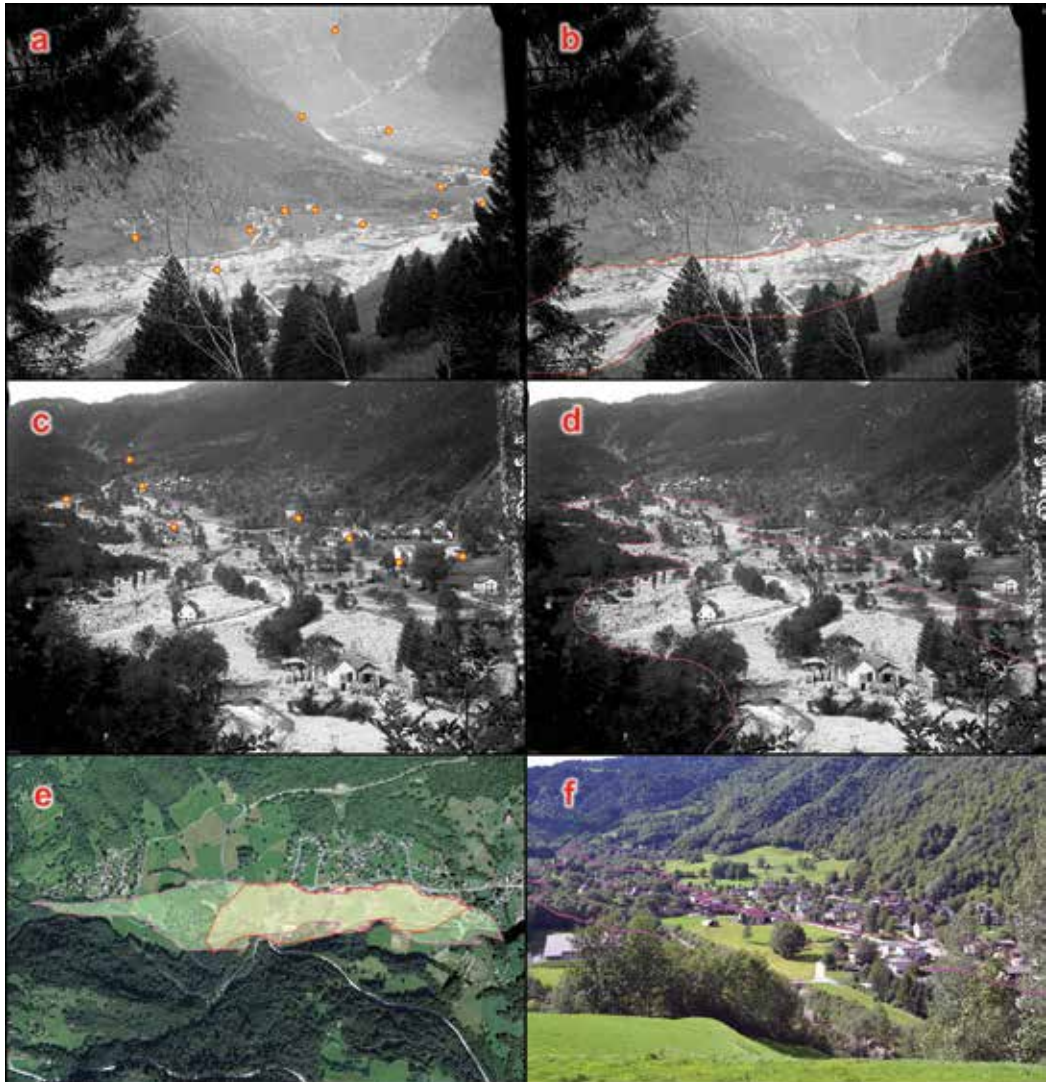

Figure 5. Flood of the Sommascona plain (Olivone, 1927). (a + b) original oblique images with control points. (c + d) Digitalization of the flood contours on the original oblique image. (e) Projection of the digitalized flood contours on the current orthophoto. (f) Projection of the digitalized flood contours on the current oblique terrestrial image (modified from Conedera et al. [21]).

4.2. Documenting natural events in real time

Real-time documentation of the fresh marks of hazardous events makes it possible to capture many important details that may enable a realistic reconstruction of the processes that occurred. Such improved understanding of underlying processes is, in turn, of paramount importance to improve the simulation and modeling of natural hazards as well as possible prevention and mitigation measures. Thanks to the monoplotting approach actual natural hazards or natural hazard-related situations can be easily processed and mapped, regardless of the remoteness or accessibility of the area in question.

4.2.1. Example 3: avalanches in Hasliberg: 2018, Meiringen

For safety reasons, the security managers of the Hasliberg ski resort record all artificially provoked and natural occurring avalanches by means of SLF pro tools, which is a map-based information system (https://www.slf.ch/en/services-and-products/protools.html). For this purpose, they roughly estimate the avalanche contour in the field. Over time, a conspicuous number of events have been entered into the system, causing the cantonal forest service to migrate all data into the official historical avalanche cadaster. Before doing this, however, the reliability of the empirical approach used by the security managers required testing. To that end, an aerial recognition mission was organized on January 24, 2018, and a number of fresh avalanches were photographically documented to be processed with the MPT_2.0.

Despite the difficulty in identifying suitable CPs in a snowy landscape, the theoretical 3D-error achieved is more than acceptable (**Table 1**), and each single registered avalanche perimeter could be measured and compared with the estimated contours by the ski resort managers. The comparison revealed significant differences with a trend toward overestimating the avalanche size by the local ski managers (**Figure 6**). Single events should thus be verified by the mean of the MPT_2.0 before their migration into the official historical avalanche cadaster.

4.2.2. Example 4: Spitzhorn rockslide: 2017, Gstaad

In October 2017, a rockslide moved a volume of ca. 50,000 m^3 downhill from the west slope of the Spitzhorn mountain. The event took place in a single main slide preceded by individual

Study case		Object	Image quality	Control points	Theoretical 3D-error (m)		
					Min	Max	Mean
1.	Airolo	Slope failure	Medium	20	0.2	3.0	0.9
2.	Olivone	Flood (a)	Good	8	0.1	2.4	0.9
		Flood (b)	Good	13	0.2	0.9	0.4
3.	Meiringen	Avalanche	Good	5	0.1	0.6	0.2
4.	Gstaad	Rockslide	Good	6	0.1	2.3	0.5
5.	Adelboden	Snow bridges	Good	6	0.1	1.0	0.3

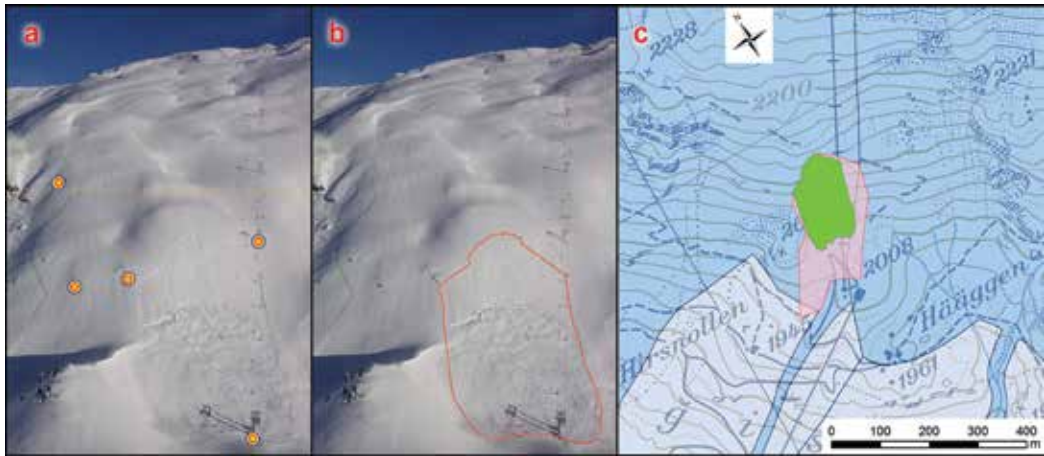**Table 1.** Achieved theoretical 3D-error for the presented study cases.

Figure 6. Avalanches in the Hasliberg ski area (Meiringen, 2018). (a) Original oblique image with control points. (b) Digitalization of the avalanche perimeter on the original image. (c) Map showing the area in question and avalanches over the years (blue), the avalanche perimeter as estimated by the ski resort managers (red), and as measured by the MPT_2.0 (green).

rockfalls, which gave security managers the opportunity to block all vehicular and pedestrian access, thus preventing fatalities. Nevertheless, the rockslide caused significant damage to the forest, the electric line, and trails.

In order to assess the involved area precisely, we used the MPT_2.0 to process an oblique picture taken during a field inspection. Despite the difficulty in selecting suitable CPs (**Figure 7**), the achieved precision (**Table 1**) and the related time investment (**Table 2**) for analyzing the image are acceptable.

4.3. Verifying the efficiency of protection infrastructures

Documenting protection infrastructures during particular events or climatic situations may also be very helpful when assessing their functional capability and reliability in preventing natural events. Our final example relates to the assessment of the dimensioning and efficiency of snow barriers as protection against avalanches under real conditions.

4.3.1. Example 5: analyzing the functionality of snow bridges: 2018, Adelboden

The functional capability of snow bridges against avalanche detachment highly depends on the correct dimensioning of the supporting structures. A prerequisite for snow bridge efficiency is that the snow never rises above the supporting area of the structure. When these conditions are not satisfied for a significant part of the snow bridge, avalanches can detach from the exceeding snow cover, damaging the snow bridges located downhill, and threatening the infrastructures in the danger zone.

Snow bridge reliability can be best assessed in real conditions during exceptional snow cover conditions. This was the case in Adelboden (Canton Berne, Switzerland) during the heavy snowfalls combined with strong snow blowing winds that repeatedly occurred in the winter
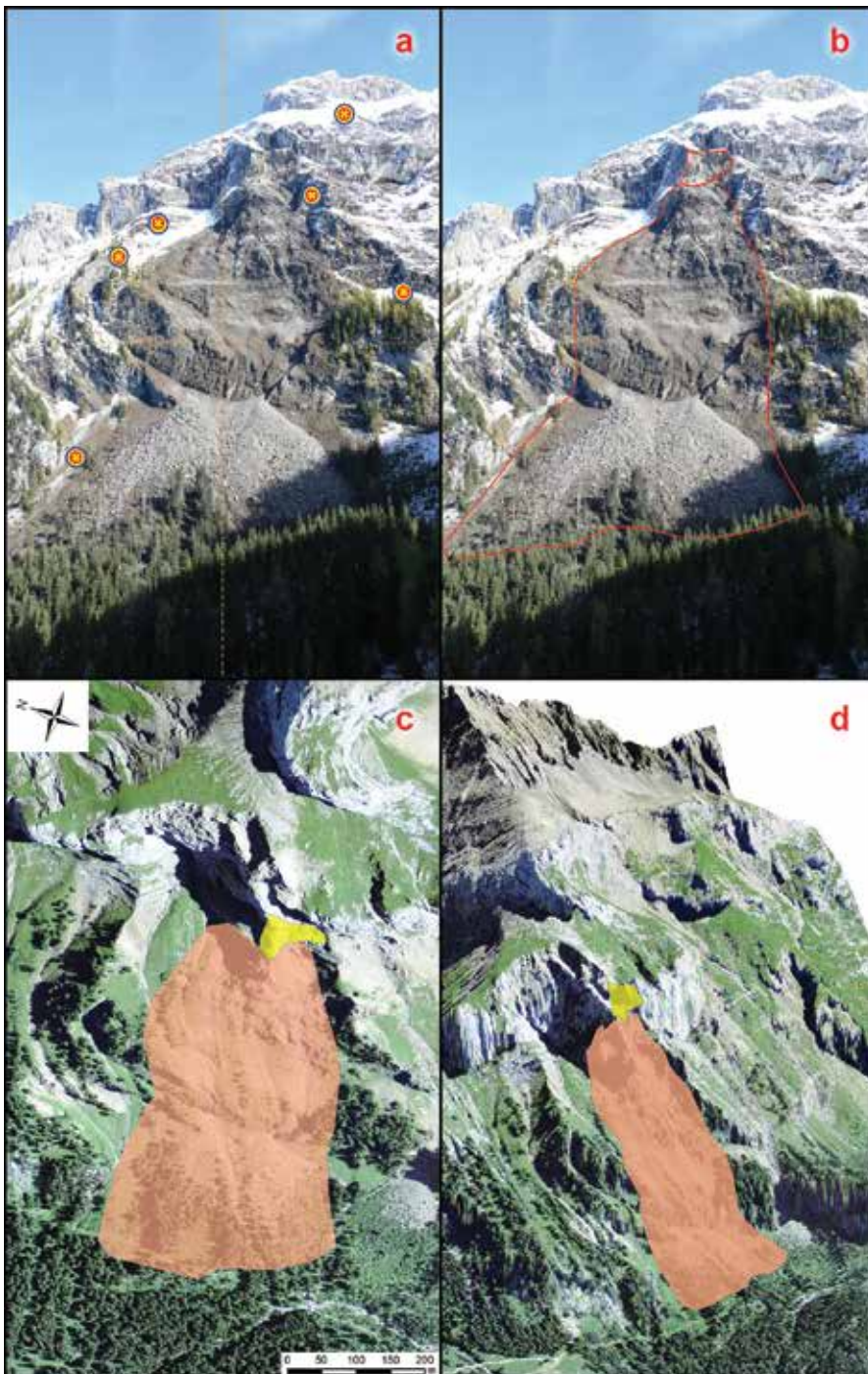
Figure 7. Spitzhorn rockslide (Gstaad, 2017). (a) Original oblique images with control points. (b) Digitalization of the detachment and transit/deposit zone on the original oblique image. (c) Projection of the digitalized contours on the current orthophoto. (d) Projection and 3D viewing of the digitalized zones in ESRI ArcScene. Yellow contours = detachment zone; orange contours = transit and deposit zone.

Working steps	Time investment (min)		
	Min	Mean	Max
Preparation of basic data for the area in question (DEM, maps, orthophotos, images)	10	20	30
Choosing and fixing control points (CPs)	10	30	90
Camera calibration	5	15	30
Digitalizing target objects	5	15	20
Import/export	5	5	5
Total	35	90	175

Table 2. Average time investment for individual working steps when processing an image with the WSL monoplotting tool.

Figure 8. Snow bridges (Adelboden, 2018). (a) Original oblique image of the snow bridge constructions with control points. (b) Digitalization of the snow bridges. (c) Projection of the digitalized bridges on the current orthophoto highlighting in blue the parts covered by snow.

season of 2017/2018, which caused a partial blanketing of the snow bridges in the upper part of the area in question. On January 24, 2018, which was 2 days after the end of a heavy snowfall event, a helicopter recognition mission was organized and the snow bridge area was photographed in order to document the blanketed parts (**Figure 8a**).

Through the georeferencing process of the MPT_2.0 (**Figure 8b**), the bridges were digitalized and exported to a GIS file, making it possible to identify the blanketed snow bridge parts, which may fail in their protection function (**Figure 8c**).

5. Discussion

The MPT_2.0 has proven to be a highly suitable instrument for georeferencing and documenting the impact of geophysical (landslides, avalanches) and hydrological (debris flows, floods) natural hazards. As reported in **Table 1**, the achieved theoretical precision for the presented study cases ranges from decimeters to a few meters, which is more than acceptable for practical purposes. In addition to the image quality and its resolution in particular, the precision of the system additionally depends on the DEM resolution and on the number, clarity, and

distribution of the control points. The combination of highly resolved DEM and unambiguous (e.g., constructions), well-distributed CPs easily result in sub-metric precision.

Local significant deviations in the reconstructed position in monoplotting with respect to the real world may, in contrast, occur when there are objects in the background landscape of an image, or when areas in the landscape display a small incidence angle with respect to the camera ray. Here, small imprecisions in clicking on the corresponding image pixel may result in a great displacement of the corresponding real point where the ray intersects the DEM. In case of crests and ridges, the ray may even overshoot the DEM and hit the background landscape or get lost in the sky.

Additional sources of error are changes in the terrain morphology that took place between the time the image was shot and the DEM measurement. These may have originated in anthropogenic mass movements or by natural events such as landslides. In the latter case, only the untouched margins of the terrain changes may be localized with the monoplotting technique (see **Figure 4**).

Similar achievement potential and limitations of the MPT_2.0 in terms of usefulness and achievable precision have been reported in independent scientific studies in the field of historical landscape reconstructions [36] and treeline ecotone dynamics [37].

According to our accumulated experience utilizing the MPT_2.0, the required time investment highly depends on (a) the epoch of the event (the further back in time, the more the landscape may have changed, and the fewer available control points), (b) the quality of the image regarding the extent and form of the object to be digitalized (from local land slide to regional floods), and (c) on the available information (shooting location in particular). Thus far, most oblique images with suitable CPs were successfully processed with the MPT_2.0 in a short time. The most time-consuming steps relate to the preparation of basic information such as the DEM, maps, orthophotos, images of the area in question, and the definition of the CPs (**Table 2**).

6. Conclusions

The main aim of using the WSL monoplotting tool (MPT_2.0) is to document in real time and reconstruct the effects of natural events before damage and signs in the landscape are removed or disappear. In this respect, the tool was found to be very flexible, enabling the operator to combine images from different epochs, and points of view that describe the same event. The possibility of georeferencing such images by reconstructing the unknown shooting point enables the use of oblique aerial photographs taken from helicopters, which in turn, opens the door to documenting natural events in highly inaccessible sites (see Example 5, blanketed snow bridges).

When suitable photographic material exists, even events dating back more than a century can be reconstructed with very satisfactory precision (see Example 1, Sasso Rosso area, Airolo). Similarly, also the extent and the severity of past pest attacks, diseases or wildfires can be

retrospectively reconstructed provided, there is a suitable photographic documentation. The MPT_2.0 could also be very useful in combination with the surveillance system cameras for automatic wildfire detection. When oblique images of the landscape from such fixed cameras are georeferenced in the monoplotting system, the pixel coordinates of the fire detection can also be immediately expressed in real-world coordinates (including the possible error) when a fire ignition spot is detected.

In contrast, less practicable is the use of the MPT_2.0 for the real-time documentation of dynamic processes such as the localization of a fire line front in fast spreading, large wildfires. In such cases, unmanned aerial vehicles (UAVs, drones) may be most suitable for producing real-time, georeferenced images of the fire front, or residual burning.

At present, the 2.0 release of the WSL Monoplotting Tool (MPT 2.0) is available at the project site (www.wsl.ch/monoplotting) and freely usable for research purposes. Please refer to this webpage for details on the terms and conditions of use, services, and tutorial options.

Acknowledgements

Author details

Conedera Marco[1]*, Bozzini Claudio[1], Ryter Ueli[2], Bertschinger Thalia[2] and Krebs Patrik[1]

*Address all correspondence to: marco.conedera@wsl.ch

1 Swiss Federal Institute for Forest, Snow and Landscape Research (WSL), Insubric Ecosystems Research Group, Cadenazzo, Switzerland

2 Forest Service Canton Berne, Natural Hazards Section, Interlaken, Switzerland

References

[1] Frey W, Wilhelm C, Gesamtbetrachtung KB N-v E z. Schweizerische Zeitschrift für Forstwesen. 2001;**152**(5):199-203. DOI: 10.3188/szf.2001.0199

[2] Wehrli A, Brang P, Maier B, Duc P, Binder F, Lingua E, Ziegner K, Kleemayr K, Dorren L. Schutzwaldmanagement in den Alpen—eine Übersicht. Schweizerische Zeitschrift für Forstwesen. 2007;**158**(6):142-156. DOI: 10.3188/szf.2007.0142

[3] Hilker N, Badoux A, Hegg C. The Swiss flood and landslide damage database 1972-2007. Natural Hazards and Earth System Sciences. 2009;**9**:913-925. DOI: 10.5194/nhess-9-913-2009

[4] Klinke A, Renn O. Nachhaltiger Umgang mit natürlichen Risiken: antizipativ, integrativ und interdisziplinär. Schweizerische Zeitschrift für Forstwesen. 2011;**162**(12):442-453. DOI: 10.3188/szf.2011.0442

[5] Schwendtner B, Papathoma-Kohle M, Glade T. Risk evolution: How can changes in the built environment influence the potential loss of natural hazards? Natural Hazards and Earth System Sciences. 2013;**13**:2195-2207. DOI: 10.5194/nhess-13-2195-2013

[6] Frei CR, Schöll R, Fukutone S, Schmidli J. Vidale PL future changes of precipitation extremes in Europe. Journal of Geophysical Research. 2006;**111**:D06105. DOI: 10.1029/2005JD005965

[7] Fowler HJ, Ekström M, Blenkinsop S, Smith AP. Estimating change in extreme European precipitation using a multimodel ensemble. Journal of Geophysical Research. 2007;**112**: D18104. DOI: 10.1029/2007JD008619

[8] Beniston M, Stephenson DB, Christensen OB, Ferro CAT, Frei C, Goyette S, Halsnaes K, Holt T, Jylhä K, Koffi B, Palutikof J, Schöll R, Semmler T, Woth K. Future extreme events in European climate: An exploration of regional climate model projections. Climatic Change. 2007;**81**:71-95. DOI: 10.1007/s10584-006-9226-z

[9] Marty C, Phillips M, Lehning M, Wilhelm C, Bauder A. Klimaänderung und Naturgefahren in Graubünden. Schweizerische Zeitschrift für Forstwesen. 2009;**160**(7):201-209. DOI: 10.3188/szf.2009.0201

[10] Papathoma-Köhle M, Promper C, Glade T. A common methodology for risk assessment and mapping of climate change related zazards—Implications for climate change adaptation policies. Climate. 2016;**4**(8):1-23. DOI: 10.3390/cli4010008

[11] Hollenstein K, Hess J. Integrales Management von gravitativen Naturrisiken in der Schweiz. Schweizerische Zeitschrift für Forstwesen. 2011;**162**(12):454-463. DOI: 10.3188/szf.2011.0454

[12] Nquot I, Kulatunga U. Flood mitigation measures in the United Kingdom. In: Proceedings of the 4th International Conference on Building Resilience, Incorporating the 3rd Annual Conference of the Android Disaster Resilience Network, Manchester (United Kingdom). September 8-11, 2014. pp. 81-87

[13] Garcia C, Blahut J, Angignard M, Pasuto A. The importance of the lessons learnt from past disasters for risk assessment. In: VanAsch T, Corominas J, Greiving S, Malet JP, Sterlacchini S, editors. Mountain Risks: From Prediction to Management and Governance. Springer; 2014. pp. 275-284. DOI: 10.1007/978-94-007-6769-0_9

[14] Uhlemann S, Thieken AH, Merz B. A quality assessment framework for natural hazard event documentation: Application to trans-basin flood reports in Germany. Natural Hazards and Earth System Sciences. 2014;**14**:189-208. DOI: 10.5194/nhess-14-189-2014

[15] Adams MS, Fromm R, Lechner V. High-resolution debris flow volume mapping with unmanned aerial systems (UAS) and photogrammetric techniques. July 12-19, 2016. pp. 749-755

[16] Hübl J, Kienholz H, Loipersberger A, editors. DOMODIS. Dokumentation alpiner Naturereignisse. Klagenfurt: Internationale Forschungsgesellschaft Interpraevent; 2006. 44 p. ISBN: 3-901164-07-3

[17] PLANALP (Platform on Natural Hazards of the Alpine Convention). Dokumentation von Naturereignissen—Feldanleitung. Innsbruck/Bern; 2006. 64 p

[18] Giordan D, Manconi A, Remondino F, Nex F. Use of unmanned aerial vehicles in monitoring application and management of natural hazards. Geomatics Natural Hazards & Risk. 2017;**8**:1-4. DOI: 10.1080/19475705.2017.1315619

[19] Huang H, Long J, Yi W, Yi Q, Zhang G, Lei B. A method for using unmanned aerial vehicles for emergency investigation of single geo-hazards and sample applications of this method. Natural Hazards and Earth System Sciences. 2017;**17**:1961-1979. DOI: 10.5194/nhess-17-1961-2017

[20] Copien C, Frank C, Becht M. Natural hazards in the Bavarian alps: A historical approach to risk assessment. Natural Hazards. 2008;**45**:173-181. DOI: 10.1007/s11069-007-9166-6

[21] Conedera M, Bozzini C, Scapozza C, Rè L, Ryter U, Krebs P. Anwendungspotenzial des WSL-Monoplotting-Tools im Naturgefahrenmanagement. Schweizerische Zeitschrift für Forstwesen. 2013;**164**(7):173-180. DOI: 10.3188/szf.2013.0173

[22] Edwards M. The United-States geophysical-data center can provide natural hazards damage photographs. Environmental Geology and Water Sciences. 1991;**18**:81-81. DOI: 10.1007/bf01704660

[23] NGDC (NOAA National Geophysical Data Center). Natural Hazards Image Database [Internet]. 2018. Available from: http://oregonexplorer.info/content/noaa-national-geophysical-data-center-ngdc-natural-hazards-image-database [Accessed: March 20, 2018]

[24] Bozzini C, Conedera M, Krebs P. A new monoplotting tool to extract georeferenced vector data and orthorectified raster data from oblique non-metric photographs. International Journal of Heritage in the Digital Era. 2013;**1**(3):500-518. DOI: 10.1260/2047-4970.1.3.499

[25] Makarovič B. Digital monoplotters. The ITC Journal. 1973;**4**:583-600

[26] Hodgson ME, Bresnahan P. Accuracy of airborne lidar-derived elevation: Empirical assessment and error budget. International Archives for Photogrammetry and Remote Sensing. 2004;**70**(3):331-339. DOI: 10.14358/PERS.70.3.331

[27] Ceruzzi PE. A History of Modern Computing. Cambridge: MIT Press; 2003. 445 p. ISBN: 0-262-53203-4

[28] Makarovič B. Data base updating by digital monoplotting. The ITC Journal. 1982;**4**:384-390

[29] Doytsher Y, Hall JK. FORTRAN programs for coordinate resection using an oblique photograph and high-resolution DTM. Computers & Geosciences. 1995;**21**(7):895-905. DOI: 10.1016/0098-3004(95)00023-2

[30] Aschenwald J, Leichter K, Tasser E, Tappeiner U. Spatio-temporal landscape analysis in mountainous terrain by means of small format photography: A methodological approach. IEEE Transactions on Geoscience and Remote Sensing. 2001;**39**(4):885-893. DOI: 10.1109/36.917917

[31] Corripio JG. Snow surface albedo estimation using terrestrial photography. International Journal of Remote Sensing. 2004;**25**(24):5705-5729. DOI: 10.1080/01431160410001709002

[32] Fluehler M, Niederoest J, Akca D. Development of an educational software system for the digital monoplotting. In: Proceedings of the International Society for Photogrammetry and Remote Sensing, Working group VI/1–VI/2 (Tools And Techniques for E-Learning), Potsdam (Germany). June 1-3, 2005. 6 p

[33] Kraus K. Photogrammetry. Fundamentals and Standard Processes. Vol. 1. Bonn: Dümmlers; 1993. 397 p. ISBN: 13: 9783427786849

[34] Ghosh SK. Fundamentals of Computational Photogrammetry. New Delhi: Concept Publishing Company; 2005. 254 p. ISBN: 13: 9788180691874

[35] Strausz DA. An Application of Photogrammetric Techniques to the Measurement of Historic Photographs. Oregon State University, Department of Geosciences; 2001

[36] Stockdale CA, Bozzini C, Macdonald SE, Higgs E. Extracting ecological information from oblique angle terrestrial landscape photographs: Performance evaluation of the WSL Monoplotting tool. Applied Geography. 2015;**63**:315-325. DOI: 10.1016/j.apgeog. 2015.07.012

[37] McCaffrey DR, Hopkinson C. Assessing fractional cover in the alpine treeline ecotone using the WSL Monoplotting tool and airborne Lidar. Canadian Journal of Remote Sensing. 2017;**43**:504-512. DOI: 10.1080/07038992.2017.1384309

Tsunamis and Volcanoes: Preventive Education and Training

Tsunami Hazard Assessment for the Hokuriku Region, Japan: Toward Disaster Mitigation for Future Earthquakes

Michihiro Ohori, Yuri Masukawa and
Keisuke Kojima

Additional information is available at the end of the chapter

Abstract

In Japan, compared with the Pacific coast, the Japan Sea coast has low seismicity and has experienced very few occurrences of historical tsunami damage. These characteristics lead to some difficulties in the promotion of disaster prevention education, because the Japan Sea coast has not often been threatened by earthquakes and tsunamis. In our study, focusing on the Hokuriku region in Japan, we conducted a tsunami simulation and examined the resulting tsunami hazard map. Three potential faults of Mw7.6 earthquake were selected to generate the tsunami. In addition, we calculated these three events with Mw7.8, given the inherent uncertainty in source parameters. Aside from tsunami height, arrival time, inundation height, and inundation area, we calculated the seismic intensity and the liquefaction occurrence rate by simplified methods. Our results indicated that Suzu City in Ishikawa Prefecture, located in the northeastern part of the Noto Peninsula, has a relatively high potential risk of tsunami as well as strong motion and liquefaction. Thus, Suzu City would represent a highly appropriate area in which to promote disaster prevention education in the Hokuriku region.

Keywords: tsunami, simulation, hazard assessment, Hokuriku region, disaster mitigation

1. Introduction

The 2011 Tohoku earthquake (Mw9) generated a giant tsunami and caused the death of more than 18,000 inhabitants (including missing persons). Surprisingly, a considerable number of people did not evacuate due to a misunderstanding regarding the early-stage warning of a

3 m-high tsunami and/or too much trust in the protection afforded by high tidal banks, despite having sufficient evacuation time after the strong ground shaking. The Pacific coast of the Tohoku region has been repeatedly threatened by tsunamis, and thus appropriate disaster prevention education and evacuation drills have been conducted. However, it was nevertheless surprising that there were such a high number of victims even in regions with high disaster prevention awareness.

Compared with the Pacific coast, the Japan Sea coast has experienced few tsunami disasters, especially in the Hokuriku region, where the seismicity is low; however, disaster prevention awareness is also low. To promote practical disaster prevention education by making full use of lessons learned from the tsunami disaster following the 2011 Tohoku earthquake, it is crucial to deepen our understanding of a devastating tsunami following strong ground shaking and relevant damage from an earthquake.

In this study, the focus of interest is the Hokuriku region (Fukui, Ishikawa, and Toyama Prefectures). To date, each prefecture has conducted its own tsunami simulation and published hazard maps in which the region is limited to its own prefecture [1–3]. When the same seismic fault is examined, source parameters differ between prefectures. Therefore, it is difficult to use hazard maps as teaching materials to gain an understanding of the whole picture of a tsunami disaster, as a tsunami obviously takes no account of administrative boundaries. In addition, cooperation between adjacent prefectures in the matter of preparedness for future tsunami disasters is not without problems.

The 2011 Tohoku earthquake (Mw9) prompted investigation on the possible occurrence of a tsunami on the Japan Sea coast in two different research projects: one by the Ministry of Land, Infrastructure and Transport [4] and the other by the Ministry of Education, Culture, Sports, Science and Technology [5]. However, since the coverage of these studies is very broad, and they do not specifically focus on the Hokuriku region, it may be difficult to make use of the project results in local disaster prevention education in our region of interest.

Here, we carried out hazard assessment of a tsunami following an earthquake in the Hokuriku region. After considering the whole region, we extracted a model district to be prioritized in future disaster education. Using a simplified method, ground shaking and liquefaction rates were evaluated to gain insight into tsunami hazard in relation to strong ground motion.

2. Analytical methods

2.1. Tsunami simulation

In the present study, we used TSUNAMI-K software, which was originally developed and published by a research group at Tohoku University as the analytical Fortran code of TUNAMI [6–8] and later incorporated with the GUI (graphical user interface) environment by Kozo Keikaku Engineering Inc. Details of the theory commentary are given in literatures [6–8]. The computer program TUNAMI developed by Tohoku University has been distributed worldwide

as part of the Tsunami Inundation Modeling Extension (TIME) project promoted by collaboration of the International Union of Geodesy and Geophysics (IUGG) and the Intergovernmental Oceanographic Commission (IOC) of the United Nations Educational, Scientific and Cultural Organization (UNESCO) during the International Decade for Natural Disaster Reduction (IDNDR). Currently it has been recognized as the UNESCO's standard evaluation method for tsunami and used by 36 institutions of 19 countries, which suffered or will suffer tsunami hazards. So, the accuracy and reliability of the code have been verified by many studies (e.g., [9–11]). Here, the outline of numerical calculations and the analytical conditions, implemented into the analytical codes, are briefly summarized.

2.1.1. Governing equations

For the tsunami analyses, the shallow-water long-wave theory is used. The governing equations are expressed in Eqs. (1)–(3).

$$\frac{\partial \eta}{\partial t} + \frac{\partial M}{\partial x} + \frac{\partial N}{\partial y} = 0 \tag{1}$$

$$\frac{\partial M}{\partial t} + \frac{\partial}{\partial x}\left(\frac{M^2}{D}\right) + \frac{\partial}{\partial y}\left(\frac{MN}{D}\right) + gD\frac{\partial \eta}{\partial x} + \frac{gn^2 M}{D^{7/3}}\sqrt{M^2 + N^2} = 0 \tag{2}$$

$$\frac{\partial N}{\partial t} + \frac{\partial}{\partial x}\left(\frac{MN}{D}\right) + \frac{\partial}{\partial y}\left(\frac{N^2}{D}\right) + gD\frac{\partial \eta}{\partial y} + \frac{gn^2 N}{D^{7/3}}\sqrt{M^2 + N^2} = 0 \tag{3}$$

Here, η is the water level, h is still water depth, D is the total water depth (h +η), g is the gravitational acceleration, n is Manning's roughness coefficient (described later), and M and N are the flow flux (flow rate per unit width) in the x- and y-direction, respectively. Eq. (1) represents a continuous equation, which corresponds to the law of conservation of mass. Eqs. (2) and (3) represent equations of motion for the x- and y-direction, respectively.

Eqs. (2) and (3) are derived from the Navier-Stokes equation, taking into account the characteristics of the tsunami: (a) the viscosity can be ignored since it is targeted for seawater, (b) the wavelength is long relative to the water depth, and (c) the seawater from the water surface to the sea bottom flows together at a uniform horizontal flow velocity. See Refs. [6–8] for detailed derivation.

Eqs. (2) and (3) are used when the tsunami height cannot be ignored with respect to the water depth in a shallow sea, usually at a water depth of 50 m (sometimes 100 m or 200 m). In the case of deep water, the second, third, and fifth terms of Eqs. (2) and (3) become small, and their solutions approach those from the linear long-wave equations. In the present study, Eqs. (2) and (3) are used as they are to calculate the tsunami inundation to the land.

2.1.2. Analytical range of seismic fault

Figure 1 shows the entire target area. The yellow frame in this figure represents the range for a detailed evaluation of the tsunami propagation. The coastal area of the western end
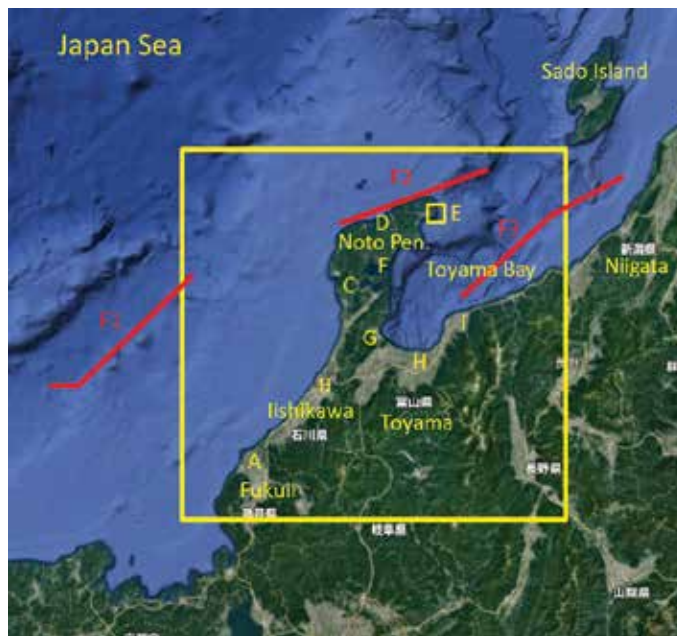
Figure 1. Map showing the entire target area. the range for a detailed evaluation of the tsunami propagation is denoted by the yellow frame. Surface projection of the three earthquake faults is denoted by a red line and labeled as F1–F3. Further explanation is described in the text. Main city locations discussed in the text labeled as A-G are Mikuni Town of Sakai City ("A"), Kanazawa City ("B"), Shiga Town ("C"), Wajima City ("D"), Suzu City ("E"), Anamizu Town ("F"), Himi City ("G"), Toyama City ("H"), and Nyuzen City ("I"). A small rectangle adjacent to "E" shows an area around Misaki Town of Suzu City illustrated in **Figures 11**, **12**. (Note that background map is from Google maps.)

(left) is Echizen Town, Fukui Prefecture, and that of the eastern end (right) is Itoigawa City, Niigata Prefecture (east of Toyama Prefecture). The seismic faults studied here are denoted by a red line in **Figure 1** and are (from the left) the Wakasa Sea Knoll Chain fault (labeled as F1), north off the Noto Peninsula fault (F2) and east off the Noto Peninsula fault (F3). Each of these three earthquake faults consists of two or three small faults with different strike angles.

2.1.3. Initial conditions

For the evaluation of crustal deformation of the seafloor accompanying the earthquake, we use the static deformation [12] of the sea bottom surface, which corresponds to the initial water level of the tsunami simulation. The fault parameters that specify the seismic fault model are set as shown in **Table 1**, referring to the report on the Ministry of Land, Infrastructure and Transport [4]. For each of the three seismic faults, two cases are calculated: Case 1 with Mw7.6 and Case 2 with Mw7.8 (in which slip displacement of the fault in Case 1 is doubled). Case 2 is intended to give inherent uncertainty in source parameters as a lesson from the 2011 Tohoku earthquake. In addition, it is assumed that the slip distribution on the fault plane is uniform and the propagation of rupture is not taken into account (the velocity of rupture propagation is assumed to be infinite).

Fault name	Segment No.	Depth* (km)	Strike angle (°)	Rake angle (°)	Slip angle (°)	Length (km)	Width (km)	Mw	
								Case 1	Case 2
Wakasa Sea-Knoll Chain	1	2.4	81	60	264	21.1	14.5	7.6	7.8
	2		47		145	36.3			
	3		54		215	29.9			
North-off Noto Pen.	1	1.1	64	45	113	48.3	19.7	7.6	7.8
	2		55		105	45.9			
East-off Noto Pen.	1	1.9	37	45	76	51.5	22.7	7.6	7.8
	2		55		102	34.1			

*Depth' represents the upper end depth of the fault plane.

Table 1. Source parameters of earthquake faults in the present study.

2.1.4. Boundary conditions

2.1.4.1. Transmitting condition at offshore side

The method in Ref. [6] is used for the amount of outflow from the calculation area on the offshore side, in which free transmission is made and reflection to the calculation area is suppressed. It is assumed that the amount of water η $(g \times h)^{1/2}$ flows out at a progressive long-wave velocity of $(g \times h)^{1/2}$, where η is the wave level just inside the boundary.

2.1.4.2. Run-up condition to the land

To calculate the tsunami's run-up to land according to shallow-water long-wave theory, the method in Ref. [13] is used. In this method, the topography at the run-up fronts is treated as steplike grids, and the flow is evaluated using Eqs. (1)–(3). When the water level η of the seaside grid is higher than the ground height z of the landside grid, the difference is defined as the actual water depth D, and the water level and the flow rate are calculated. $D > 10^{-5}$ (m) is often used as a criterion for considering a tsunami's run-up to land (e.g., [14]). This kind of boundary to treat tsunami's run-up is called the moving boundary [8]. After comparison of several methods to treat the moving boundary, the method in Ref. [13] is selected and implemented into the computational code TUNAMI because of its accuracy [8].

2.1.4.3. Tide level conditions

The average sea level in the Japan Sea is 0.2 m higher than T. B. (mean sea level in Tokyo Bay). In the present study, the tide level is set to ± 0 m.

2.1.5. Submarine topography data and land altitude data

For tsunami simulation, the seafloor depth data and land altitude data are required. For the offshore, we use the 1 km grid water depth data of the Japan Sea area from JTOPO30 (30-s grid

water depth data in Japan's coastal waters) [15] published by the Marine Information Research Center of the Japan Hydrographic Association. For the nearshore, we use the coastal 500 m grid water depth data [16] published by the Japan Coast Guard. Furthermore, for the land data necessary for the run-up analysis, we use the 50 m grid land altitude data [17] published by the Geospatial Information Authority of Japan.

2.1.6. Numerical scheme

For numerical calculations, Eqs. (1)–(3) are discretized and solved by using the finite difference method. An orthogonal coordinate grid is used in the spatial domain, and a staggered grid is used in the variable placement. The leapfrog method is used in the time domain, which provides neutral stability with no dissipation error. In the discretization of the spatial domain, three grid sizes are used: 450 m for the whole region, 150 m for the intermediate region, and 50 m for the nearshore and the land. The whole region for analysis is shown in **Figure 1**, in which the yellow frame is the region discretized into 50 m grids. We analyze the calculations performed in the time domain with a time step of 0.1 s and tsunami propagation for 180 min after an earthquake fault ruptures.

2.1.7. Manning's roughness

The fifth term in Eqs. (2) and (3) represents the friction effect against the sea bottom during tsunami propagation, which varies rapidly when Manning's roughness n changes. In the present study, n is fixed at 0.025, with a reference to [10].

2.2. Evaluation of strong motion

To provide an overview of a disaster not only from the perspective of tsunami inundation but also from the damage occurrence of strong ground shaking and liquefaction, simplified methods based on the attenuation formula of the maximum velocity are used to calculate the seismic intensity and the liquefaction occurrence rate in the whole region. Here, the methodologies are briefly summarized.

2.2.1. Seismic intensity

The seismic intensity (The Japan Meteorological Agency seismic intensity scale) is evaluated through three steps: (1) the evaluation of the maximum velocity on the engineering bedrock, (2) the evaluation of the amplification factor of the maximum velocity from the engineering bedrock to the ground surface, and (3) the evaluation of the seismic intensity from the maximum velocity at the surface.

In the first step, the maximum velocity on the engineering bedrock (a layer with the S-wave velocity of 600 (m/s)) is evaluated using Eq. (4) by the empirical formula [18–19]:

$$log_{10}\, PGV_{600} = 0.58\, M_w + 0.0038D + d - 1.29 - log_{10}\left(X + 0.0028 \times 10^{0.50Mw}\right) - 0.002X \quad (4)$$

where PGV is abbreviation of "peak ground velocity", PGV_{600} is the maximum velocity (cm/s) on the engineering bedrock with S-wave velocity of 600 m/s, Mw is the moment magnitude, D

is the depth of the source (km), d is the coefficient depending on the earthquake type (d = 0 for a crustal earthquake, d = −0.02 for an interplate earthquake, and d = 0.12 for an in-plate earthquake), and X is the fault's shortest distance between the fault plane and the target site (km). In the present study, the maximum velocity is estimated for a crustal earthquake. Eq. (4) is obtained by the regression analysis based on 543 data of the maximum velocity from 21 earthquakes that occurred in Japan (Mw5.8–8.2). Its validity and usefulness have been confirmed by many researchers in many earthquakes (e.g., [20–24]).

In the second step, the amplification factor of the maximum velocity from the engineering bedrock to the surface is calculated by the following relationship [25]:

$$log_{10} \, ARV = -0.852 \, log_{10} \, (AVS30/600) \tag{5}$$

where ARV (m/s) represents the amplification rate factor of the maximum velocity from the engineering bedrock to the surface and AVS30 (m/s) represents the average S-wave velocity from the surface to a depth of 30 m, ranging between 100 and 1500 m/s. According to Eq. (5), the ground motion becomes larger when AVS30 is lower than 600 m/s, whereas it becomes smaller when AVS30 is higher than 600 m/s. The maximum velocity at the ground surface, PGV, can be obtained by multiplying the maximum velocity at the engineering velocity, PGV_{600}, in Eq. (4) by the amplification factor ARV in Eq. (5):

$$log_{10} \, PGVs = log_{10} \, (PGV_{600} \times ARV) = log_{10} \, PGV_{600} + log_{10} \, ARV$$
$$= log_{10} \, PGV_{600} - 0.852 \, log_{10} \, (AVS30/600) \tag{6}$$

In the third step, according to Refs. [26, 27], the seismic intensity on the ground surface can be calculated using the following formula:

$$I = 2.286 + 2.088 \times log_{10} \, PGVs \tag{7}$$

Using the above three-step procedure, it is possible to calculate the seismic intensity at an arbitrary point from a given seismic fault. In the present study, using the AVS30 of a 250 m grid based on the geomorphologic classification published by NIED's Japan Seismic Hazard Information Station (J-SHIS) [28, 29], the seismic intensity of the targeted area is evaluated.

2.2.2. Liquefaction occurrence rate

The relationship between the seismic intensity and the liquefaction occurrence rate [30, 31] is expressed as:

$$P_{liq}(I) = \Phi\big((I - \mu)/\sigma\big) \tag{8}$$

where $P_{liq}(I)$ represents the liquefaction occurrence rate at the seismic intensity I, Φ is the cumulative normal distribution function, μ is the mean value, and σ is the standard deviation; μ and σ are determined by classifying 15 types of geomorphologic classification—representing the potential to liquefy—into 4 groups according to liquefaction risk and by performing a regression analysis for each group with the least squares method based on the data of seismic intensity and liquefaction occurrence rate (see Refs. [30, 31] for details). Parameters to evaluate

Group	Geomorphologic classification liable to liquefy	μ	σ
1	Natural levee, abandoned river channel, lower slopes of dune, lowland between coastal dunes and bars, reclaimed land, filled land	6.960	0.761
2	Alluvial fan, alluvial fan with slope angle of less than 1/100, marine sand, and gravel bars	7.160	0.773
3	Back marsh, delta and coastal lowland, sand dune	7.906	0.933
4	Gravelly terrace, valley bottom lowland, valley bottom lowland with slope angle of less than 1/100	7.231	0.628

Table 2. Parameter to evaluate the liquefaction occurrence rate from Refs. [30, 31].

the liquefaction occurrence rate, μ and σ, are summarized in **Table 2**. For example, liquefaction begins to occur near seismic intensity 5.0. in group 1, which is the most liable to liquefy (natural levees, abandoned river channels, lower slopes of dunes, lowland between coastal dunes and bars, reclaimed land, and filled land). Note that parameters μ and σ in **Table 2** are determined based on the liquefaction data over 1400 from the recent 9 damaging earthquakes in Japan [30, 31] and applied to successfully reproduce the liquefaction occurrence locations due to the 2011 Tohoku earthquake [32].

3. Results

3.1. Overview of tsunami propagation

For each of the three earthquake faults, we conducted a tsunami simulation on two cases with different magnitudes: Case 1 Mw7.6 and Case 2 Mw7.8. The maximum tsunami height is shown in **Figures 2–7**. The displayed range of these figures corresponds to the yellow frame inside **Figure 1**, with the southwestern end as the origin, the distance in the east-west and north-south direction (km) is taken in the horizontal direction, and the maximum tsunami
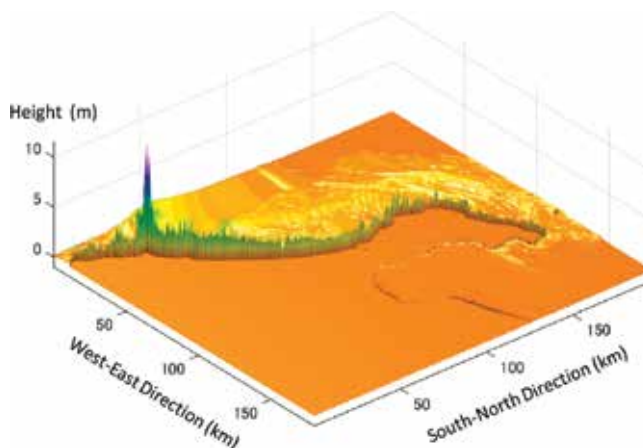

Figure 2. Map showing the maximum tsunami height for Case 1 (Mw7.6) of the Wakasa Sea knoll chain fault. The displaying range corresponds to the yellow frame inside **Figure 1**.

height is taken in the vertical direction (m). Similar plots have been done for the inundation depth and tsunami arrival time but omitted because of space. The general features from these results are discussed below.

3.1.1. Wakasa Sea knoll chain fault

The tsunami height in Case 1 (Mw7.6) (**Figure 2**) reaches a maximum of 9.0 m in Sakai City (Mikuni Town), Fukui Prefecture; ∼2.0 m in the vicinity of Kanazawa City, Ishikawa Prefecture; 0.5–2.0 m on the western side of the Noto Peninsula; and ∼0.1 cm in the coastal area of Toyama Prefecture. The spatial distribution characteristics of the inundation depth of the tsunami are similar to those of the tsunami height. Many areas are flooded from Fukui Prefecture to the western coast of the Noto Peninsula in Ishikawa Prefecture. The maximum inundation depth reaches 8.5 m in Sakai City (Mikuni Town), Fukui Prefecture.

The tsunami height in Case 2 (Mw7.8) (**Figure 3**) reaches a maximum of 13 m in Sakai City (Mikuni Town) in Fukui Prefecture; ∼4.0 m in the coastal area around Kanazawa City, Ishikawa Prefecture; 3.1 m in Hakui City, Ishikawa Prefecture; 0.3 m in Himi City, Toyama Prefecture; and ∼0.2 m in Toyama City, Toyama Prefecture. As for the inundation of the tsunami, many areas are flooded from Fukui Prefecture to the northern Noto Peninsula in Ishikawa Prefecture. The maximum inundation depth reaches 12 m in Mikuni Town in Sakai City, Fukui Prefecture.

Since the Wakasa Sea Knoll Chain fault is located offshore compared with the other two faults, the arrival time of the tsunami is prolonged. In the vicinity of Sakai City (Mikuni Town), Fukui Prefecture, where the maximum tsunami height occurs, the arrival time is ∼29 min from the occurrence of the earthquake. On the western coast of the Noto Peninsula in Ishikawa Prefecture, it is 29–37 min.
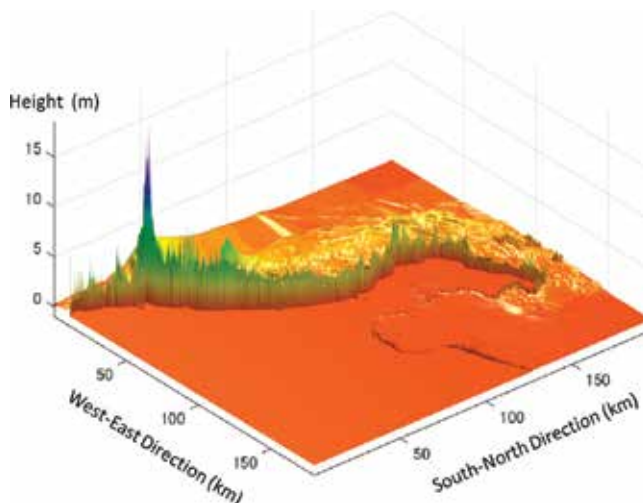

Figure 3. Map showing the maximum tsunami height for Case 2 (Mw7.8) of the Wakasa Sea knoll chain fault. Other conditions are the same as in **Figure 2**.

3.1.2. North off the Noto Peninsula fault

The maximum height of the tsunami in Case 1 (Mw7.6) (**Figure 4**) occurs in Suzu City, Ishikawa Prefecture, reaching 7.1 m. It is 1.0–3.5 m in the northern Noto Peninsula near the earthquake fault, 0.5–2.0 m in Toyama prefecture, 1.0–2.0 m in the coastal area around Kanazawa City, and 0.5–1.0 m in Sakai City (Mikuni Town) in Fukui Prefecture. The inundation depth of the tsunami is similar to that of the tsunami height. Many areas are flooded from the northeastern tip of the Noto Peninsula to its western coast. The maximum inundation depth reaches ∼4.0 m on the eastern coast of Suzu City, Ishikawa Prefecture (around Horyu Town), 1.0–3.0 m on the western coast, and 1.0–4.0 m in Wajima City (around Wajima Port).

The maximum height of the tsunami height in Case 2 (Mw7.8) (**Figure 5**) occurs in Suzu City, Ishikawa Prefecture, reaching 9.6 m. It is 3.0–6.0 m in the northern side of Noto Peninsula;
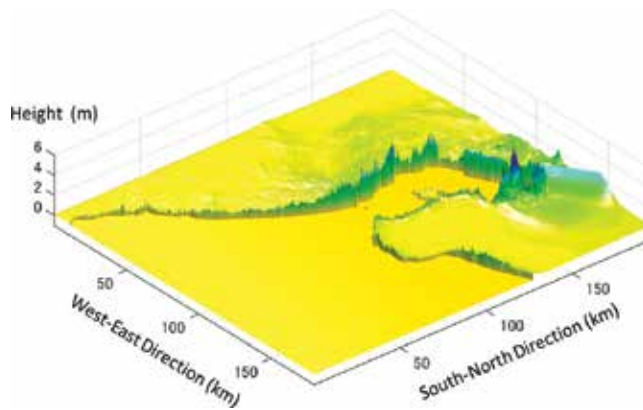

Figure 4. Map showing the maximum tsunami height for Case 1 (Mw7.6) of the north off the Noto Peninsula fault. Other conditions are the same as in **Figure 2**.
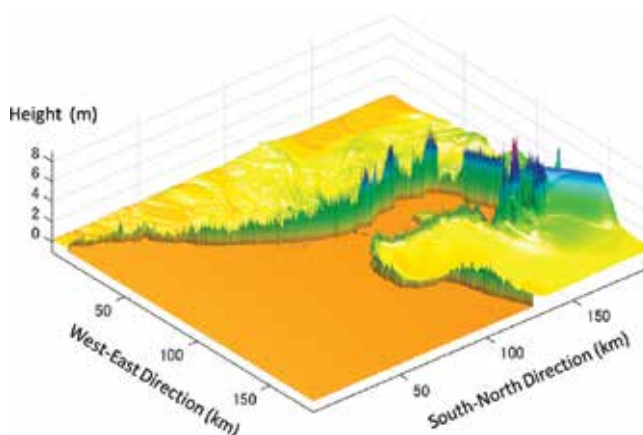

Figure 5. Map showing the maximum tsunami height for Case 2 (Mw7.8) of the north off the Noto Peninsula fault. Other conditions are the same as in **Figure 2**.

1.0–3.0 m in Toyama Prefecture; 2.0 m in the coastal area around Kanazawa City; and 1.5 m in Sakai City (Mikuni Town), Fukui Prefecture. The inundation depth of the tsunami has distribution characteristics similar to the tsunami height. Many areas are flooded from the northeastern tip of the Noto Peninsula to its western coast. The maximum inundation depth
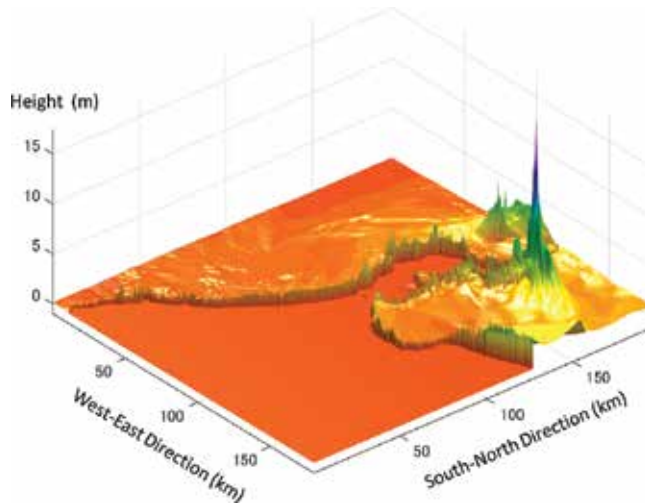

Figure 6. Map showing the maximum tsunami height for Case 1 (Mw7.6) of the east off the Noto Peninsula fault. Other conditions are the same as in **Figure 2**.
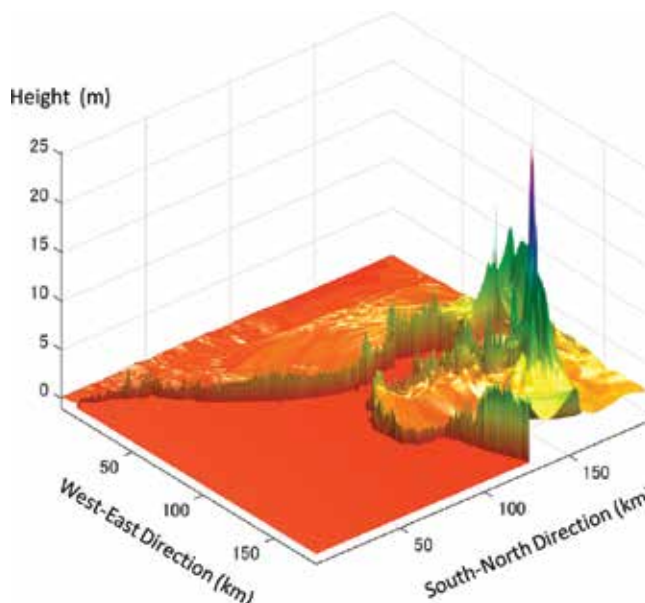

Figure 7. Map showing the maximum tsunami height for Case 2 (Mw7.8) of the east off the Noto Peninsula fault. Other conditions are the same as in **Figure 2**.

reaches 7.0 m in Suzu City (around Horyu Town). In addition, other areas of Suzu City, Wajima City (around Wajima Port), and Shiga Town (around the Togi river mouth) have an inundation depth of 1.0–4.0 m.

North off the Noto Peninsula fault is close to the land area, and the tsunami arrives within 3 min at its fastest. Going around the Noto Peninsula, the tsunami takes 12 min to Suzu City, Ishikawa Prefecture. It reaches the prefectural border between Toyama and Niigata Prefectures in ∼15 min and arrives in Fukui Prefecture in 100 min.

3.1.3. East off the Noto Peninsula fault

The tsunami height in Case 1 (Mw 7.6) (**Figure 6**) reaches a maximum of 13.8 m in Suzu City (Kodomari), Ishikawa Prefecture; 6.0–8.0 m in the vicinity of the prefectural border between Toyama and Niigata Prefectures; ∼2.5 m in the coastal area around Toyama City; ∼2.0 m in the coastal area near Kanazawa City; and 1.0–2.5 m in Sakai City (Mikuni Town), Fukui Prefecture. The spatial distribution characteristics of the inundation depth of the tsunami are similar to those of the tsunami height. The maximum inundation depth reaches ∼12.0 m in Suzu City (around Misaki Town). It is 1.0–7.0 m in other coastal areas of Suzu City and 1 m in Himi City, Toyama Prefecture (around Himi Fishing Port).

The maximum height of the tsunami in Case 2 (Mw 7.8) (**Figure 7**) is 21.4 m in Suzu City, Ishikawa Prefecture. It reaches 6.5 m in Anamizu Town, Ishikawa Prefecture; 3.0–6.0 m on the northern side of the Noto Peninsula; 2.0–3.0 m in the coastal area around Toyama City; ∼7.5 m in the vicinity of the prefectures border between Toyama and Niigata prefectures; 2.0 m in the coastal area around Kanazawa City; and 1.0–2.0 m around Sakai City (Mikuni Town), Fukui Prefecture. The inundation depth of the tsunami shows distribution characteristics similar to those of the tsunami height. Many areas are flooded from the northeastern tip of the Noto Peninsula to the coast of Toyama Bay. The maximum inundation depth reaches about 20 m in Suzu City (around Misaki Town) and is 1.0–3.0 m in Himi City, Toyama Prefecture (around Himi Fishing Port).

East off the Noto Peninsula fault is also close to the land area, and the tsunami arrives within 3 min at its fastest. The arrival time is ∼6 min near the prefectures border between Niigata and Toyama prefectures, ∼8 min in Sado Island, and 12 min in Suzu City, Ishikawa Prefecture. It takes about 105 min to arrive in the vicinity of Kanazawa City, Ishikawa Prefecture, and 135 min in Sakai City (Mikuni Town) in Fukui Prefecture.

3.1.4. Other findings

In Case 2, the slip displacement on the fault is double that of Case 1, meaning that the tsunami height is nearly double in the vicinity of the fault, although in the coastal area away from the fault the height is ∼1.5 times. In this analysis, the nonlinear long-wave equations are solved for the whole area, and in the coastal area near the land, the water becomes shallow and the effect of the submarine friction term increases.

The overall distribution characteristics of tsunami height change significantly for each of the three faults; except in the vicinity of the fault, the tsunami height at the Noto Peninsula tends to be high. In particular, it is predicted that Suzu City, Ishikawa Prefecture, located at the tip of the Noto Peninsula, has a high tsunami and broad inundation areas compared with other areas.
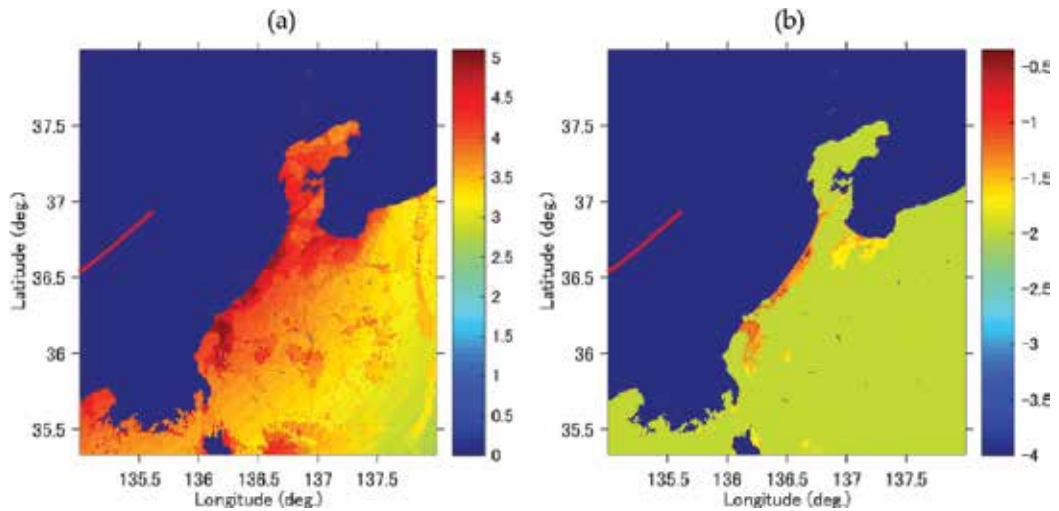

Figure 8. Map showing the seismic intensity (a) and the liquefaction occurrence rate (b) for Case 1 (Mw7.6) of the Wakasa Sea knoll chain fault. Note that color chart for the liquefaction occurrence rate (%) is expressed in log scale.
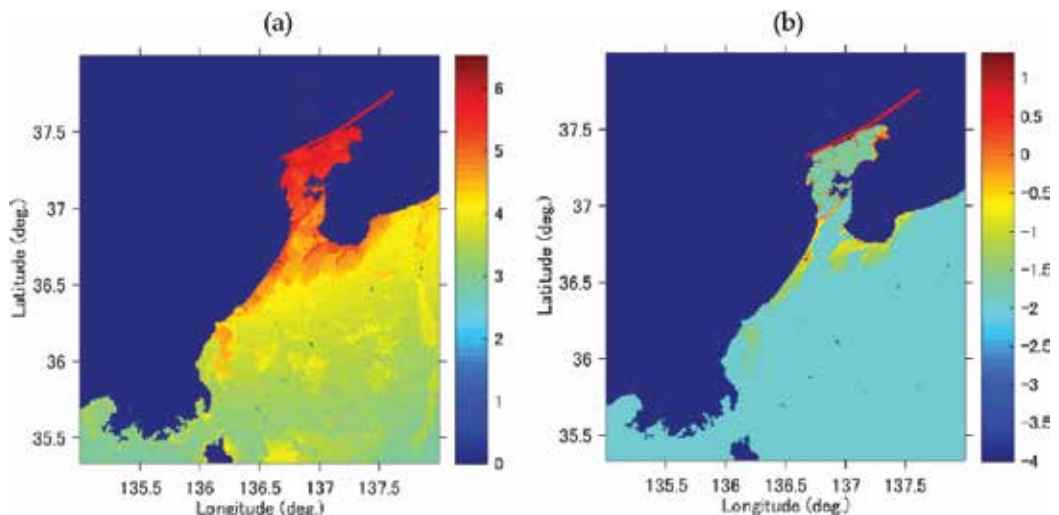

Figure 9. Map showing the seismic intensity (a) and the liquefaction occurrence rate (b) for Case 1 (Mw7.6) of the north off the Noto Peninsula fault. Other conditions are the same as in **Figure 8**.
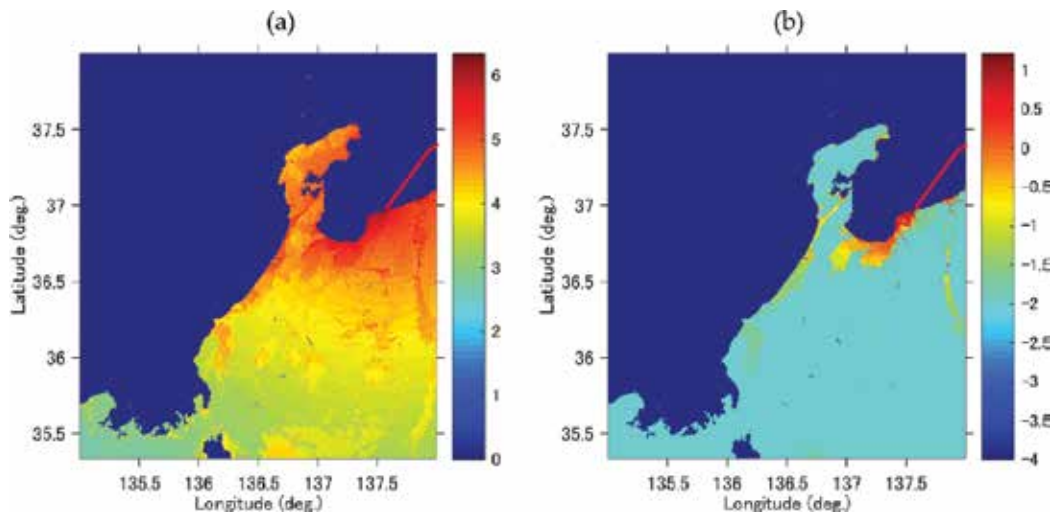
Figure 10. Map showing the seismic intensity (a) and the liquefaction occurrence rate (b) for Case 1 (Mw7.6) of the east off the Noto Peninsula fault. Other conditions are the same as in **Figure 8**.

3.2. From the perspective of strong ground motion

For a better understanding of a tsunami in a series of disasters triggered by an earthquake, the ground shaking and liquefaction occurrence rates were calculated for each fault. The seismic intensity and the liquefaction occurrence rate depend on the maximum velocity evaluated by Eq. (4). As can be seen from this equation, the difference of 0.2 in Mw between Cases 1 and 2 leads to a difference of 5–25% in the maximum velocity, depending on the fault distance. It also leads to a difference of 0.04–0.2 in the seismic intensity. These differences become smaller when the site is closer to the epicenter. Therefore, for the seismic intensity and liquefaction occurrence rate, here the results only for Case 1 are shown and discussed.

The maximum seismic intensity across the whole range is 5+ for the Wakasa Sea Knoll Chain fault (**Figure 8(a)**), 6+ for north off the Noto Peninsula fault (**Figure 9(a)**), and 6+ for east off the Noto Peninsula fault (**Figure 10(a)**). The maximum liquefaction occurrence rate across the whole range is 0.45% for the Wakasa Sea Knoll Chain fault (**Figure 8(b)**), 21% for north off the Noto Peninsula fault (**Figure 9(b)**), and 16% for east off the Noto Peninsula fault (**Figure 10(b)**).

4. Discussion

Calculation of the inundation area in the target area using a geographic information system (GIS) showed that the largest inundation area was estimated to be about 38 km^2 in Case 2 east off the Noto Peninsula fault, followed by ~17 km^2 in Case 2 north off the Noto Peninsula fault. In Case 2 of the Wakasa Sea Knoll Chain fault, the inundation area was ~7.6 km^2, which is slightly smaller

than the area of $\sim$9.0 km^2 in Case 1 east off the Noto Peninsula fault. Comparing Case 2 with Case 1, the inundation area increased 2.2 times in the Wakasa Sea Knoll Chain fault and 2.9 times north off the Noto Peninsula fault, 4.2 times east off the Noto Peninsula fault. In Case 2, the slip displacement on the fault is double that of Case 1, but the inundation area of the tsunami is much greater than that.

After observing the inundation area using the GIS, we decided to focus on Suzu City, Ishikawa Prefecture, which is expected to have the largest inundation area from both north off the Noto Peninsula fault and east off the Noto Peninsula fault. As an example, the inundation area of the city from the east off the Noto Peninsula fault is illustrated in **Figures 11** and **12**, which highlight the area around Misaki Town, Suzu City. In Case 2 (**Figure 12**), the tsunami runs up $\sim$1.9 km from the mouth of the Kino River, which is 1.5 times further than in Case 1 (**Figure 11**). In other inundation areas of the city, the tsunami runs up 1.5–1.7 km further from the coast in Case 2, which is two to four times the distance in Case 1. The inundation area of Suzu City from east off the Noto Peninsula fault is $\sim$5.3 km^2 in Case 1, and $\sim$17.4 km^2 in Case 2, which is $\sim$3.3 times larger. The inundation area of Suzu City from north off the Noto Peninsula fault is $\sim$2.3 km^2 in Case 1, and $\sim$7.4 km^2 in Case 2, which is $\sim$3.2 times larger (the figures are omitted due to space constraints).

Next, for the tip of the Noto Peninsula including Suzu City in Ishikawa Prefecture, an enlarged map of the seismic intensity and the liquefaction occurrence rate for north off the Noto Peninsula fault and east off the Noto Peninsula fault is shown in **Figures 13** and **14**. The lowland along the coast of Suzu City is subjected to strong shaking, with the seismic intensity
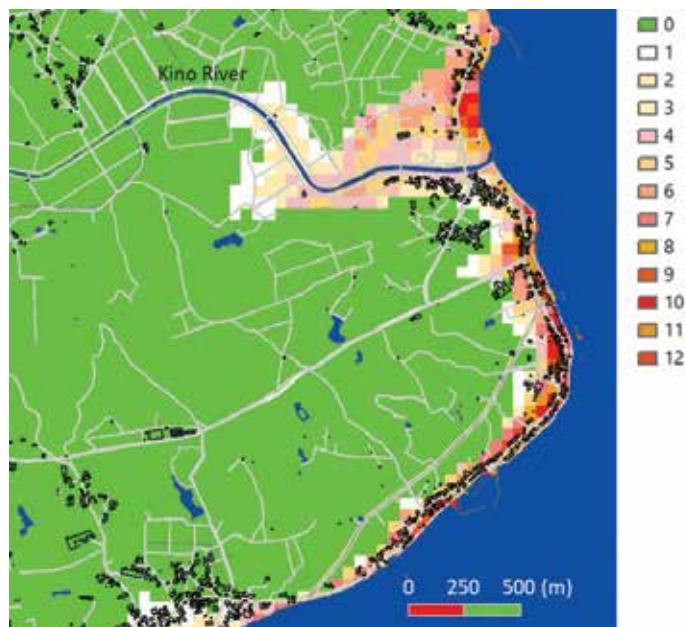

Figure 11. Enlarged map showing the inundation area (around Misaki Town) of Suzu City for Case 1 (Mw7.6) of the east off the Noto Peninsula fault. Note that color chart shows the inundation height (m).
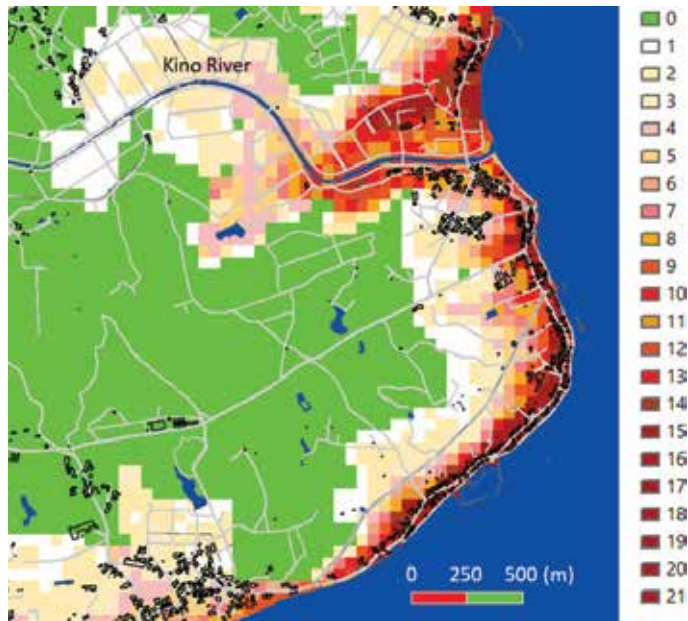
Figure 12. Enlarged map showing the inundation area (around Misaki Town) of Suzu City for Case 2 (Mw7.8) of the east off the Noto Peninsula fault. Other conditions are the same as in **Figure 11**.
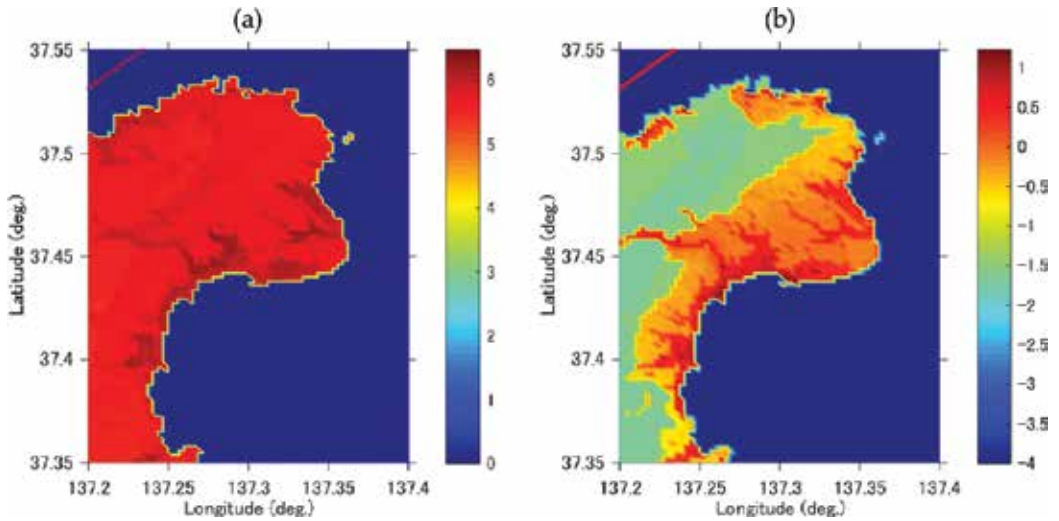

Figure 13. Enlarged map around the tip of the Noto Peninsula including Suzu City showing the seismic intensity (a) and the liquefaction occurrence rate (b) for Case 1 (Mw7.6) of the north off the Noto peninsula fault. Other conditions are the same as in **Figure 8**.
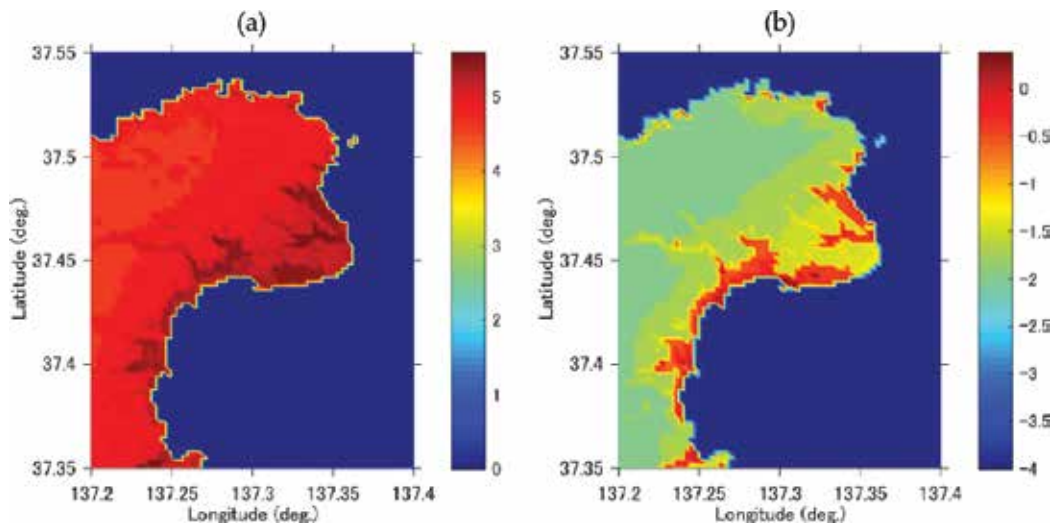
Figure 14. Enlarged map around Suzu City showing the seismic intensity (a) and the liquefaction occurrence rate (b) for Case 1 (Mw7.6) of the east off the Noto Peninsula fault. Other conditions are the same as in **Figure 8**.

reaching 6+ for the north off the Noto Peninsula fault and 6– for the east off the Noto Peninsula fault. Their liquefaction occurrence rate reaches 16 and 2.4%, respectively.

The inundation area of a tsunami is likely to occur in the coastal lowland, where strong ground motion may induce building damage and soil liquefaction. Therefore, it is important to examine the impact of damage caused by ground shaking on evacuation route and evacuation time. This is not limited to Suzu City but is common to the entire area where there is flooding caused by the tsunami and provides an important perspective for future damage estimation.

As noted, in the Hokuriku region, relatively few earthquakes are felt, and disaster prevention awareness is low. The resources (people, time, budget, etc.) that can be input for the promotion of disaster education are always limited. Under these circumstances, to obtain the maximum effect from limited resources, it is preferable to introduce intensive resources in a specific area with a high disaster risk, rather than treating the whole area equally. In this respect, Suzu City may be a model district, and if the promotion of disaster prevention is successful in the city, it could be fruitfully expanded to other areas.

5. Conclusions

In our study, focusing on the Hokuriku region in Japan, we conducted a tsunami simulation and examined the resulting tsunami hazard map. Three potential faults of Mw7.6 earthquake were selected to generate the tsunami: the Wakasa Sea Knoll Chain fault, north off the Noto Peninsula fault, and east off the Noto Peninsula fault. In addition, we calculated these three

events with Mw7.8, given the inherent uncertainty in source parameters. Aside from tsunami height, arrival time, inundation height, and inundation area, we calculated the seismic intensity and the liquefaction occurrence rate by simplified methods. Our findings in the present study are summarized as follows.

- In Case 2 (Mw7.8), the slip displacement on the fault is double that of Case 1 (Mw7.6), meaning that the tsunami height is nearly double in the vicinity of the fault, although in the coastal area away from the fault the tsunami height is ~1.5 times. In this analysis, the nonlinear long-wave equations are solved for the whole region, and in the coastal area near the land, the water becomes shallow and the effect of the submarine friction term increases.

- Comparing Case 2 with Case 1, the inundation area increased 2.2 times in the Wakasa Sea Knoll Chain fault and 2.9 times north off the Noto Peninsula fault, 4.2 times east off the Noto Peninsula fault. In Case 2, the slip displacement on the fault is double that of Case 1, but the inundation area of the tsunami is much greater than that.

- The overall distribution characteristics of tsunami height change significantly for each of the three faults; except in the vicinity of the fault, the tsunami height at the Noto Peninsula tends to be high. In particular, it is predicted that Suzu City, Ishikawa Prefecture, located at the tip of the Noto Peninsula, has a high tsunami and broad inundation areas compared with other areas.

- Our results indicated that Suzu City in Ishikawa Prefecture, located in the northeastern part of the Noto Peninsula, has a relatively high potential risk of tsunami as well as strong motion and liquefaction. Thus, Suzu City would represent a highly appropriate area in which to promote disaster prevention education in the Hokuriku region.

- The inundation area of a tsunami is likely to occur in the coastal lowland, where strong ground motion may induce building damage and soil liquefaction. Therefore, it is important to examine the impact of damage caused by ground shaking on evacuation route and evacuation time. This is not limited to Suzu City but is common to the entire area where there is flooding caused by the tsunami and provides an important perspective for future damage estimation.

Acknowledgements

Author details

Michihiro Ohori[1]*, Yuri Masukawa[2,3] and Keisuke Kojima[4]

*Address all correspondence to: ohorim@u-fukui.ac.jp

1 Research Institute of Nuclear Engineering, University of Fukui, Tsuruga, Japan

2 Graduate School, University of Fukui, Fukui, Japan

3 CTI Engineering Co., Ltd., Japan

4 Department of Architecture and Civil Engineering, University of Fukui, Fukui, Japan

References

[1] Fukui Prefecture. The Tsunami Simulation Results in Fukui Prefecture http://www.pref. fukui.lg.jp/doc/kikitaisaku/kikitaisaku/tunami-soutei.html (in Japanese, last accessed in April 30, 2018)

[2] Ishikawa Prefecture. The Tsunami Hazard Map in Ishikawa Prefecture http://www.pref. ishikawa.lg.jp/bousai/kikikanri_g/tsunami_info.htm (in Japanese, last accessed in April 30, 2018)

[3] Toyama Prefecture. The Outline of the Results of the Tsunami Simulation Survey http:// www.pref.toyama.jp/cms_pfile/00017580/01067018.pdf (in Japanese, last accessed in April 30, 2018)

[4] Ministry of Land, Infrastructure and Transport, Study Group on Large Earthquakes in the Japan Sea, Report on the Study Group on Large Earthquakes in the Japan Sea. September, 2014 http://www.mlit.go.jp/river/shinngikai_blog/daikibojishinchousa/ (in Japanese, last accessed in April 30, 2018)

[5] Ministry of Education, Culture, Sports, Science and Technology. Japan Sea Earthquake and Tsunami Research Project http://www.eri.u-tokyo.ac.jp/project/Japan_Sea/index.html (in Japanese, last accessed in April 30, 2018)

[6] Goto C, Ogawa Y. Numerical Method of Tsunami Simulation with the Leap-Frog Scheme, Report of Department of Civil Engineering. Faculty of Engineering, Tohoku University; 1982. p. 52 (in Japanese)

[7] Intergovernmental Oceanographic Commission. Numerical Method of Tsunami Simulation with the Leap-Frog Scheme (Manuals and Guides 35), IUGG/IOC TIME PROJECT, UNESCO. 1997; Part 1, Chapter 1, 1–19 http://tsunami190245.tripod.com/tsh.pdf (last accessed in April 30, 2018)

[8] Imamura F, Yalcine A C, Ozyurt G. Tsunami Modelling Manual; April 2006. 58p. http://www.tsunami.civil.tohoku.ac.jp/hokusai3/J/projects/manual-ver-3.1.pdf (last accessed in April 30, 2018)

[9] Goto K, Fujima K, Sugawara D, Fujino S, Imai K, Tsudaka R, Abe T, Haraguchi T. Field measurements and numerical modeling for the run-up heights and inundation distances of the 2011 Tohoku-oki tsunami at Sendai plain, Japan. Earth, Planets and Space. 2012;**64**: 1247-1257

[10] Oishi Y, Imamura F, Sugawara D. Near-field tsunami inundation forecast using the parallel TUNAMI-N2 model: Application to the 2011 Tohoku-Oki earthquake combined with source inversions. Geophysical Research Letters. 2015;**42**(4):1083-1091

[11] Tsushima H, Hirata K, Hayashi Y, Tanioka Y, Kimura K, Sakai S, Shinohara M, Kanazawa T, Hino R, Maeda K. Near-field tsunami forecasting using offshore tsunami data from the 2011 off the Pacific coast of Tohoku earthquake. Earth, Planets and Space. 2011;**63**:821-826

[12] Mansinha L, Smylie DE. The displacement fields of inclined faults. Bulletin of the Seismological Society of America. 1971;**61**:1433-1440

[13] Iwasaki T, Mano A. Two-Dimensional Numerical Simulation of Tsunami Run-ups in Eulerian Description, Proc. 26th Conference on Coastal Engineering, Japan Society of Civil Engineers; 1979. pp. 70-74 (in Japanese)

[14] Satake K, Nanayama F, Yamaki S. Source models of the unusual tsunami in the 17th century in eastern Hokkaido. Annual Report on Active Fault and Paleoearthquake Researches. 2003;**3**:315-362 (in Japanese)

[15] Japan Hydrographic Association. JTOPO30 (30-second grid water depth data in Japan's coastal waters http://www.mirc.jha.jp/products/finished/JTOPO30/ (in Japanese, last accessed in April 30, 2018)

[16] Japan Oceanographic Data Center, Japan Coast Guide. The coast 500 m grid water depth http://jdoss1.jodc.go.jp/vpage/depth500_file.html (last accessed in April 30, 2018)

[17] Geospatial Information Authority of Japan. The Land Altitude Data of 50 m Grid. https://fgd.gsi.go.jp/download/menu.php (in Japanese, last accessed in April 30, 2018)

[18] Si H, Midorikawa S. New relationship for peak acceleration and velocity considering effects of fault type and site condition. Journal of Structural and Construction Engineering, Architectural Institute of Japan. 1999;**523**:63-70 (in Japanese)

[19] Si H, Midorikawa S. New attenuation relations for peak ground acceleration and velocity considering effects of fault type and site condition, Proc. 12th World Conference on Earthquake Engineering. Paper No. 0532. 30 January - 4 February 2000; Auckland, New Zealand. 8p

[20] Midorikawa S, Ohtake Y. Variance of peak ground acceleration and velocity in attenuation relationships. Proc. 13th World Conference on Earthquake Engineering. Paper No. 325. 1-6 August 2004; Vancouver, Canada. 10p

[21] Honda R, Aoi S, Morikawa N, Sekiguchi H, Kunugi T, Fujiwara H. Ground motion and rupture process of the 2003 Tokachi-oki earthquake obtained from strong motion data of K-NET and KiK-net. Earth, Planets and Space. 2004;**56**:317-322

[22] Aoi S, Sekiguchi H, Morikawa N, Kunugi T. Source process of the 2007 Niigata-ken Chuetsu-oki earthquake derived from near-fault strong motion data. Earth, Planets and Space. 2008;**60**:1131-1135

[23] Aoi S, Kunugi T, Suzuki W, Morikawa N, Nakamura H, Senna S, Fujiwara H. Strong motion characteristics of the 2011 Tohoku-Oki earthquake. Zisin (Journal of Seismological Society of Japan). 2012;**64**:169-182 (in Japanese)

[24] Suzuki W, Aoi S, Kunugi T. Strong motions observed by KNET and KiK-net during the 2016 Kumamoto earthquake sequence, earth. Planets and Space. 2017;**69**:19, 12

[25] Fujimoto K, Midorikawa S. Empirical method for estimating J.M.A. Instrumental seismic intensity from ground motion parameters using strong motion records during recent major earthquakes. Journal of Social Safety Science. 2005;**7**:241-246 (in Japanese)

[26] Fujimoto K, Midorikawa S. Relationship between average shear-wave velocity and site amplification inferred from strong motion records at nearby station pairs. Journal of Japan Association for Earthquake Engineering. 2006;**6**:11-22 (in Japanese)

[27] Fujimoto K, Midorikawa S. Simplified method for predicting average shear-wave velocity of ground at strong-motion stations. Proc. 14th World Conference on Earthquake Engineering. Paper No. 02-0016; 12–17 October 2008; Beijing, China. 10p

[28] National Research Institute for Earth Science and Disaster Prevention. Japan Seismic Hazard Information Station (J-SHIS). http://www.j-shis.bosai.go.jp/ (last accessed in April 30, 2018)

[29] Wakamatsu K, Matsuoka M. Nationwide 7.5-arc-second Japan engineering geomorphologic classification map and Vs30 zoning. Journal of Disaster Research. 2013;**8**:90-911

[30] Matsuoka M, Wakamatsu M, Hashimoto M. Liquefaction potential estimation based on the 7.5-arc-second Japan engineering geomorphologic classification map. Journal of Japan Association for Earthquake Engineering. 2011;**1**:20-39 (in Japanese)

[31] Matsuoka M, Wakamatsu M, Hashimoto M, Senna S, Midorikawa. Evaluation of liquefaction potential for large areas based on geomorphologic classification. Earthquake Spectra. 2015;**31**:2375-2395

[32] Senna S, Hasegawa N, Maeda T, Fujiwara H. Liquefaction damage of the Tonegawa basin caused by the 2011 off the Pacific Coast of Tohoku Earthquake. Proc. International Symposium on Engineering Lessons Learned from the 2011 Great East Japan Earthquake. 1-4 March 2012; Tokyo, Japan. pp. 719-730

Disaster Mitigation Model of Eruption Based on Local Wisdom in Indonesia

Eko Hariyono and Solaiman Liliasari

Abstract

Kelud is one of the most active volcanoes in Indonesia and suffered a major eruption in 2014. Although they are not part of the super volcano, the impact of the eruption is extraordinary. However, the eruption is not too worrying for the surrounding community. The lack of disaster victims caused by the eruption in 2014 became a successful representation of disaster mitigation models owned by local communities in answering the eruption problem. The easy evacuation process and quickly post-eruption rehabilitation illustrate a pattern of environmental adaptation around the volcano. This discussion focuses on how the people behavior around the volcano in responding to the challenge of eruption? How the role of local government in preparing the community in the face of an eruption, and what actions are done so that the rehabilitation process can take place quickly? To answer all these questions, the researchers collected relevant data through observation, documentation, and interviews with the local communities and local government representatives directly involved in disaster mitigation measures. In addition, the researchers also revealed local traditions that are considered capable of supporting the process of preparing the community in answering the eruption challenges and becoming part of disaster mitigation in the volcanic region.

Keywords: disaster mitigation model, volcanic eruption, natural disaster, local wisdom in Indonesia

1. Introduction

Indonesia is one of the countries in the world most vulnerable to natural disasters and climate change [1]. Based on the world disaster statistics accessed from Centre for Research on the Epidemiology of Disasters (CRED; **Figure 1**), Indonesia ranks fourth after the Republic of

China Province, India and Philippines in terms of geophysical disasters [2]. This is due to the location of Indonesia in the equatorial region and is at the meeting of three giant plates (Pacific, Indo-Australian and Eurasia). In addition to the fertile land of agriculture, beautiful scenery and great geothermal potential, the negative impacts are occurrence provided various geological disasters such as earthquakes, tsunamis, volcanic eruptions and landslides [3]. The consequences of the geological disaster caused terrible human casualties, social and economic losses and environmental damage [4].

The various of natural disasters that struck Indonesia demanded the people to be ready, responsive and alert. The presence of hundreds of active volcanoes as a consequence of Indonesia be a part of the Ring of Fire, it should be a sign that the terrestrial disaster can be present at any time and everywhere and become a threat to the community. An effort to build a safe life against for people in disaster area becomes a challenge for the government and the people of Indonesia. Through the improvement of the volcanic disaster program of monitoring and communication system and community preparedness planning will be able to minimize disaster risk [5].

A disaster is a traumatic event that has the potential to inflict injury and even death [6]. Among natural disasters, volcano eruption is considered the most dangerous natural disaster [7]. The eruption catastrophe greatly affects the people, both directly and indirectly [8] and gives various impacts to the surrounding environment and society [9, 10]. The eruptions can also causes other disasters, like volcanic earthquakes, tsunamis, the change of weather and climate that caused by increased concentrations of aerosols in the earth atmosphere [11, 12].

Based on the history of volcanic eruption, Indonesia had experienced the biggest eruption in the history of the world. The Krakatau eruption in Java (1883), Tambora in Flores (1815) and an eruption of super-volcano Toba rebellion in 76,000 years ago [13] with terrible impacts on a local, regional and global scale [14]. The eruption of Tambora with the death reached 92,000 people and caused global climate change that known as "The year without summer." This

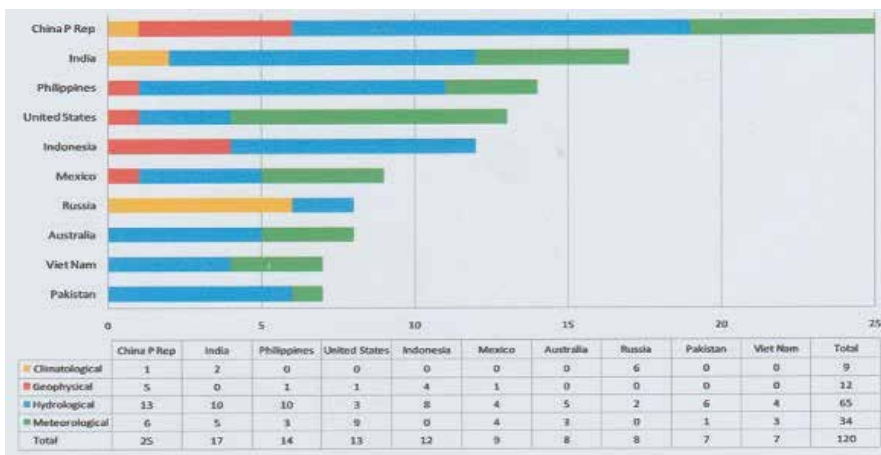|	China P Rep	India	Philippines	United States	Indonesia	Mexico	Australia	Russia	Pakistan	Viet Nam	Total
Climatological	1	2	0	0	0	0	0	6	0	0	9
Geophysical	5	0	1	1	4	1	0	0	0	0	12
Hydrological	13	10	10	3	8	4	5	2	6	4	65
Meteorological	6	5	3	9	0	4	3	0	1	3	34
Total	25	17	14	13	12	9	8	8	7	7	120

Figure 1. Indonesia ranks fourth in geophysical disasters after China's Republican Province, India and Philippines [2].

eruption impact is the occurrence of a prolonged winter in Europe and northeastern North America for 1 year [15]. The eruption of Krakatau caused victim more than 36,500 people and caused tsunami in coastal Java and Sumatra [16, 17]. Another major eruption was the eruption of Galunggung in West Java in 1822 with the death toll of 5500 people and Mount Agung in Bali in 1963 with a total victim of 1900 people [18].

The great eruption that occurred in the last decade was the eruption of Merapi. As the most active volcano in Java [19], its eruption always accompanied by lava bursts and pyroclastic flows along as several kilometers [20]. Due to the eruption, approximately 339 people died [21, 22]. The magnitude of the victims of Merapi eruption is caused by the increasing population of the people living around the volcano, so that when the disaster occurrence causes multiple casualties [23].

The biggest eruption challenge in the last decade in Indonesia comes from the Mount Sinabung in Karo province of North Sumatra. This volcano has the last eruption around the year 1200 and back to erupt in 2010 [24], and continues to the present [25]. Sinabung eruption strength is smaller than Merapi [26], but it caused the extraordinary economic losses of IDR 42,796 billion (USD 3295 million) [27].

In general, the Indonesian people are less ready to face the volcanic eruption disaster resulted from the lack of knowledge in preparing for disaster [28]. This is caused because of the fact that the public does not understand the impact of the eruption and low skill in planning and preparing for the volcanic activity [29]. Knowledge is a key factor for the community in understanding the process of natural disaster, so it will be calmer in facing it [30]. However, the public awareness of the environment around the volcano is also very important to the readiness of society in facing eruption disaster [31].

Various experiences of the eruption faced by the Indonesian nation prove that the Indonesian people are very strong in facing the natural disaster. Many efforts have been made to improve the resilience of communities [22]. Although recorded in history is not a few victims of volcanic eruption disaster, but the community has been survived in the vicinity. The eruption has built the emotional closeness of people who experience the same disaster. Traumatic events due to volcanic eruption can improve both social and individual of the community life [21].

Along with the development of time, Indonesian people matured in seeing the eruption disaster. They realize that the eruption disaster is God's will that cannot be prevented but also need not worry too much in facing it. Success in the face of disaster is determined by the ability to adapt to the environment [32]. Building a life in harmony with nature is the key to success in addressing all the challenges of natural disasters and the Indonesian people have presented it in the form of local wisdom. A jargon "Disaster brings blessings" always conveyed by the local government in motivating people to remain grateful for all the calamities that hit make the community stronger in the face of disaster. This jargon implies that the eruption is not only seen from the negative side of the damage, but the blessing behind the eruption disaster is much greater than the damage received [33]. Increased fertility of the soil as a result of volcanic ash [34] becomes one of the blessing forms of an eruption which can be used as a soil stabilization material [35]. This is a promising prospect for the communities around volcano who are mostly farmers.

Integration with local wisdom is very important in an eruption disaster mitigation because cultural roles in local wisdom are proven crucial in disaster risk reduction, but in the planning of disaster risk reduction strategies is often largely be ignored [36]. Therefore, it becomes a consideration of the need to integrate local wisdom in developing a new design of volcano mitigation model based on local wisdom that is assessed the most appropriate to the condition of Indonesian people.

2. The various experiences of eruption of several volcanoes in Indonesia

Mount Kelud is one of the stratovolcano that became proud of the community of East Java Indonesia. An active volcano with an altitude of 1731 m above sea level is located at 7°56'00″ SL (South Latitude) and 112°18'30″ EL (East Longitude). This mountain is produced from a subduction process between the Indo-Australian and Eurasian plates in the south of Java Island [37]. The magnificence of Mount Kelud is increasingly visible because it is flanked by three volcanoes that are currently in a resting condition, namely Mount Wilis in the West, and in the east, there is a complex of Mount Kawi and Butak. From a distance, Mount Kelud looks like a stunning natural building with tremendous geographic and geological potential.

Geographically, Mount Kelud is located in three districts, namely Malang, Kediri and Blitar (**Figure 2**). In addition to storing a variety of beauty, Mount Kelud promises a good life for the surrounding community. The fertile volcanic soil around Kelud makes the land in this mountainous region very good for developing agriculture industry and a variety of productive local plants to support the improvement of the welfare of the surrounding community.

Based on monitoring results from the volcanology center, Mount Kelud has three eruption characteristics, namely semi-magmatic, magmatic and effusive. Semi-magmatic eruption is a phreatic eruption triggered by evaporation of crater's lake water that seeps through a crack at the bottom of the crater and exhaled to the surface. This eruption started the magmatic eruption. The magmatic eruption is the eruption followed by the exit of volcanic material
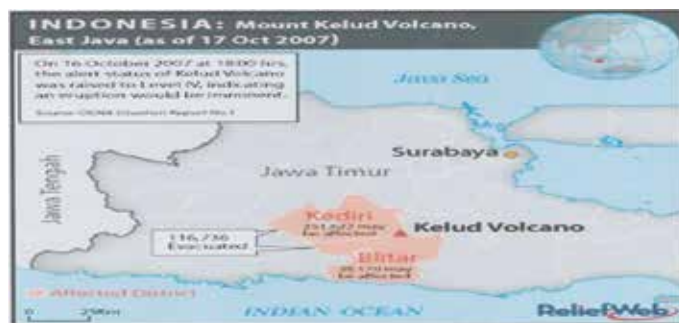

Figure 2. Kelud location map in East Java and the impact of its eruption in 2007 (https://volcano.si.edu/volcanoes/region06/java/kelut/3303kel7.jpg).

from the body mountain. These eruptions are generally explosive due to increased volcanic gas and eruptive energy. The effusive eruption is an eruption accompanied by magma flow to the surface that can form a lava dome [37]. Based on **Figure 2**, the 2007 eruption had a major impact on residents in two districts, 251,622 residents in Malang Regency and 38,170 people in Blitar Regency. The total evacuation reached 116,736 people.

Mount Kelud has experienced seven times of eruptions during 1900–2015, that is, in 1901, 1919, 1951, 1966, 1990, 2007 and 2014 with the decreasing number of fatalities (**Figure 3**). The latest eruption of Mount Kelud occurred on 13 February 2014 with a level of an eruption (VEI) is quite powerful to be able to vibrate the Earth's ionosphere layer. Volcanic ash bursts are expected to reach a height of 17 km with 76,000 people evacuated [38]. As informed from PVMBG, the eruption characteristic of Kelud 2014 is different from the previous eruption (1990). The eruption in 2014 has a considerable impact on a number of big cities in Java.

In addition to storing geological potential and extraordinary natural charm, Mount Kelud also has the substantial potential disaster after an eruption that must be wary of. The Kelud people called cold lava flood (**Figure 4**). This disaster is no less terrible than the catastrophic eruption. The characteristics of Kelud's lava are quite unique. Basalt-andesitic lava type with relatively middle silica content makes the distribution not sufficiently extensive or only in the center of the eruption and its surroundings. However, the presence of post-eruption rain around the volcano causes the lava that mixed with other eruption material to be carried over several kilometers by the flow and destroying the area around it. Besides causing casualties, the lava floods making the breakdown of communication lines and some areas around the mountain become isolated.

One of the characteristics of Kelud eruption is very horrible and accompanied by a roar and thundering. The eruption is also accompanied by terrible lightning flashes due to the process of

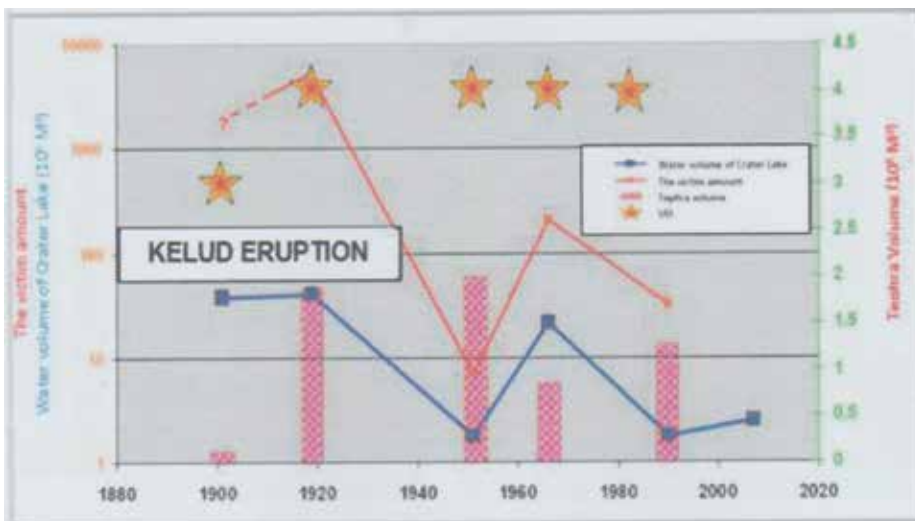

Figure 3. Kelud eruption profile since the eighteenth century. This graph shows the relationship between the volume of crater lake water and the number of fatalities (modified from: https://geologi.co.id/2007/11/05/bagaimana-letusan-kelud/).

Figure 4. The cold lava flood. Another terrible disaster that following of Kelud eruption (https://www.merdeka.com/foto/peristiwa/323649/20140218200905-dahsyatnya-banjir-lahar-dingin-gunung-kelud-001-debby.html).

ionization of clouds caused the electrical charges carried by the volcanic ash into space and in contact with other charges in the atmosphere. The combination of electric flashes and a puff of ash into the sky displays a gigantic figure that is terribly believed by local people as the incarnation of Mount Kelud who is angry (**Figure 5**). This condition is used by the local government in instructing people to immediately leave from dangerous areas around Mount Kelud.

Although its eruption is assessed by geologists as a powerful eruption, it does not mean cause the occurrence of many casualties. This condition illustrates the success of disaster mitigation actions implemented by local communities and Kediri regency government. The government works collaboratively with local communities to help protect communities from the physical and psychological impact [39].

Besides Kelud, Mount Merapi (2986 m asl) is one of the legendary mountains in Java Island. Geographically, Mount Merapi lies on 7°32′30″ SL and 110°26′30″ EL, bordering four districts,

Figure 5. Kelud eruption in 2014. The combination of electric flash and volcanic ash resembles an angry gigantic figure.

namely Sleman in Yogyakarta and Magelang, Boyolali and Klaten in Central Java Province (**Figure 6**), as a subduction product between plates Indo-Australia and Eurasia in Java [37]. The historical record of Merapi eruption began in 1768. From that time until now, Merapi has erupted 80 times with varying strength and periodization [37]. The eruption impact not only caused a lot of casualties and environmental damage but also deep trauma for the people living around it [40].

The large eruption of Mount Merapi in the last decade occurred in 2010. This eruption is considered the largest eruption since 1870 with the death toll reaching 277 people [21]. Although the same type of stratovolcano like Mount Kelud, the eruption characteristics is different from Kelud. Merapi eruption characteristic is lower explosive with eruption index level between 1 and 3. Merapi rocks are basaltic-andesitic [41] with silica (SiO_2) content of 52–56% (greater than the silica content of Kelud volcano). However, it does not mean that the Merapi eruption is safe for people living around it.

The volatile material of Merapi cause in every eruption always followed by a lava dome [42] that produces hot clouds or "Wedus Gembel" and greatly endangers the surrounding population. Hot clouds Merapi glide has a speed of 200 km/h with temperatures reaching 1000°C, with decreasing temperature between 23 and 27°C/km [43]. This hot cloud is a vertical pyroclastic flow explosion product [44] and flows gravitationally along the leaf and rivers and will stop when its energy is exhausted [38]. Recorded by BNPB, Merapi's biggest victim was inflicted by the hot clouds that attacked the settlements (**Figure 7**).

The ancient of Javanese believes, people believe in the relationship between Merapi, Keraton and the South Sea Ruler [45]. They believe that the Mount Merapi has supernatural powers

Figure 6. Merapi location map and settlement around it (wikipidia.org).

Figure 7. Hot clouds of Merapi or "Wedus Gembel" should destroy the surrounding settlements.

that can affect the lives of surrounding communities [46]. Merapi eruption always associates with the anger of the spirit of guardians; therefore, people on the slopes of Merapi are always careful in every attitude, words, and deeds and always maintain the hereditary traditions that are considered capable of muffling the anger of it.

The people around Merapi have ecological wisdom in terms of rearing, farming and living [47]. Before starting agricultural activities, the average community organizes a salvation event that aims to ask for blessing and safety in farming. To get fertile agricultural land people are advised to use a sharp machete to open the forest and use the intercropping system in farming. This can keep the soil fertility level. In the livestock system, the people of Merapi take grasses of feed animals in places that are considered not haunted. They went to the forest together and guarded each other against the disturbance of the spirits around Merapi. This is very impacting on the forest around Mount Merapi stay awake. At the time of taking grasses food in the forest which is considered haunted, the community must keep the environmental ethics. The wisdom of people in living is also owned by the people of Merapi. All buildings should not face Mount Merapi and Merbabu as it is deemed disrespectful to both mountains.

The story of Merapi eruption cannot be separated from the role of the figure of public figures who became the icon of obedience to the existence of volcano. He is Mbah Marijan, a caretaker who devotes his entire life to the Merapi volcano to become a victim of Merapi eruption malignancy in 2010. Communities around Merapi tend to be more obedient to the status information of volcanic activity from caretaker Mbah Marijan compared with information from the government. Although for sometimes the eruption experience is accurate, but not able to provide guarantees for the community because the decision taken by the caretaker is not based on proper geological studies. As a result, it is not a few casualties from the last eruption in 2010.

However, this does not mean that this experience is a bad history of the Indonesian people in facing the threat an eruption of Mount Merapi, especially for the people of Yogyakarta and its surroundings. The low level of public knowledge of the geological information presented in the technique is still difficult to understand, so there is a need for tools to communicate to the community related to volcanic activity. The contribution of Mbah Marijan with his experience in dealing with eruptions is considered very large in helping save the people from the Merapi eruption.

3. Community behavior and the challenges of volcano eruption

The volcano disaster provides a meaningful example of how communities apply cultures, religions and ceremonies to communicate and remember disaster risks and mitigation strategies [45]. The understanding of that society has based only on myth and not based on scientific knowledge so that the existence of the culture is not widely understood by the public. Therefore, it is necessary to conduct an in-depth study related to the culture of the community and local knowledge as material for the development of disaster mitigation model that is more suitable to the characteristics of the local community on the mountain slopes.

Communities located in disaster-prone areas are suspected of having traditional intelligence in dealing with disasters formed from the introduction of the physical environment [48]. Local knowledge of the environment around volcano plays a significant role in the impact of the eruption disaster [31]. As did Sugihwaras society in predicting eruptions based on changes in natural signs. People believe that if a python is present at the villagers' means Kelud volcano will soon erupt. The python is believed by the villagers as a mountain guard manifestation that conveys the message that "celebration" will begin soon and remind people to move temporarily. The people of Kediri also abstain from cutting down Bamboo trees and Banyan at random because they are considered as sacred trees. Both trees are very important in maintaining the quality of water and soil in the surroundings of Mount Kelud.

The history of Mount Kelud and Merapi eruption, as well as several volcanoes in Indonesia, cannot be separated from the traditions of the surrounding community. A belief that the eruption of a volcano is a manifestation of the anger of the mountain guard makes the community always obedient to the tradition to perform the ceremony of honor. Scientifically, this context is very unusual, but adherence to local traditions and cultures provides a distinct advantage for people to remain secure in the face of volcanic eruption threats. One of the evidence is an offering performed by the community around Kelud mountain on 1 Suro (Javanese month). Based on the field study, most of the people of Kediri (82.61%) consider the offering ceremony to be important. One of the reasons is to obtain salvation from God Almighty from the danger of Mount Kelud eruption (65.22%). The spiritual power makes people feel secure and protected from natural disaster [21]. The culture role is very important in disaster risk reduction because through the power of culture is able to reduce the vulnerability of society to disaster [36].

This finding is highly relevant to the results of the previous study. The communities around the volcano have their own way of dealing with the threat of eruption. They have developed a system to live around the volcano through naturalization, familiarization and domestication toward all threats from volcanoes [19]. Various forms of ritual are carried out by communities around the volcano which aims to respect the volcano that seen as a source of life [49]. People consider that the volcano is a part of their daily culture and life. They have a unique culture that portrays volcano as the center of the God and the symbol of greatness [33].

Local wisdom is a basic knowledge that achieved in the balance of life with nature and related to the culture in the community with its main character is that wisdom comes from experience or truth derived from life [50]. A ritual ceremony is a form of local wisdom as it connects the balance of nature with life. The main purpose of this ritual is to express gratitude to God Almighty who has given the fertility of the land in the mountain of Kelud and Merapi and

so that people avoid the eruption disaster. This ritual is a cultural framework that reflects the social structure and provides a sense of security like their ancestors [51].

The wisdom of the people around Kelud is also visible from the house building designed to minimize the impact of the eruption disaster. Various types of houses are built with small size and have a sturdy pole and a tapered roof (less than 45°) (**Figure 8**). This is done with the consideration of volcanic ash will more easily fall to the ground, so that the house does not become collapsed due to support a load of ash erupted. In addition, the community uses roof tile from clay. They believe that the clay is more weather resistant both in the rainy season and drought and more environmentally friendly. The use of clay tile is very suitable for settlement in the mountains because it can stabilize the temperature inside the house so it remains warm and comfortable.

The ability of communities around the volcano in the face of the eruption disaster becomes a model that can be developed in different regions with the same geological background. Differences in social, cultural and economic factors play an important role in the ability of communities to understand disasters and how they cope with disaster risks [51]. Like the Tenggerese people of the Bromo Mountains, they have five cultural adaptations that enable them to survive in the mountainous areas of resilience and high ability to return to their original state, attachment to place and knowledge of danger, the source of social and moral order, and catalyst for the process of change [33].

Compliance with the traditions and beliefs against the signs of nature helps the people to save themselves from the dangers of an eruption. But the traditions of the people and the signs of nature have not been studied scientifically, so that they cannot be understood by the wider community. Although people have an indigenous knowledge and use it daily, they are not aware that it can be used to reduce disaster risk [52].

The natural environment around the volcano determines the natural conditions for animals and plants in it. This illustrates the importance of preserving the environment. At a time when the environment is disturbed, the animals and plants can longer serve as a messenger
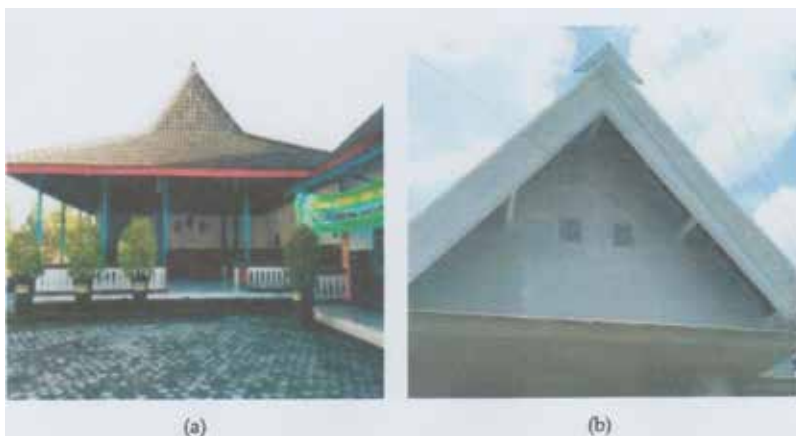

Figure 8. The changes of residential model around mount Kelud. (a) Joglo-shaped roof commonly called the "Tuo" building form and (b) the roof of a cone-shaped house is commonly called the "Enom.".

of nature against the disaster. The abstinence of not wearing red shirts on the slopes of Kelud, ringing the whistle with the mouth to produce high-frequency sounds, not destroying the environment around mountain, and not doing immoral acts is essentially an ethno-pedagogy to keep the environment order to stay natural and sustainable. When the natural conditions are well preserved, then nature will work in accordance with its role.

Success in facing the danger of eruption is not just the success of the government alone, but the wisdom of society in protecting the environment and building a life in harmony with nature makes the impact of the eruption is not so influential in the community. Evacuation and recovery process that runs quickly to make people can survive the eruption disaster and his life can be restored quickly as usual and even better. There are two patterns of adaptation conducted by communities around the mountains of Merapi, the pattern of economic-ecological adaptation and magical belief [53].

A comprehensive system of risk management and preventive measurement is essential in order to reduce potential losses from disasters [39]. Reducing disaster risk requires an integrated approach between social science and the natural sciences [28]. The integration of local knowledge and ethno-science approach into a contemporary framework for the conservation and sustainability of natural resource management will be increasingly important at both national and international levels, especially in developing countries [54].

4. Disaster mitigation model based on local wisdom

The decreasing number of deaths due to eruption from year to year show the disaster management techniques carried out by the government through the National Disaster Management Agency or Badan Nasional Penanggulangan Bencana (BNPB) are better, although not balanced with the level of public awareness in maintaining the environment as an effort to minimize the disaster risk. The high environmental damage caused by some people who are not responsible to be one of the factors triggers the high risk of geological disasters in Indonesia. The low public awareness of the dangers of eruption is a serious concern as a matter to be solved. Not only the responsibility of the government, but also the entire community. All government, non-governmental and international organizations have responsibilities in disaster recovery programs with mutual cooperation between them and the community [55].

Dealing with eruption problems, the government selected effective measures, such as land use arrangements, lava control systems, development of monitoring and early warning systems, evacuation plans, relocation of the population and education and community preparedness programs [4]. By synergizing local wisdom and government programs, disaster mitigation plans can be well implemented.

Disaster mitigation is an effort by the government and the community as an action to minimize disaster risk. This is because volcanic hazards can cause total destruction of the path through which pyroclastic material flows, so that communities must be temporarily displaced. However, the implementation of mitigation is not as easy as imagined. Not all

communities living around the volcano are willing to be evacuated even though disaster early warning has been submitted by the government.

Often people do not understand the geological information presented by the government, but the public better understands the environmental changes of the natural signs. This fact reinforces the need to integrate geological information and local wisdom in making accurate decisions to face of natural disasters. Successful experience in dealing with earthquake and tsunami disaster for Simeulue-Aceh community proves that local wisdom is very important in minimizing disaster risk. They have a way of responding to disaster challenges through traditional communication tools, construction methods and residential planning, and traditional ceremonies [56].

Based on the results of field studies that have been conducted on communities around Mount Kelud associated with disaster mitigation measures, 36.36% said they chose to be evacuated. This means no less than 60% of people still choose to live in the area of disaster eruption. In the vicinity of volcanoes, innovation in disaster mitigation models is required by incorporating local wisdom in it. This needs to be done so that mitigation and recovery process can be quick and easy [56].

Figure 9 is a model of a local wisdom-based disaster mitigation plan implemented in the village of Pelem Sari Yogyakarta. This model integrates the local wisdom in responding to Merapi eruption disaster and very interesting to discuss. Based on the picture, local wisdom serves as a traditional signal when the eruption does not suddenly erupt. There are conditions that have not been able to be completed especially at the time of Mount Merapi erupted suddenly and accompanied by a dangerous eruption. In these circumstances, the main priority is the safety of the population and necessary hard efforts from the government to take a quick decision for evacuating people immediately and leave dangerous areas to get to the safest location as quickly as possible.

Related to the development of volcanic disaster mitigation model, we can learn from Maori indigenous people by integrating local, science and art. They have three important steps: (1) communication understanding of geological and volcanic processes from different perspectives, (2) optimizing local communities living around the volcano to improve preparedness, and (3) develop learning tools for current and future generations that can be used in various community levels [49].

There are four approaches to consider in assisting communities in reducing disaster risk based on local wisdom, including (1) understanding, communicating and managing vulnerabilities and risks and perceptions of local communities about risks and vulnerabilities that come to threaten the life of the community in the future, (2) maximizing community benefits about volcanic environments, especially during rest periods without increasing vulnerability, (3) managing crises, and (4) managing settlements after the crisis [57].

Reducing disaster risks related to efforts to improve community resilience that can be implemented through the preparation of disaster mitigation plans [32]. A comprehensive system of risk management and preventive measurement is essential in order to reduce potential losses from disasters [39]. Reducing disaster risk requires an integrated approach between social
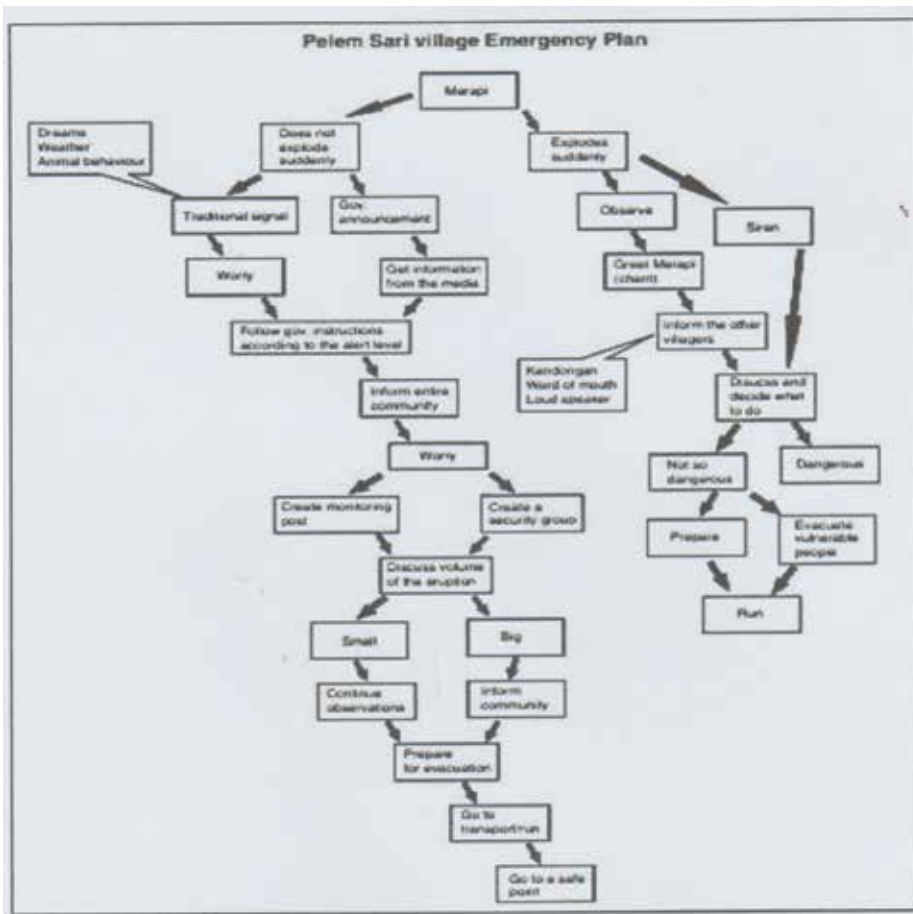
Figure 9. A model of a mitigation plan that integrates local wisdom in the Pelem Sari village Yogyakarta [36].

science and the natural sciences [28]. The integration of local knowledge and ethno-science approaches into a contemporary framework for the conservation and sustainability of natural resource management will be increasingly important at both national and international levels, especially in developing countries [54].

Success in disaster mitigation is strongly influenced by the experience and local knowledge of communities in the face of disasters [58]. Community knowledge is acquired from within and outside the community as a way of dealing with problems [50]. The ways in which the community represents knowledge in dealing with disasters become the local wisdom of the local community. The integration of traditional knowledge and scientific knowledge will get an overview of how to engage communities in vulnerability and risk management [57]. Natural environment around the Kelud Mountain determine the natural conditions for animals and plants in it. This illustrates the importance of preserving the environment. At a time the environment is disturbed, the animals and plants can no longer serve as a messenger of nature against the disaster.

Technology is not the only tool capable of ensuring the safety of people around the mountain, but technology needs to be supported with the local knowledge of people who have more experience related to the surrounding environmental conditions. This became a recommendation in developing a model of volcanic disaster mitigation although in the millennial era. The combination of traditional knowledge and scientific knowledge resulted in a new pattern in addressing disaster challenges and making communities more actively involved in disaster risk management [57].

5. Conclusion

The fruitfulness in facing volcanic eruption in Indonesia is an implementation of disaster management mitigation model that is interesting to be socialized. Ability to utilize local wisdom in building the value of togetherness and wisdom in maintaining and preserving the environment became one of the keys to its success. Building a resilient community while maintaining local cultural values will become a force in building disaster mitigation management of volcano. People remain convinced that behind the disaster there will be a blessing that will be better for the future.

Based on the results of the study on the behavior of the community around Kelud and Merapi mountains, two important concepts were found in developing a disaster mitigation model based on local wisdom that is the compliance of the community in building a harmony with nature by maintaining the natural environment condition to stay sustainable and building the spirit of togetherness in emotional bond through ritual ceremonies. These two aspects become the basic capital in facing all the threats of volcanic disaster and illustrate the importance of local wisdom in building a society that has resilience in the face of eruption disaster.

The meaning of local wisdom needs to be studied and developed scientifically so that it can be understood by the community at large and become an important part to be conserved as an effort to build a community that is resilience to disaster. The action that can be done is to integrate local wisdom in education and training.

Author details

Eko Hariyono[1] and Solaiman Liliasari[2]*

*Address all correspondence to: liliasari@upi.edu

1 Physics Department, Mathematics and Natural Science Faculty, State University of Surabaya, Surabaya, Indonesia

2 Science Education Program, School of Postgraduate Studies, Indonesia University of Education, Bandung, Indonesia

References

[1] Djalante R. Research trends on natural hazards, disasters, risk reduction and climate change in Indonesia: A systematic literature review. Natural Hazards and Earth System Sciences Discussions. 2016;**342**. DOI: 10.5194/nhess-2016-342

[2] Guha-Sapir D, Vos F, Below R, with Ponserre S. Annual Disaster Statistical Review 2010: The Numbers and Trends. Brussels: CRED; 2011. Available from: http://www.cred.be/sites/default/files/ADSR_2010.pdf

[3] Mukhlis T, Syakur T, Dharma D, Anhorn J. School preparedness and training for geological hazard mitigation: An example from Indonesia. Disaster Management and Human Health Risk. 2017;**173**:113-119. DOI: 10.2495/DMAN170111

[4] Carter WN. Disaster Management: A Disaster Manager's Handbook. Mandaluyong City, Phil.: Asian Development Bank; 2008

[5] Wilkinson E, Lovell E, Carby B, Barclay J, Robertson RE. The dilemmas risk-sensitive development on a small volcanic island. Resources. 2016;**5**(21):1-20. DOI: 10.3390/resources5020021

[6] Christia M. Experiences of People Affected Merapi Eruption in 2010, A Qualitative Study Conducted in Krinjing Village Indonesia [Thesis]. University of Oslo; 2012

[7] Caldera J, Wirasinghe S. Analysis and classification of volcanic eruption. In: 10th International Conference of the International Institute for Infrastructure Resilience and Reconstruction (I3R2). West Lafayette, Indiana, USA: Purdue University; 2014. pp. 128-133

[8] Lavigne F, De Coster B, Juvin N, Flohic F, Gaillard JC, Texier P, et al. People's behaviour in the face of volcanic hazards: Perspectives from Javanese communities, Indonesia. Journal of Volcanology and Geothermal Research. 2008:273-287. DOI: 10.1016/j.jvolgeores.2007.12.013

[9] Jenkins SF, Barsotti S, Hincks TK, Neri A, Phillips JC, Sparks RSJ, Sheldrake T, Vougioukalakis G. Rapid emergency assessment of ash and gas hazard for future eruptions at Santorini Volcano, Greece. Journal of Applied Volcanology. 2015;**4**:16. DOI: 10.1186/s13617-015-0033-y

[10] Raga GB, Baumgardner D, Ulke AG, Torres Brizuela M, Kucienska B. The environmental impact of the Puyehue-Cordon Caulle 2011 volcanic eruption on Buenos Aires. Natural Hazards and Earth System Sciences. 2013;**13**;2319-2330. DOI: 10.5194nhess-13-2319-2013

[11] Frölicher TL, Joos F, Raible CC. Sensitivity of atmospheric CO_2 and climate to explosive volcanic eruptions. Biogeosciences. 2011;**8**:2317-2339. DOI: 10.5194/bg-8-2317-2011

[12] Frölicher TL, Joos F, Raible CC, Sarmiento JL. Atmospheric CO_2 response to volcanic eruptions: The role of ENSO, season, and variability. Global Biogeochemical Cycles. 2013;**27**:239-251. DOI: 10.1002/gbc.20028.2013

[13] Smyth R, Crowley QG, Hall R, Kinny PD, Hamilton PJ, Schmidt DN. A Toba-scale eruption in the Early Miocene: The Semilir Eruption, East Java, Indonesia. Lithos. 2011: **126**;198-211. DOI: 10.1016/j.lithos.2011.07.010

[14] Chesner CA. The Toba caldera complex. Quaternary International. 2011. DOI: 10.1016/j.quaint.2011.09.025

[15] Gertisser R, Self S. The great 1815 eruption of Tambora and future risks from large scale volcanism. Geology Toda. 2015;**31**:132-136

[16] Whelan F, Kelletat D. Submarine slides on volcanic islands—A source for mega-tsunamis in the quaternary. Process in Physical Geography. 2003;**27**:198-216

[17] Egorov Y. Tsunami wave generation by the eruption of underwater volcano. Natural Hazards and Earth System Sciences. 2007;**7**:65-69

[18] Kusky T. The Hazardous Earth Volcanoes Eruption and Other Volcanic Hazards. New York: Facts on File, Inc; 2008

[19] Dove MR. Perception of volcanic eruption as agent of change: On Merapi volcano, Central Java. Journal of Volcanology and Geothermal Research. 2008;**172**:329-337

[20] Iguchi M, Ishihara K, Surono HM. Learn from 2010 Eruption at Merapi and Sinabung Volcanoes in Indonesia. Vol. 54B. Kyoto Univ.: Annuals of Disaster Prevention Research Institute; 2011

[21] Subandi MA, Achmad T, Kurniati H, Febri R. Spirituality, gratitude, hope and post-traumatic growth among the survivors of the 2010 eruption of Mount Merapi in Java, Indonesia. Australasian Journal of Disaster and Trauma Studies. 2014:**18**(1)

[22] Tuswadi & Hayashi T. Disaster prevention education in Merapi volcano area primary schools: Focusing on student's perception and teacher's performance. Procedia Environmental Sciences. 2014;**20**:668-677

[23] Surono M, Jousset P, Pallister J, Boichu M, Buongiorno MF et al. The 2010 explosive eruption of Java's Merapi volcano—A '100-year' event. Journal of Volcanology and Geothermal Research, Elsevier. 2012:**241-242**;121-135

[24] Gunawan H, Surono BA, Kristianto PO, McCausland W, Pallister J, Iguchi M. Overview of the eruptions of Sinabung eruption, 2010 and 2013-present and details of the 2013 phreatomagmatic phase. Journal of Volcanology and Geothermal Research. 2017. DOI: 10.1016/j.jvolgeores.2017.08.005

[25] Muzambiq S, Syafriadi, Wijaksana BS, Rosaidi U. Characteristic of Sinabung volcano deformation of 2011-2012 estimated based on GPS data. Australian Journal of Basic and Applied Sciences. 2017:**11**(9);59-71

[26] Kadavi PR, Lee WJ, Wook-Lee C. Analysis of the pyroclastic flow deposits of mount Sinabung and Merapi using Landsat imagery and the artificial neural networks approach. Applied Sciences. 2017;**7**:935. DOI: 10.3390/app7090935

[27] Daniel J. CATDAT: Damaging Volcanoes Database 2010—The Year in Review. Available from: https://www.cedim.de/download/CATDAT_VOLC_Data_-_1st_Annual_Review_-_2010_-_James_Daniell_-_02.02.2011.pdf

[28] Donovan A, Eiser JR, Sparks RSJ. Scientists' views about lay perceptions of volcanic hazard and risk. Journal of Applied Volcanology. 2014;**3**:15. DOI: 10.1186/s 13617-014-0015-5

[29] Gonzáles-Mellado AO, De la Cruz-Reyna S. A simple semi-empirical approach to model thickness of ash-deposits for different eruption scenarios. Natural Hazards and Earth System Sciences. 2010;**10**:2241-2257. DOI: 10.5194/nhess-10-2241-2010

[30] King TA, Tarrant RAC. Children's knowledge, cognitions and emotions surrounding natural disasters: An investigation of year 5 students, Wellington, New Zealand. Australasian Journal of Disaster and Trauma Studies. 2013;**2013**:1

[31] Hariyono E, Liliasari S. The characteristics of volcanic eruption in Indonesia. In: Volcanoes. Tech Open Access; 2018. ISBN: 978-953-51-5610-9

[32] Cho SE, Won S, Kim S. Living in harmony with disaster: Exploring volcanic hazard vulnerability in Indonesia. Sustainability. 2016;**13**. DOI: 10.3390/su8090848

[33] Bachri S, Stotter J, Monreal M, Sartohadi J. The calamity of eruptions, or an eruption benefits? Mt. Bromo human-volcano system a case study of open risk perception. Natural Hazards and Earth System Sciences. 2015;**15**:277-290

[34] Wilson T, Kaye G, Stewart C, Cole J. Impacts of the 2006 eruption of Merapi volcano, Indonesia, on agriculture and infrastructure. GNS Science Report. 2007;**7**;69

[35] Latif DO, Rifa'i A, Suryolelono KB. Chemical characteristics of volcanic ash in Indonesia for soil stabilization: Morphology and mineral content. International Journal of GEOMATE. 2016;**11**:2606-2610

[36] Donovan K. Doing social volcanology: Exploring volcanic culture in Indonesia. Area. 2010;**42**(1):117-126. DOI: 10.1111/j.1475-4762.2009.00899.x

[37] PVMBG. Data Dasar Gunungapi Indonesia [Basic Data of Indonesia Volcanoes]. Ministry of Energy and Mineral Resource, Geology Department; 2010

[38] Kristiansen NI, Prata AJ, Stohl A, Carn SA. Stratospheric volcanic ash emissions from the 13 February 2014 Kelut eruption. Geophysical Research Letters. 2015;**42**:588-596. DOI: 10.1002/2014GL062307

[39] Schwendtner B, Papathoma-Köhle M, Glade T. Risk evolution: How can changes in the built environment influence the potential loss of natural hazards? Natural Hazards and Earth System Sciences. 2013:**13**;2195-2207. DOI: 10.5194/nhess-13-2195-2013

[40] Fatwa T, Asti MS, Wahyuni ST, Widodo H. The effectiveness of trauma healing methods to reduce post-traumatic stress disorder (PTSD) on teenage victims of Mount Merapi eruption. International Journal of Research Studies in Psychology. 2014;**3**:101-111

[41] Chadwick JP, Troll VR, Ginibre C, Morgan D, Gertisser R, Waight TD, Davidson JP. Carbonate assimilation at Merapi volcano, java, Indonesia: Insights from crystal isotope stratigraphy. Journal of Petrology. 2007;**48**:1793-1812

[42] Gertisser R, Charbonnier SJ, Keller J, Quidelluer X. The geological evolution of Merapi volcano, Central Java, Indonesia. Bulletin of Volcanology. 2012;**74**:1213-1233

[43] Indresputra F, Rahayu S, Widiyanto S. Effect of pyroclastic cloud from Merapi volcano to the survival of Uromycladium tepperianum on Falcataria moluccana in Yogyakarta, Indonesia. The 3rd International Conference on Sustainable Future for Human Security SUSTAIN 2012. Procedia Environmental Sciences. 2013:**17**;70-78

[44] Newhall CG, Bronto S, Alloway B, Banks NG, Bahar I, del Marmol MA, et al. 10,000 years of explosive eruptions of Merapi Volcano, Central Java: Archaeological and modern implications. Journal of Volcanology and Geothermal Research. 2000;**100**:9-50

[45] Troll VR, Deegan FM, Jolis EM, Budd DA, Dahren B, Schwarzkoff LM. Ancient oral tradition describes volcano earthquake interaction at Merapi volcano Indonesia. Swedish Society for Anthropology and Geography. 2015;**97**:137-166

[46] Gunawan H. The wisdom of the community on the southern slopes of Merapi, Sleman District – The special region of Yogyakarta. Sosio Informa. 2015:**1**(02)

[47] Fatkhan M. Kearifan lingkungan masyarakat lereng Gunung Merapi (Environmental wisdom community slope of Mount Merapi). Aplikasia. 2006;**VII**:107-121

[48] Setyawati S, Pramono H, Ashari A. Kecerdasan tradisional dalam mitigasi bencana erupsi pada masyarakat lereng Baratdaya Merapi (Traditional intelligence in eruption disaster mitigation on peoples of the south-western slopes of Merapi). SOCIA: Jurnal Ilmu-Ilmu Sosial. 2015;**12**(2):100-110

[49] Pardo N, Wilson H, Procter JN, Lattughi E, Black T. Bridging Maori indigenous knowledge and western geosciences to reduce social vulnerability in active volcanic regions. Journal of Applied Volcanology. 2015;**4**:5. DOI: 10.1186/s13617-014-0019-1

[50] Mungmachon MR. Knowledge and local wisdom: Community treasure. International Journal of Humanities and Social Science. 2012;**2**:174-181

[51] Jóhannesdóttir G, Gisladóttir G. People living under threat of volcanic hazard in southern Iceland: Vulnerability and risk perception. Natural Hazards and Earth System Sciences. 2010;**10**:407-420

[52] Maferetlhane OI. The role of indigenous knowledge in disaster risk reduction: A critical analysis [Mini Dissertation]. Master of Development and Management at the North-West University, Potchefstroom Campus. 2012

[53] Nazaruddin, M. Natural Hazard and Semiotic Changes on the Slope of Mt. Merapi, Indonesia [Master Thesis]. University of Tartu Faculty of Philosophy, Department of Semiotics; 2013

[54] Rist S, Guebas FD. Ethnoscience—A step toward the integration of scientific and indigenous forms of knowledge in the management of natural resource for the future. Environment, Development and Sustainability. 2006;**8**:467-493

[55] Arain F. Knowledge-based approach for sustainable disaster management: Empowering emergency response management team. Procedia Engineering. 2015;**11**:232-239

[56] Syahputra H. Role of local wisdom in acceleration of disaster risk reduction in Aceh (Kabupaten Simeulue case). In: 5th Annual International Workshop & Expo on Sumatra Tsunami Disaster & Recovery 2010. 2010

[57] Kelman I, Mather TA. Living with volcanoes: The sustainable livelihoods approach for volcano-related opportunities. Journal of Volcanology and Geothermal Research. 2008;**172**:189-198

[58] Texier-Teixeira P, Chouraqui F, Perrillat Coulomb A, Lavigne F, Cadag JR, Grancher D. Reducing volcanic risk on Fogo volcano, Cape Verde, through a participatory approach: Which outcome?. Natural Hazards and Earth System Sciences. 2014:**14**;2358-2374. DOI: 10.5194/nhess-14-2374-2014

Edited by José Simão Antunes do Carmo

This book addresses different aspects of natural hazards and vulnerabilities, with a focus on prevention and protection. It consists of nine chapters, five on flood events addressing vulnerabilities, risk assessments, impacts, sensitivity analyses, and mitigation measures, two on climate change and reconstruction of natural hazard events such as avalanches and rockslides, and two on tsunamis and volcanoes.

All chapters provide relevant information and useful elements for readers interested and concerned about the lack of action or its ineffectiveness in containing the vulnerabilities and risks of possible natural hazards worldwide.

IntechOpen